Aims

The *Seminario Matematico* is a society of members of mathematics-related departments of the University and the Politecnico in Turin. Its scope is to promote study and research in all fields of mathematics and its applications, and to contribute to the diffusion of mathematical culture.

The *Rendiconti* is the official journal of the Seminario Matematico. It publishes papers and invited lectures. Papers should provide original contributions to research, while invited lectures will have a tutorial or overview character. Other information and the contents of recent issues are available at `http://seminariomatematico.dm.unito.it/rendiconti/`

Instructions to Authors

Authors should submit an electronic copy (preferably in the journal's style, see below) via

e-mail: `rend_sem_mat@unito.it`

English is the preferred language, but papers in Italian or French may also be submitted. The paper should incorporate the name and affiliation of each author, postal and e-mail addresses, a brief abstract, and MSC classification numbers. Authors should inform the executive editor as soon as possible in the event of any change of address.

The final decision concerning acceptance of a paper is taken by the editorial board, based upon the evaluation of an external referee. Papers are typically processed within two weeks of arrival, and referees are asked to pass on their reports within two months.

Authors should prepare their manuscripts in LaTeX, with a separate BibTeX file whenever possible. To avoid delays in publication, it is essential to provide a LaTeX version once a paper has been accepted. The appropriate style file and instructions can be downloaded from the journal's website. The editorial board reserves the right to refuse publication if the file does not meet these requirements.

RENDICONTI DEL SEMINARIO MATEMATICO

Università e Politecnico di Torino

CONTENTS

Volume 72, N. 1–2 **2014**

RENDICONTI DEL SEMINARIO MATEMATICO 2014

Autorizzazione del Tribunale di Torino N. 2962 del 6.VI.1980

DIRETTORE RESPONSABILE

Alberto Collino

QUESTO FASCICOLO È STAMPATO CON IL CONTRIBUTO DI:
UNIVERSITÀ DEGLI STUDI DI TORINO
POLITECNICO DI TORINO

Preface: Special issue on rate-independent evolutions and hysteresis modelling

The interest in hysteresis and rate-independent phenomena is shared by scientists with a great variety of different backgrounds. We can encounter these processes in several situations of common life: for instance in elasto-plasticity, ferromagnetism, shape-memory alloys, phase transitions. Beyond physics, hysteresis and rate-independent phenomena appear also in engineering, biology, economics as well as in many other settings, playing an important role in many applications. The complexity arising in these fields necessarily requires a joint contribution of experts with different backgrounds and skills. Therefore, only synergy and cooperation among these several people can lead to concrete advances in the technological capabilities of our society.

This special issue of *Rendiconti del Seminario Matematico* is devoted to the latest advances and trends in the modelling and in the analysis of this family of complex phenomena, motivated by the *Spring School on Rate-independent Evolutions and Hysteresis Modelling*, held at the Politecnico di Milano and University of Milano on May 27-31, 2013. In particular, we gathered contributions from different area of mathematics, with the intent of presenting an updated picture of current research directions, offering a new perspective in the study of these processes.

We wish to thanks all the referees, who kindly agreed to devote their time and effort to read and check all the papers carefully, providing useful comments and recommendations. We are also grateful to all the authors for their great job and the high quality of their contributions. We finally wish to express our gratitude to Prof. Marino Badiale for the opportunity to publish this special issue and for the technical support.

Guest editors:

Stefano Bosia
Michela Eleuteri
Elisabetta Rocca
Enrico Valdinoci

Rend. Sem. Mat. Univ. Politec. Torino
Vol. 72, 1–2 (2014), 3 – 16

S. Dipierro*

ASYMPTOTICS OF FRACTIONAL PERIMETER FUNCTIONALS AND RELATED PROBLEMS

Abstract. In this paper we review some recent results concerning the asymptotics of a fractional perimeter and the regularity of the corresponding minimizers. We also provide an elementary example of set with infinite s-perimeter.

1. Introduction

In [4] the notion of nonlocal perimeter was introduced. Namely, given $s \in (0,1/2)$ and a bounded open set $\Omega \subset \mathbb{R}^n$ with $C^{1,\gamma}$-boundary, for some $\gamma \in (0,1)$, the s-perimeter of a (measurable) set $E \subseteq \mathbb{R}^n$ in Ω is defined as

$$\begin{aligned}\mathrm{Per}_s(E;\Omega) :=& \mathscr{L}(E\cap\Omega, (\mathscr{C}E)\cap\Omega)\\ &+\mathscr{L}(E\cap\Omega, (\mathscr{C}E)\cap(\mathscr{C}\Omega)) + \mathscr{L}(E\cap(\mathscr{C}\Omega), (\mathscr{C}E)\cap\Omega),\end{aligned} \tag{1}$$

where $\mathscr{C}E = \mathbb{R}^n \setminus E$ denotes the complement of E. The interaction $\mathscr{L}$ considered in [4] is the following

$$\mathscr{L}(A,B) := \int_A\int_B \frac{dx\,dy}{|x-y|^{n+2s}}$$

for any measurable sets A and B.

We mention also [22, 23], where the author analyses some functionals related to the one defined in (1), also in connection with fractal dimensions.

The idea behind definition (1) is that each point in E interacts with each point in the complement of E, in such a way that the set Ω is taken into account. More precisely, in Figure 1 we can see that Ω splits E, which is the set below the line, and the complement of E into four parts: the black set $E\cap(\mathscr{C}\Omega)$, the dark gray set $E\cap\Omega$, the light gray set $(\mathscr{C}E)\cap\Omega$ and the white set $(\mathscr{C}E)\cap(\mathscr{C}\Omega)$. Then, the functional in (1) takes into account the interactions between all these sets, with the exception of the interaction between the black one and the white one. The reason for this is that in [4] the authors were interested in minimizing the functional in (1), and therefore the interaction of the two sets outside Ω is assumed as a fixed boundary datum.

Notice that, when $s \in (-\infty,0]\cup[1/2,+\infty)$, the integrals in (1) may diverge even for smooth sets. In the case $s \leqslant 0$ the problem comes from the interaction between

Acknowledgements. The author has been supported by EPSRC grant EP/K024566/1 "Monotonicity formula methods for nonlinear PDEs".

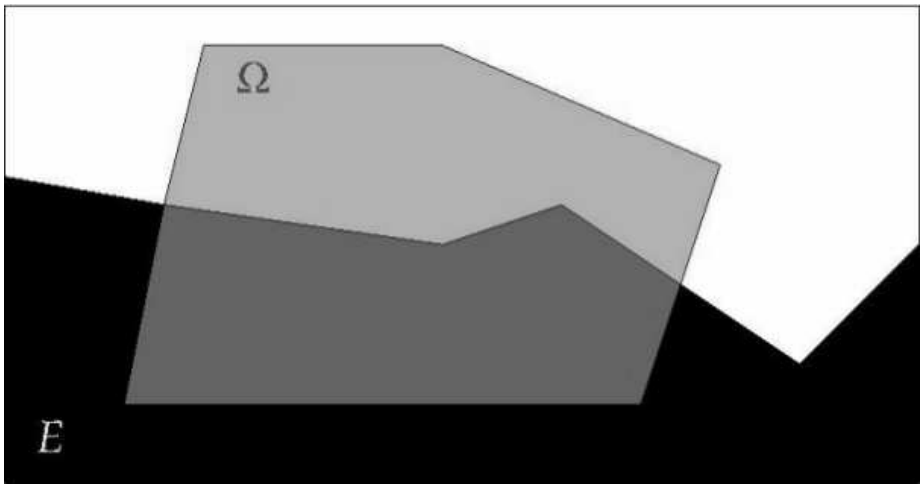

Figure 1: The sets considered in the nonlocal perimeter (1).

points x and y that are very far away from each other, while in the case $s \geqslant 1/2$ from the interaction between points x and y that are very close to each other, since the contribution to the integrals in (1) of these interactions becomes unbounded. On the contrary, when $s \in (0,1/2)$, the integrals in (1) are finite, for instance, if the set E is smooth, see [5].

As already mentioned, in [4] the minimization problem corresponding to (1) was introduced. That is, we say that a set E is s-minimal in Ω if

$$\mathrm{Per}_s(E,\Omega) \leqslant \mathrm{Per}_s(F,\Omega)$$

for any measurable set F that coincides with E outside Ω, i.e. $F \setminus \Omega = E \setminus \Omega$.

The existence of an s-minimizer is ensured by the following result, which is proved using the lower semicontinuity of the functional in (1) and a compactness property, see Section 3 in [4]:

THEOREM 1. *(Theorem 3.2 in [4]) Let Ω be a bounded Lipschitz domain, and $E_0 \subset \mathbb{R}^n \setminus \Omega$ be a given set. Then, there exists a set E, with $E \setminus \Omega = E_0$ such that*

$$\mathrm{Per}_s(E,\Omega) \leqslant \mathrm{Per}_s(F,\Omega)$$

for any F such that $F \setminus \Omega = E_0$.

Moreover, in [4] the authors established the Euler-Lagrange equation associated to the functional in (1): that is, if E is an s-minimizer in Ω and $x \in \Omega \cap (\partial E)$, then

$$\int_{\mathbb{R}^n} \frac{\chi_E(x+y) - \chi_{\mathscr{C}E}(x+y)}{|y|^{n+2s}}\, dy = 0. \tag{2}$$

We remark that the integral equation in (2) is the fractional counterpart of the zero mean curvature equation, that is the equation satisfied by classical minimal surfaces (i.e. surfaces that minimize the classical perimeter). Therefore, the integral in (2) can be seen as a sort of fractional mean curvature, see [1] where this notion was introduced and compared with the classical one.

From a geometric point of view, we can say that (2) means that there is a balance between a suitable average of the set E, centred at points of the boundary ∂E, and the average of its complement.

In [4], equation (2) is taken in the viscosity sense for any measurable set E, since the denominator may be singular if E is not smooth. An interesting thing is that, setting $\widetilde{\chi}_E := \chi_E - \chi_{\mathscr{C}E}$, (2) reads

$$(-\Delta)^s \widetilde{\chi}_E = 0 \quad \text{along } \partial E,$$

we refer to [20, 10] for a basic introduction to the fractional Laplace operator.

As a consequence of the Euler-Lagrange equation (2), in [4] the authors proved a comparison principle, namely if an s-minimizer is contained in a strip outside Ω then it is contained in the same strip inside Ω too.

Using this comparison principle, one can see that the half-plane in an s-minimizer in any domain Ω (see Corollary 5.3 in [4]). As far as we know, actually the half-plane is the only explicit example of s-minimizer.

Recently, the s-perimeter has attracted a lot of attention and inspired many works in different directions, both in the pure mathematical setting (see, for instance, the papers [3, 6, 19], where the problem of the regularity of the s-minimal surfaces was studied) and in view of concrete applications (such as phase transition problems with long range interactions, see [16, 17, 18, 21]).

The limits as $s \searrow 0$ and $s \nearrow 1/2$ are somehow the critical cases for the s-perimeter, due to the fact that the functional in (1) diverges as it is. Nevertheless, if suitably rescaled, these limits seem to give useful information on the problem, concerning, for instance, the regularity of the nonlocal minimal surfaces, see [6].

The paper is organized as follows. In Sections 2 and 3 we discuss the asymptotics of the s-perimeter when $s \nearrow 1/2$ and $s \searrow 0$, respectively. In Section 4 we give an example of set E which has infinite s-perimeter for any $s \in (0, 1/2)$ (and therefore it does not make sense to talk about the asymptotics for such a set E). In Section 5 we review the state of the art concerning the regularity of s-minimal surfaces. Finally, in Section 6 we recall the Bernstein problem and some related results obtained in the nonlocal setting.

2. Asymptotic of the s-perimeter when $s \nearrow 1/2$

One of the reasons for which the functional defined in (1) is called s-perimeter relies on the asymptotic as $s \nearrow 1/2$. Indeed, one can prove that, when $s \nearrow 1/2$, the fractional perimeter, suitably renormalised, approaches the classical perimeter, as stated in the following:

THEOREM 2. *([5, 2])*

i) Let $\alpha \in (0,1)$, $R>0$ and $s_k \nearrow 1/2$. Suppose that E is a set with $C^{1,\alpha}$-boundary in B_R. Then,

$$\lim_{k\nearrow+\infty} (1-2s_k)\,\mathrm{Per}_{s_k}(E,B_r) = \omega_{n-1}\,\mathrm{Per}(E,B_r) \quad \text{a.e. } r\in(0,R).$$

ii) Let $R>r>0$, $s_k \nearrow 1/2$ and E_k be such that

$$\sup_{k\in\mathbb{N}} (1-2s_k)\,\mathrm{Per}_{s_k}(E_k,B_R) < +\infty.$$

Then, up to subsequence,

$$\chi_{E_k} \to \chi_E \quad \text{in } L^1(B_r),$$

for a suitable set E with finite perimeter in B_r.

iii) Let $R>r>0$, $s_k \nearrow 1/2$ and E_k be s_k-minimizers in B_R such that

$$\chi_{E_k} \to \chi_E \quad \text{in } L^1(B_R).$$

Then, E is a minimizer for the perimeter in B_r. Also, E_k approach E uniformly in B_r, that is for any $\varepsilon>0$ there exists k_0, possibly depending on r and ε, such that if $k\geqslant k_0$ then $E_k\cap B_r$ and $B_r\setminus E_k$ are contained, respectively, in an ε-neighbourhood of E and of $\mathbb{R}^n\setminus E$.

We observe that in the first statement i) of Theorem 2 the convergence holds true for almost any ball, since pathological sets may exist. Namely, one can construct a set E whose boundary hits the boundary of a ball B_r and then has a segment that lies on it. Since in the definition of the classical perimeter one considers open balls, the part of ∂E that coincides with ∂B_r is not taken into account. On the other hand, the integrals in the definition of the s-perimeter do not "feel" the difference between open and closed balls, and therefore also the part of ∂E that coincides with ∂B_r plays a role in the interactions. This means that for such a set E and such a ball the convergence is not true. Anyway, notice that one can slightly decrease or increase the radius of the ball to obtain the convergence of the s-perimeter of E into $B_{r\pm\varepsilon}$ to its classical perimeter.

Theorem 2 was proved in [5] from a geometric point of view, while in [2] the authors proved the convergence of the fractional perimeter to the classical perimeter as $s\nearrow 1/2$ in a Γ-convergence setting. In both the cases the authors obtained the (locally uniformly) convergence of s-minimizers to classical minimizers.

3. Asymptotic of the s-perimeter when $s\searrow 0$

In order to deal with the limit as $s\searrow 0$ of the functional in (1), we recall that the fractional Sobolev space $H^s(\mathbb{R}^n)$ is defined as

$$H^s(\mathbb{R}^n) := \left\{ u\in L^2(\mathbb{R}^n) : \frac{|u(x)-u(y)|}{|x-y|^{\frac{n}{2}+s}} \in L^2(\mathbb{R}^n\times\mathbb{R}^n) \right\}.$$

[1] As usual, we denote by $\omega_{n-1} := \mathscr{H}^{n-1}(S^{n-1})$ the surface of the $(n-1)$-dimensional sphere.

This space is endowed with the norm

$$\|u\|_{H^s(\mathbb{R}^n)} := \left(\int_{\mathbb{R}^n} |u(x)|^2 dx + \int_{\mathbb{R}^n}\int_{\mathbb{R}^n} \frac{|u(x)-u(y)|^2}{|x-y|^{n+2s}}\, dx\, dy\right)^{1/2},$$

where the term

$$[u]_{H^s(\mathbb{R}^n)} := \left(\int_{\mathbb{R}^n}\int_{\mathbb{R}^n} \frac{|u(x)-u(y)|^2}{|x-y|^{n+2s}}\, dx\, dy\right)^{1/2} \tag{3}$$

is the so-called Gagliardo seminorm, see [10] for a basic introduction to the fractional Sobolev spaces.

Now, a first result regarding the asymptotic of the s-perimeter when $s \searrow 0$ is the following:

THEOREM 3. *(Theorem 3 in [15]) Suppose that $u \in H^{s_0}(\mathbb{R}^n)$ for some $s_0 \in (0,1/2)$. Then,*

$$\lim_{s\searrow 0} s \int_{\mathbb{R}^n}\int_{\mathbb{R}^n} \frac{|u(x)-u(y)|^2}{|x-y|^{n+2s}}\, dx\, dy = \omega_{n-1}\int_{\mathbb{R}^n} |u(x)|^2 dx. \tag{4}$$

This means that the Gagliardo seminorm of u converges, up to a multiplicative constant, to the L^2-norm when $s \searrow 0$.

A proof of Theorem 3 when u is in the Schwartz space of rapidly decaying smooth functions goes as follows (see also Remark 4.3 in [10]). For these functions the definition in (3) agrees, up to a multiplicative constant (depending on n and s), with the Fourier definition

$$[u]_{H^s(\mathbb{R}^n)} = c(n,s)\int_{\mathbb{R}^n} |\xi|^{2s} |\widehat{u}(\xi)|^2\, d\xi,$$

where $\widehat{u}$ denotes the Fourier transform of u, see [10]. The normalising constant $c(n,s)$ is such that

$$\lim_{s\searrow 0} c(n,s)s = \omega_{n-1},$$

see Proposition 3.4 and Corollary 4.2 in [10]. Hence, applying the Plancherel Theorem, one has

$$\begin{aligned}\lim_{s\searrow 0} s\,[u]_{H^s(\mathbb{R}^n)} &= \lim_{s\searrow 0} c(n,s)\, s \int_{\mathbb{R}^n} |\xi|^{2s} |\widehat{u}(\xi)|^2\, d\xi \\ &= \omega_{n-1}\int_{\mathbb{R}^n} |\widehat{u}(\xi)|^2\, d\xi = \omega_{n-1}\|\widehat{u}\|_{L^2(\mathbb{R}^n)} = \omega_{n-1}\|u\|_{L^2(\mathbb{R}^n)},\end{aligned}$$

which is (4).

As a particular case, one can take $u := \chi_E$ in (4), for some set $E \subseteq \Omega$ such that $\mathrm{Per}_{s_0}(E,\Omega) < +\infty$ (and so $\chi_E \in H^{s_0}(\mathbb{R}^n)$) for some $s_0 \in (0,1/2)$. Since $E \cap (\mathscr{C}E) = \varnothing$, from (1) one has that

$$\mathrm{Per}_s(E,\Omega) = \mathscr{L}(E\cap\Omega, (\mathscr{C}E)\cap\Omega) + \mathscr{L}(E\cap\Omega, (\mathscr{C}E)\cap(\mathscr{C}\Omega)) = \mathscr{L}(E, \mathscr{C}E),$$

and so

$$\begin{aligned}\lim_{s\searrow 0} 2s\,\mathrm{Per}_s(E,\Omega) &= \lim_{s\searrow 0} 2s\,\mathscr{L}(E,\mathscr{C}E)\\ &= \lim_{s\searrow 0} 2s\int_E\int_{\mathscr{C}E}\frac{dx\,dy}{|x-y|^{n+2s}}\\ &= \lim_{s\searrow 0} s\int_{\mathbb{R}^n}\int_{\mathbb{R}^n}\frac{\chi_E(x)-\chi_E(y)}{|x-y|^{n+2s}}\,dx\,dy\\ &= \lim_{s\searrow 0} s\,[\chi_E]^2_{H^s(\mathbb{R}^n)} = \omega_{n-1}\|\chi_E\|^2_{L^2(\mathbb{R}^n)} = \omega_{n-1}|E|,\end{aligned} \tag{5}$$

where $|E|$ denotes the Lebesgue measure of E.

The general case was treated in [11]. Given a set E, possibly unbounded, the authors introduced the following parameter

$$\widetilde{\alpha}(E) := \lim_{s\searrow 0}\frac{2s}{\omega_{n-1}}\int_{E\setminus B_1}\frac{dy}{|y|^{n+2s}}, \tag{6}$$

called the "weighted volume of E towards infinity", and the normalized Lebesgue measure $\mathscr{M}(E) := \omega_{n-1}|E|$. Then, the result proved in [11] is the following:

THEOREM 4. *(Theorems 2.5 and 2.7 in [11]) Suppose that* $\mathrm{Per}_{s_0}(E,\Omega) < +\infty$ *for some* $s_0 \in (0,1/2)$*, and that the limit in* (6) *exists. Then,*

$$\lim_{s\searrow 0} 2s\,\mathrm{Per}_s(E,\Omega) = (1-\widetilde{\alpha}(E))\mathscr{M}(E\cap\Omega) + \widetilde{\alpha}(E)\mathscr{M}(\Omega\setminus E). \tag{7}$$

Also, if $\mathrm{Per}_{s_0}(E,\Omega) < +\infty$ *for some* $s_0 \in (0,1/2)$ *and* $|E\cap\Omega| \neq |\Omega\setminus E|$*, then the existence of the limit in* (6) *is equivalent to the existence of the limit in* (7)*.*

Notice that $\widetilde{\alpha}(E) \in [0,1]$ and therefore the limit in (7) is a convex combination of the normalized Lebesgue measure of the sets $E\cap\Omega$ and $\Omega\setminus E$. In particular, if $E \subseteq \Omega$ then $\widetilde{\alpha}(E) = 0$ (notice that E is bounded and recall Footnote 2) and so (7) boils down to (5).

In some sense, (7) says that the s-perimeter "localizes" in Ω when $s \searrow 0$, because it takes into account only the Lebesgue measure of two sets which are contained in Ω. This is not completely true, since the parameter $\widetilde{\alpha}(E)$ in the convex combination takes into account the contribution of E coming from infinity. Hence, the nonlocal character of the s-perimeter is preserved also in the limit, by means of the parameter that interpolates the two Lebesgue measures which are set in Ω.

[2] Notice that in (6) one can take the integral over $E\setminus B_R$ for any $R>0$, instead of $E\setminus B_1$. Indeed

$$\int_{B_R\setminus B_1}\frac{dy}{|y|^{n+2s}} = \omega_{n-1}\int_1^R\frac{\rho^{n-1}\,d\rho}{\rho^{n+2s}} = \frac{\omega_{n-1}}{2s}(1-R^{-2s}),$$

and therefore

$$\lim_{s\searrow 0}\frac{2s}{\omega_{n-1}}\int_{B_R\setminus B_1}\frac{dy}{|y|^{n+2s}} = 0.$$

In Theorem 4 the assumption of the existence of the limit in (6) cannot be removed, since the limit in (6) (and hence the limit in (7)) may not exist. Indeed, in [11] the authors provide an example of set for which such limit does not exist (see also Section 1.1 in [21]). Roughly speaking, the idea is constructing a set which looks like a cone of variable opening angle: one starts with a cone of small opening in an annulus, then changes his mind and enlarges the opening of the cone in the subsequent annulus, and so on, alternating cones of small and big opening angles in the subsequent annuli (see Figure 2 where the set is grossly drawn). In this way, the parameter $\widetilde{\alpha}(E)$ "detects" the different openings and this creates an oscillation of the value of $\widetilde{\alpha}(E)$ in the different annuli. As a consequence, the limit in (6) does not exist.

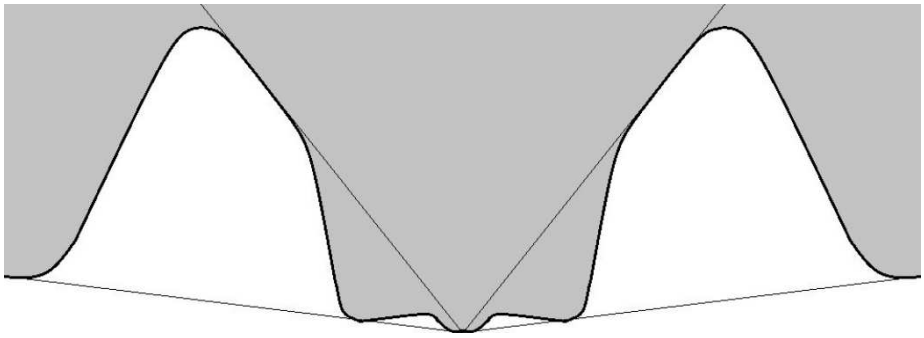

Figure 2: An example for which the limit as $s \searrow 0$ of the fractional perimeter does not exist.

In Theorem 4 it is also required that the set E has finite s_0-perimeter for some $s_0 \in (0,1/2)$. We point out that this assumption cannot be dropped in general, since there are sets that do not satisfy it (and for them the limit of the functional in (1) as $s \searrow 0$ does not make any sense), see the subsequent Section 4.

4. Example of set with infinite s-perimeter for any $s \in (0,1/2)$

In this section we give an example of sets E and Ω for which

$$\mathrm{Per}_s(E,\Omega) = +\infty \quad \text{for any } s \in (0,1/2).$$

For this, we take $n \geqslant 1$ and a real number β such that

$$0 < \beta < \frac{2s}{n-2s}. \tag{8}$$

Notice that β is well defined, since $n \geqslant 1$ and $s \in (0,1/2)$. Moreover, for any $k \geqslant 1$, we consider

$$i_k := \frac{C_\beta}{k^{\beta+1}}, \tag{9}$$

where $0 < C_\beta < 1$ is a constant depending on β, such that the following holds true

$$\sum_{k=1}^{+\infty} i_k = 1.$$

For any $k \geqslant 1$, we set

$$r_k := 1 - \sum_{j=1}^{k} i_j.$$

Thanks to (9), we have that

$$r_k = \sum_{j=k+1}^{+\infty} i_j \geqslant \frac{C_\beta}{k^\beta}, \tag{10}$$

up to relabeling C_β.

Now, for any $k \geqslant 1$, we consider the annulus A_k of thickness i_k. Notice that each A_k can be covered by the union of balls $B_{i_k/2}(x)$ of radius $i_k/2$ and centred at points lying on the sphere of radius $r_k + (i_k/2)$. Namely,

$$A_k = \bigcup_{x \in \partial B_{r_k+(i_k/2)}} B_{i_k/2}(x).$$

Since, for any $k \geqslant 1$ and $x \in \partial B_{r_k+(i_k/2)}$, the radius of the ball $B_{i_k/2}(x)$ is $i_k/2 < +\infty$, we can apply the Vitali's covering Theorem (see e.g. [12]), obtaining that, for any $k \geqslant 1$, there exists a countable subcollection of disjoint balls $B_{i_k/2}(x_j)$, $j = 1, \dots N_k$, such that

$$A_k = \bigcup_{x \in \partial B_{r_k+(i_k/2)}} B_{i_k/2}(x) \subseteq \bigcup_{j=1}^{N_k} B_{5i_k/2}(x_j). \tag{11}$$

We claim that, for any $k \geqslant 1$,

$$N_k < +\infty. \tag{12}$$

For this, notice that

$$\bigcup_{j=1}^{N_k} B_{i_k/2}(x_j) \subseteq A_k,$$

and therefore

$$c_n N_k i_k^n = N_k |B_{i_k/2}(x_j)| \leqslant |A_k|, \tag{13}$$

for a suitable positive constant c_n depending on n, where $|B_{i_k/2}(x_j)|$ and $|A_k|$ denote the Lebesgue measures of $B_{i_k/2}(x_j)$ and A_k, respectively. Since $|A_k|$ is finite, (13) implies (12).

Moreover, we claim that

$$N_k \geqslant C\left(\frac{r_k}{i_k}\right)^{n-1}, \tag{14}$$

for some constant $C>0$ (only depending on n). To show this, we use the Binomial Theorem and (11) to get

$$|B_1|\, r_k^{n-1} i_k \leqslant |B_1|\,[(r_k+i_k)^n - r_k^n] = |A_k| \leqslant \sum_{j=1}^{N_k} |B_{5i_k/2}(x_j)| = C_1 N_k\, i_k^n,$$

for some $C_1>0$ depending on the dimension, and this implies (14).

Notice that from (9), (10) and (14) we have

$$N_k \geqslant C k^{n-1}, \tag{15}$$

up to renaming the constant C.

Let us make the following observation. We consider the unit ball B_1 and a smooth non-empty set $S_1 \subset B_1$. Notice that any smooth set would do the job, we will take a smiley face for typographical convenience in Figure 3. Since the boundary of S_1 is smooth and both S_1 and $B_1 \setminus S_1$ are not empty, from Lemma 11 in [5] we obtain that

$$0 < C_* := \int_{S_1}\int_{B_1\setminus S_1} \frac{dx\,dy}{|x-y|^{n+2s}} < +\infty.$$

Hence, setting B_ρ the ball of radius ρ and S_ρ the scaled version of S_1 by a factor ρ, for any $\rho>0$, we have

$$\begin{aligned}\int_{S_\rho}\int_{B_\rho\setminus S_\rho} \frac{dx\,dy}{|x-y|^{n+2s}} &= \int_{S_1}\int_{B_1\setminus S_1} \frac{\rho^{2n} d\widetilde{x}\,d\widetilde{y}}{\rho^{n+2s}|\widetilde{x}-\widetilde{y}|^{n+2s}}\\ &= \rho^{n-2s}\int_{S_1}\int_{B_1\setminus S_1} \frac{d\widetilde{x}\,d\widetilde{y}}{|\widetilde{x}-\widetilde{y}|^{n+2s}}\\ &= C_*\,\rho^{n-2s},\end{aligned} \tag{16}$$

where we have used the change of variables $\widetilde{x}=x/\rho$ and $\widetilde{y}=y/\rho$.

Now, in each annulus A_k we have N_k disjoint balls of radius $i_k/2$, and in each of these balls we insert a smiley face S_k^j, $j=1,\dots,N_k$. We define the set E as the union of these smiley faces, that is

$$E := \bigcup_{k=1}^{+\infty}\bigcup_{j=1}^{N_k} S_k^j$$

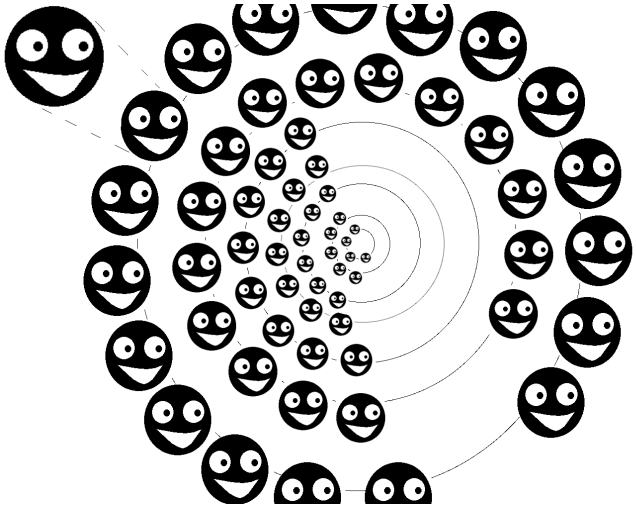

Figure 3: The set E with the smiley faces.

(as depicted in Figure 3). Notice that $E \subset B_1$, and therefore, using (16), (9), (15) and (8), we get

$$\begin{aligned}
\mathrm{Per}_s(E,B_1) &= \mathscr{L}(E,\mathscr{C}E)\\
&\geqslant \sum_{k=1}^{+\infty}\sum_{j=1}^{N_k} \mathscr{L}(S_k^j, B_{i_k/2}(x_j)\setminus S_k^j)\\
&= \sum_{k=1}^{+\infty}\sum_{j=1}^{N_k} \int_{S_k^j}\int_{B_{i_k/2}(x_j)\setminus S_k^j} \frac{dx\,dy}{|x-y|^{n+2s}}\\
&= C_2 \sum_{k=1}^{+\infty} N_k i_k^{n-2s}\\
&\geqslant C_3 \sum_{k=1}^{+\infty} \frac{k^{n-1}}{k^{(1+\beta)(n-2s)}}\\
&= C_3 \sum_{k=1}^{+\infty} \frac{1}{k^{\beta(n-2s)-2s+1}}\\
&= +\infty,
\end{aligned}$$

for suitable positive constants C_2 and C_3. This gives the desired result.

We mention that in [11] an example in one dimension of a set with infinite s-perimeter for any $s \in (0,1/2)$ was constructed (see Subsection 3.10 there).

5. Regularity of s-minimal surfaces

One of the main problems considered in [4] is the one of the regularity of the s-minimizers:

THEOREM 5. *(Theorem 2.4 in [4]) If E is an s-minimizer in B_1, then $\partial E \cap B_{1/2}$ is a $C^{1,\alpha}$-hypersurface around each of its points, possibly except a closed set Σ of finite $(n-2)$-Hausdorff dimension.*

We observe that the boundary of E is supposed to have dimension $n-1$, and so the fact that Σ can be at most an $(n-2)$-dimensional object implies that it is negligible inside ∂E. Hence, Theorem 5 says that if E is an s-minimizer then its boundary is smooth at "most of its points".

Anyway, as far as we know, there are no examples of s-minimizers with a non-empty singular set. One may be tempted to say that, for instance, the classical cone in the plane

$$\mathscr{C} := \{(x,y) \in \mathbb{R}^2 : xy > 0\}$$

is an s-minimizer, since it satisfies the Euler-Lagrange equation (2). But in fact, there is an original idea of L. Caffarelli (explained in Section 1.2 of [21]) which shows that the cone $\mathscr{C}$ is not s-minimal. Notice that this says that the s-minimality implies, but is not equivalent to, the Euler-Lagrange equation (2).

Even though the regularity obtained in Theorem 5 is only $C^{1,\alpha}$, in [3] it was proved by non trivial bootstrap arguments that one can improve it towards C^∞.

Now, concerning the regularity of minimizers of the functional in (1), at the moment, there are only other two results in two different directions: the first result says that one can recover the classical minimal surface theory in any dimensions but only when s is sufficiently close to $1/2$, while the second result is valid for any s in the range $(0,1/2)$ but only in the plane.

In particular, starting from Theorem 2, in [6] the authors proved the following:

THEOREM 6. *([6]) For any $n \in \mathbb{N}$ there exists $\varepsilon_n \in (0,1/2]$ such that if $s \in ((1/2)-\varepsilon_n, 1/2)$ then s-minimal surfaces are "as regular as the classical minimal surfaces", that is*

- *if $n \leqslant 7$, then any s-minimal surface is locally C^∞,*
- *if $n = 8$, then any s-minimal surface is locally C^∞ except, at most, at countably many isolated points,*
- *if $n > 8$, then any s-minimal set is locally C^∞ outside a closed set $\Sigma \subset \partial E$ with finite $(n-8)$-Hausdorff dimension.*

Although there are no examples of singular sets in any dimension and for any $s \in (0,1/2)$, as far as we know, Theorem 6 seems to be the only improvement of Theorem 5 about the regularity of s-minimal surfaces valid in any dimension (even if only for s

close to $1/2$). On the other hand, the proof of Theorem 6 is based on a compactness argument, and therefore the value of the quantity ε_n is not explicit (we only know that it is a universal constant that depends only on the dimension).

As we already said, the proof of Theorem 6 relies on the asymptotic of the functional in (1) as $s \nearrow 1/2$. Although the proof is very technical and delicate, morally, the idea is that, since the s-perimeter converges to the classical perimeter as $s \nearrow 1/2$, the s-minimal surfaces inherit the regularity of the classical minimal surfaces when s is sufficiently close to 1/2. For this, some care is needed in order to obtain uniform regularity estimates in s, which can pass to the limit.

Concerning the second result that we mentioned about the regularity of s-minimal surfaces, it is contained in [19] and states the following:

THEOREM 7. *([19]) Let $n = 2$. Suppose that $R > r > 0$ and that E is an s-minimal set in B_R, then $(\partial E) \cap B_r$ is a C^∞-curve.*

Also, if E is an s-minimal set in B_ρ for every $\rho > 0$, then ∂E is a straight line.

Theorem 7 says that in the plane any s-minimal surface is smooth, and this is exactly what happens in the classical case. In particular, as a byproduct, one obtains an improvement of Theorem 5: the singular set Σ has finite $(n-3)$-Hausdorff dimension, instead of $n-2$. Still, we do not know if this is optimal, see Theorem 6.

A consequence of the above result is also that in the plane global s-minimal sets (i.e. s-minimal sets in any ball) are straight lines.

Now, it seems very difficult to obtain further information from the asymptotic as $s \searrow 0$, since for s close to 0 the minimizers of the s-perimeter seem to be somehow related to the minimizers of the Lebesgue measure (see Theorem 4), which can have very wild boundary.

On the other hand, in [7] the authors proved that when s is close to 0 all symmetric cones are unstable if the dimension $n \leqslant 6$ and stable if $n = 7$. This tells us that, when $n \leqslant 6$, a symmetric cone is not an s-minimizer, but, still, we are not able to conclude that the singular set Σ in Theorem 5 is empty, since the example of a non-smooth s-minimizer can be a non symmetric cone.

We also mention a very recent paper [8], where the authors constructed an example of surface that satisfies the equation in (2) for s sufficiently close to $1/2$, that is the so-called "nonlocal catenoid" (see Theorem 1 there).

6. The Bernstein problem

The regularity theory for minimal surfaces is related to the Bernstein problem: if the graph of a function on $\mathbb{R}^n$ is a minimal surface in $\mathbb{R}^{n+1}$, is it true that the function is affine?

In the classical case, the result is true in dimension $n \leqslant 8$ and false when $n \geqslant 9$, see e.g. [13].

In the nonlocal setting, there is only a very recent paper [14], where the authors

were able to extend a result of De Giorgi for minimal surfaces (see [9]), showing that Bernstein's Theorem holds true in dimension $n+1$ if there are no singular s-minimal cones in $\mathbb{R}^n$.

For this, we recall that a s-minimal surface E is a "s-minimal graph" if it can be written as a global graph in some direction. Namely, up to rotation, there exists a function $u : \mathbb{R}^n \to \mathbb{R}$ such that

$$E := \{(x,t) \in \mathbb{R}^n \times \mathbb{R} : t < u(x)\}.$$

Then, we have the following:

THEOREM 8. *(Theorem 1.2 in [14]) Let $E := \{(x,t) \in \mathbb{R}^n \times \mathbb{R} : t < u(x)\}$ be a s-minimal graph, and suppose that there are no singular s-minimal cones in $\mathbb{R}^n$. Then u is an affine function.*

This means that if the only s-minimal cone in $\mathbb{R}^n$ is the half-space and E is a s-minimal graph, then E is a half-space.

If $n = 1$ in Theorem 8 we obtain a particular case of Theorem 7.

If $n = 2$, since there are not s-minimal cones in the plane (see Theorem 7), as a byproduct of the general result in Theorem 8 one obtains that s-minimal graphs have C^∞-boundary in $\mathbb{R}^3$. Unfortunately, this is not enough to further improve Theorem 5, that is we cannot say that the singular set Σ has $(n-4)$-Hausdorff dimension, because of the assumption that E is a s-minimal graph.

On the other hand, combining Theorems 6 and 8 we have that, when s is sufficiently close tp $1/2$, Bernstein Theorem holds true up to dimension 8.

References

[1] N. ABATANGELO, E. VALDINOCI, *A notion of nonlocal curvature*, Numer. Funct. Anal. Optim., 35 (2014), no. 7-9, 793–815.

[2] L. AMBROSIO, G. DE PHILIPPIS, L. MARTINAZZI, *Γ-convergence of nonlocal perimeter functionals*, Manuscripta Math. **134** (2011), 377–403.

[3] B. BARRIOS, A. FIGALLI, E. VALDINOCI, *Bootstrap regularity for integro-differential operators and its application to nonlocal minimal surfaces*, Ann. Sc. Norm. Super. Pisa Cl. Sci. (5) 13 (2014), no. 3, 609–639.

[4] L. CAFFARELLI, J.-M. ROQUEJOFFRE, O. SAVIN, *Nonlocal minimal surfaces*, Comm. Pure Appl. Math. **63** (2010), 1111–1144.

[5] L. CAFFARELLI, E. VALDINOCI, *Uniform estimates and limiting arguments for nonlocal minimal surfaces*, Calc. Var. Partial Differential Equations **41** (2011), no. 1–2, 203–240.

[6] L. CAFFARELLI, E. VALDINOCI, *Regularity properties of nonlocal minimal surfaces via limiting arguments*, Adv. Math. **248** (2013), 843–871.

[7] J. DÁVILA, M. DEL PINO, J. WEI, *Nonlocal minimal Lawson cones*, Preprint (2013), `http://arxiv.org/abs/1302.0276`

[8] J. DÁVILA, M. DEL PINO, J. WEI, *Nonlocal s-minimal surfaces and Lawson cones*, Preprint (2014), `http://arxiv.org/pdf/1402.4173.pdf`

[9] E. DE GIORGI, *Una estensione del teorema di Bernstein*, Ann. Scuola Norm. Sup. Pisa (3) **19** (1965), 79–85.

[10] E. DI NEZZA, G. PALATUCCI, E. VALDINOCI, *Hitchhiker's guide to the fractional Sobolev spaces*, Bull. Sci. math. **136** (2012), no. 5, 521–573.

[11] S. DIPIERRO, A. FIGALLI, G. PALATUCCI, E. VALDINOCI, *Asymptotics of the s-perimeter as* $s \searrow 0$, Discrete Contin. Dyn. Syst. **33** (2013), no. 7, 2777–2790.

[12] L. C. EVANS, R. F. GARIEPY, *Measure Theory and Fine Properties of Functions*, CRC press (1992), pp. 27.

[13] A. FARINA, E. VALDINOCI, *The state of the art for a conjecture of De Giorgi and related problems*, Recent progress on reaction-diffusion systems and viscosity solutions, World Sci. Publ., Hackensack, NJ (2009).

[14] A. FIGALLI, E. VALDINOCI, *Regularity and Bernstein-type results for nonlocal minimal surfaces*, J. Reine Angew. Math., DOI 10.1515/crelle-2015-0006.

[15] V. MAZ'YA, T. SHAPOSHNIKOVA, *On the Bourgain, Brezis, and Mironescu theorem concerning limiting embeddings of fractional Sobolev spaces*, J. Funct. Anal. **195** (2002), 230–238.

[16] G. PALATUCCI, O. SAVIN, E. VALDINOCI, *Local and global minimizers for a variational energy involving a fractional norm*, Ann. Mat. Pura Appl. (4) **192** (2013), no. 4, 673–718.

[17] O. SAVIN, E. VALDINOCI, *Density estimates for a variational model driven by the Gagliardo norm*, J. Math. Pures Appl. (9) **101** (2014), no. 1, 1–26.

[18] O. SAVIN, E. VALDINOCI, *Γ-convergence for nonlocal phase transitions*, Ann. Inst. H. Poincaré Anal. Non Linéaire **29** (2012), 479–500.

[19] O. SAVIN, E. VALDINOCI, *Regularity of nonlocal minimal cones in dimension 2*, Calc. Var. Partial Differential Equations **48** (2013), no. 1–2, 33–39.

[20] L. SILVESTRE, *Regularity of the obstacle problem for a fractional power of the Laplace operator*, Ph.D. Thesis, University of Texas at Austin (2005).

[21] E. VALDINOCI, *A fractional framework for perimeters and phase transitions*, Milan J. Math. **81** (2013), no. 1, 1–23.

[22] A. VISINTIN, *Nonconvex functionals related to multiphase systems*, SIAM J. Math. Anal. **21** (1990), 1281–1304.

[23] A. VISINTIN, *Generalized coarea formula and fractal sets*, Japan J. Industrial Appl. Math. **8** (1991), 175–201.

AMS Subject Classification: 28A75, 49Q05, 49Q20, 60G22

Serena DIPIERRO,
Maxwell Institute for Mathematical Science and School of Mathematics
University of Edinburgh, James Clerk Maxwell Building, Peter Guthrie Tait Road
Edinburgh EH9 3FD, UNITED KINGDOM
e-mail: serena.dipierro@ed.ac.uk

Lavoro pervenuto in redazione il 29.01.2015.

Rend. Sem. Mat. Univ. Politec. Torino
Vol. 72, 1–2 (2014), 17 – 36

D. Flynn[1]

A SURVEY OF HYSTERESIS MODELS OF MAMMALIAN LUNGS

Abstract. In this paper, a survey of mathematical models accounting for the pressure-volume relationship with and without hysteresis in mammalian lungs is given. It is shown that a model with a Preisach operator with no additional parameters, based on Venegas' non-hysteretic model, could capture most of the behaviour of observed data. However, the model does not capture the full sigmoidal character of the inflation loop and needs to be further extended.

1. Introduction.

The mammalian lung is a complex organ necessary for respiration. It consists of an inverted tree-like structure shown in Figure 1, which starts at the wind-pipe, branches into two bronchial tubes, which in turn branch into thinner tubes called bronchioles. These bronchioles finally terminate at the alveoli - the tiny air sacs which perform gas exchange with the blood.

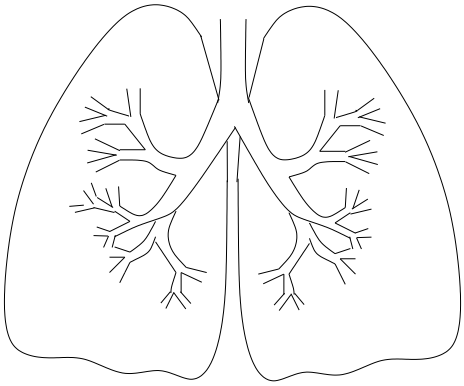

Figure 1: Tree-like structure of the mammalian lungs.

Knowledge of the static mechanical properties of the lung is the basis for understanding the distribution of ventilation, the work of breathing and other parameters of pulmonary function [30]. The static mechanical properties are reflected in the pressure-volume relationship, which is represented by a sigmoidal shaped curve as shown in Figure 2, where the input is the pressure and the output is the volume. This relationship becomes more complex when the pressure is allowed to change direction, in this

[1]CET, ITAM, Academy of Sciences of the Czech Republic

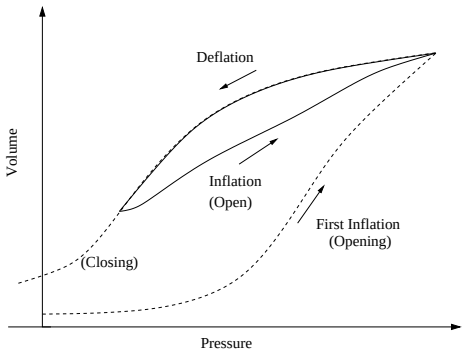

Figure 2: Hysteresis in the pressure-volume relationship of the lungs. Adapted from [10].

case it exhibits hysteresis also shown in Figure 2. In fact it has been found that the qualitative behaviour of Pressure-Volume (P-V) characteristic loops does not vary a whole lot between different species[4].

According to [28], the first measurement of the static pressure-volume relationship of human lungs obtained post mortem, was made by [20] in 1849. However, these measurements were made during inflation only [27]. Measurements for both inflation and deflation of mammalian lungs were first obtained by [11] in 1913, and these measurements exhibited static hysteresis [27].

Early models of the pressure-volume relationship in lungs initially focused on either the inhalation or exhalation limb only [30]. When modelling of hysteresis was initially tackled, the focus was on the rate-dependent aspect. These models were similar to electrical circuits [32], where resistance, impedance, inertance and frequency determined the shape of the P-V loops.

In 1970, Hildebrandt [18] was probably the first to develop a model of rate-independent hysteresis. He found that his linear viscoelastic model accounted for two-thirds of the hysteresis in his data and postulated that the remainder came from a rate-independent plastic strain. He went on to develop a model based on Prandtl bodies, which displayed the qualitative behaviour observed in his data.

In this paper we will briefly outline the medical motivations and background of the lungs and the importance of the knowledge of the P-V relationship. Following this, the mechanisms which are responsible for hysteresis in this relationship will be discussed. In section 5 a brief review of the mathematical modelling efforts will be given. In section 7, we will present mathematical models which we developed and the subsequent results from applying these models to experimental data will also be presented. Finally, conclusions will be drawn in section 8.

2. Medical motivations: mechanical ventilator settings and lung damage

According to [3], P-V curves are used for protective ventilation strategies for patients with lung disease. If the ventilator is set incorrectly, there is a possibility of damage to the patient's lungs, especially those with an underlying condition [2]. Knowledge of these curves when the lungs are in a diseased state such as ARDS (Acute Respiratory Distress Syndrome) [40] is also beneficial. One property that is used quite often is *compliance*, which is a measure of ease of expansion of the lungs. Compliance C is defined as the slope of the P-V relationship i.e. $C = \frac{dV}{dp}$, usually taken at its maximum value [13]. It can change due ageing, inflammation, swelling and denaturalisation of surfactant (which causes increased surface tension) [9].

It has been broadly agreed that a minimum setting should be chosen so as to prevent the alveoli from collapsing, a state known as atelectasis [17, 28, 29]. This minimum setting is known as Positive End-Expiratory Pressure (PEEP) and is set as low as possible that results in acceptable oxygenation [2, 31]. There are various strategies for setting ventilators as outlined by [22] for setting PEEP in patients with ALI (Acute Lung Injury). They introduce a new technique based on the hysteresis of the P-V loops, utilising the vertical distance between the inflation and deflation limbs. It was found that their technique gave the same oxygenation but with lower airway pressures and less over-inflation than other methods. In addition, it was demonstrated during clinical trials by [1, 2], that a ventilator strategy guided by P-V curves resulted in reduced trauma and improved survival compared with conventional strategy without P-V curve guidance [3].

3. Mechanisms of hysteresis

It is understood that hysteresis in the lungs arises from the recruitment and the derecruitment of alveoli and from the surface tension of the surfactant [8, 19] on the interior of alveoli. We will look at these mechanisms in this section.

3.1. Recruitment and derecruitment of alveoli

According to [14], air spaces inflate non-uniformly from the atelectatic (collapsed) state, they inflate in patches and suddenly pop-open, however, they close uniformly during deflation, without collapsing. However, if the surfactant is depleted or chemically altered, the individual alveoli will become unstable during both inflation and deflation.

Suki et al. [35] demonstrated that recruitment of alveoli is the dominant mechanism during *first* inflation. Subsequent inflations are primarily influenced by surface film and connected tissue of the parenchyma. In Cheng et al. [10], derecruitment occurs when the excised lung is deflated below a critical pressure (in rats it was 4 ± 1cm H_2O), at which lung units are sequentially closed. They also noted that additional energy is required to overcome these closed units on inflation and this is reflected in an increase of hysteresis area.

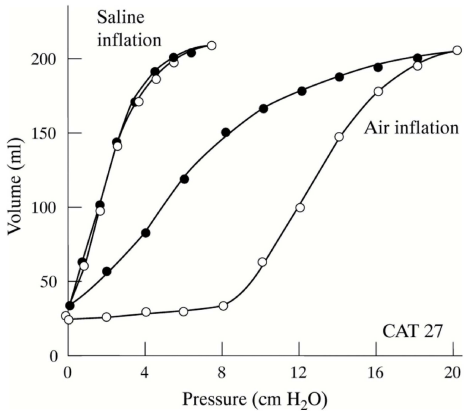

Figure 3: Pressure-volume curves of the respiratory system. The narrow loop on the left was obtained from excised lungs with warm saline solution instead of air. The wider loop on right is formed from inflation (open circles) and deflation (closed circles) of excised lungs. Taken from [21].

In fact the main aim for mechanical ventilators is to keep alveoli from closing, and this is achieved by setting a positive end-expiratory pressure (PEEP) above this critical derecruiting threshold.

The inflation limb of the hysteresis loops generated during first inflation exhibits a plateau as can be seen in Figure 3 (open circles between 0 and 8 cm H_2O), where almost no recruitment occurs. Thereafter, crossing a critical pressure a sudden avalanche [35, 36] of recruitment occurs over a small pressure range. This contrasts significantly with subsequent inflation curves, which contain no such plateau.

3.2. Surface tension of the surfactant

The interior surfaces of alveoli are coated in a thin liquid layer known as the surfactant. It has many properties which facilitate the proper functioning of the lungs and is more than a saline solution, it consists of a liquid layer with a mixture of lipids (90%) and proteins (10%) [8].

Laplace's law, states that pressure p is proportional to the tension T and inversely proportional to the radius R, i.e. $p \propto \frac{T}{R}$, predicts that two unequal alveoli should not remain in equilibrium as shown in Figure 4. The surfactant prevents this collapse [5, 8, 16], as it has the property that its surface tension varies as the area of the surface layer changes, so that T and R in Laplace's equation vary proportionately and p remains equal in all alveoli [8].

According to [15], it was Von Neergaard [38] who in 1929 discovered that the main determinant of hysteresis is air-liquid surface force in alveoli.

In [8], they describe the classic experiment where excised lungs are degassed and P-V curves are measured during a stepwise inflation and deflation manoeuvre,

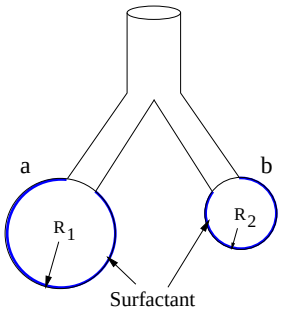

Figure 4: Balancing of alveoli with surfactant.

thus producing the hysteresis loop, shown in Figure 3. This manoeuvre is repeated with warm (37°C) saline solution instead of air, this time it is producing almost no hysteresis, as shown in Figure 3. They make the point, that surface tension disappears as a consequence of the absence of the air-liquid interface.

According to [24], many studies reach the same conclusion, that the air-liquid interface at the alveoli plays an important role in lung mechanics. This is reiterated by [8]. In conclusion, both recruitment and surfactant tension contribute to hysteresis, but dominate at different pressure ranges and pressure histories.

4. Measurements of P-V hysteresis

According to [15], the equations of motion describing the pressure changes of the respiratory system, assuming isotropic expansion, can be written as:

$$p_{AO} = \frac{V}{C} + \dot{V}R + \ddot{V}I - p_{mus}, \tag{1}$$

where the dots denote time-derivatives, p_{AO} is the airway pressure, p_{mus} is the respiratory muscle pressure, $\dot{V}$ is the gas flow, R is the airway resistance and I is the impedance. If the subject is sedated or paralysed then p_{mus} can be eliminated, otherwise the P-V loops may include effects from the respiratory muscle [15]. The term C is the compliance and is one of the main goals in measuring P-V curves. If rate-independence is assumed, the resistance and impedance terms from equation (1) vanish, leaving only the compliance term to be assessed, in fact these *static* P-V curves are often called *compliance curves* [15].

4.1. Static, quasi-static and dynamic hysteresis

In the lung physiology literature [15] the term *static hysteresis* is used instead of *rate-independent hysteresis*. The term *static* denotes that the lung is neither inhaling nor exhaling when measurements are taken. However, it is not advisable to stop the lungs

of a live subject from breathing for too long [15], therefore *quasi-static* measurements are taken.

There are a number of possibilities for measuring quasi-static P-V curves e.g. they can be measured by a stepwise approach, i.e. breathing is paused, and after a relaxation period of about five seconds, measurements are made [15, 37] and the same process is continued. Another approach is to take measurements at a very slow flow rate, at less than 9 L/min, as this minimises the effects of the resistive elements of the respiratory system [15].

The behaviour of P-V curves of the continuously working lung is also of interest to clinicians [15]. In this case *rate-dependent* hysteresis is also observed and is referred to as *dynamic hysteresis* in the literature [15]. However, these curves depend on the frequency, and vary qualitatively from those from the static/quasi-static loops.

5. Mathematical models

Some of the earlier work focused on modelling the P-V curve either during inflation or deflation limb, i.e. without accounting for hysteresis. However, it is possible fit these models to either limb, but it requires a new set of parameters for each inflation or deflation curve. Subsequently hysteresis models were proposed and were based on the idea of either sums or integrals of elements, which had a distribution of threshold values to denote their opening or closure.

5.1. Models without hysteresis

Salazar and Knowles exponential model

One of the earliest expressions used to model the P-V curve during inflation or deflation, was suggested by Salazar and Knowles [33] in 1964. Starting with the assumption that the compliance, $\frac{dV}{dp}$, is proportional to the difference between maximum volume V_M and actual volume V, i.e. $\frac{dV}{dp} = K(V_M - V)$, where K is a constant, and by introducing the half inflation pressure h, such that $e^{-Kh} = \frac{1}{2}$, they came up with the expression

$$V = V_M(1 - e^{-\frac{p\ln 2}{h}}). \tag{2}$$

However, this model did not go far enough to capture the full sigmoidal shape and neither did several subsequent models, which are documented by [30].

Murphy and Engel's sigmoidal model

It was Murphy and Engel [30] who were the first to model the P-V relationship below functional residual capacity (FRC), thus capturing the full sigmoidal shape. Note, however, that the independent variable in their model was volume V instead of p. It

consists of five parameters, as follows:

$$p = \frac{k_1}{V_M - V} + \frac{k_2}{V_m - V} + k_3, \tag{3}$$

where V_M is the upper asymptote, V_m is the lower asymptote and k_1, k_2 are shape parameters and the constant k_3 shifts the curve to the left or to the right [30].

Venegas' four parameter model

An improved model, which was also a sigmoid, was developed by Venegas et al. [39]. Their expression gave an improved fit to P-V data and had one less parameter than [30]. The expression is given by:

$$V = a + \frac{b}{\left(1 + e^{(p-c)/d}\right)}, \tag{4}$$

where V and p are again volume and pressure respectively. Parameter a is the lower asymptote volume, b is the vital capacity or the total change in volume between the lower and upper asymptotes. The parameter c is the pressure at which the inflection point of the sigmoidal curve occurs and which also corresponds to the pressure at the point of highest compliance. Finally parameter d is proportional to the pressure range within which most of the volume changes take place. In addition, [39] showed that the derivative of their expression was a closed form approximation to the normal distribution. They argued that as such the sigmoidal shape of the inflation limb of the P-V curve in ARDS could be reflecting the progressive recruitment of alveolar units with a distribution that follows the normal distribution.

5.2. Models with hysteresis

There have been numerous approaches to the treatment of hysteresis, both for the rate-independent and dependent cases. We will outline these below.

Hildebrandt's Prandtl-bodies model

In the 1970's, Hildebrandt [18] initially developed a linear viscoelastic model to interpret P-V data from cat lungs. He applied pressure in the form of a sinusoid with varying amplitude and varying frequency, in a stepwise fashion to isolated cat lungs. His model was able to account for the stress-relaxation which occurred after each step. It was found that his model was in quantitative agreement with the frequency-dependent compliance of the loops, however, it only accounted for two-thirds of the observed hysteresis. This remaining hysteresis was postulated to be due to the rate-independent plastic strain. He was also able to show that a model based on Prandtl bodies with a distribution of yield points exhibited some of the essential characteristics required to described the dependence of both loop area and amplitude of deformation.

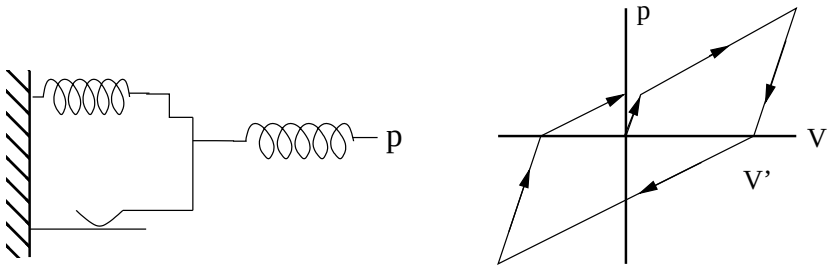

Figure 5: Prandtl body which Hildebrandt used as the smallest element in his static hysteresis model [18].

Starting with the Prandtl body in Figure 5, which is perfectly elastic up to its yield point, after which it undergoes retarded flow. He formulated a model consisting of an arbitrary large number of these units in series, and with a distribution of thresholds representing the strengths of intermolecular linkages. Each unit had a compliance c and the compliance of the system was C. When the pressure $p > p_{T_i}$, i.e. crossed the threshold of the *i-th* unit, stretching of that unit would commence.

The total number of units N would depend on the p. He chose the distribution of thresholds for ease of computation, such that

$$N = \alpha p^{\beta}, \tag{5}$$

where $\alpha > 0, \beta > 0$ were constants. The compliance of the system was then given by:

$$\frac{dV}{dp} = C + cN. \tag{6}$$

From equations (5) and (6), he obtained:

$$V = Cp + rp^{\beta+1}, \tag{7}$$

where $r = \alpha c/(\beta+1)$. This is plotted as curve 1 in Figure 6. To plot curve 2, he translated the coordinate system to point L in Figure 6 and rotated the axis by 180°. To change direction, the force had to be changed by $2p_{T_i}$ and had to be applied, with this force p_1, N_1 elements were moved to the left, where

$$N_1 = \alpha \left(\frac{p_1}{2}\right)^{\beta}, \tag{8}$$

$$\frac{dV_1}{dp_1} = C + cN_1. \tag{9}$$

Similarly, these equations are combined to form:

$$V_1 = Cp + \frac{rp_1^{\beta+1}}{2^{\beta}}, \tag{10}$$

and is plotted as curve 2 in Figure 6. This procedure is repeated to produce further evolution of the system.

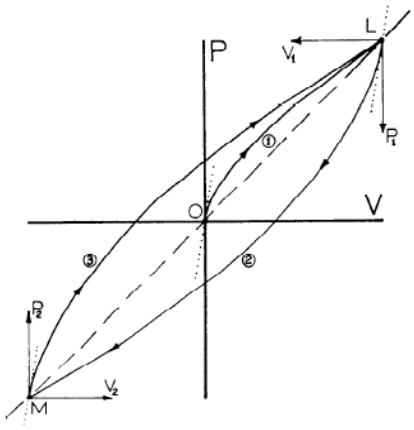

Figure 6: Hildebrandt's [18] plot of the mechanical behaviour of a large number of Prandtl bodies in series.

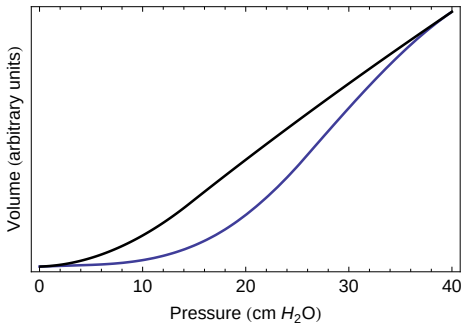

Figure 7: Hickling model: graph of volume vs. pressure, where pressure varied from 0 to 40 cm H_2O for inflation, and back to zero for deflation, completing a full loop.

Hickling's discrete element model

In [17], Hickling models the lungs as a combination of discrete elements, each of which represents an alveolus. These elements are grouped into compartments representing horizontal slices of the lungs, with an increasing gravitational superimposed pressure starting at 0 cm H_2O at the upper compartment and finishing at 15 cm H_2O at the lowermost compartment.

Each element has an associated threshold opening pressure (TOP) or a range of TOPs to simulate alveolar or small airway openings after collapse. While the model was presented as a BASIC programming in [17], it shall be expressed here in a more

concise form to aid with the description:

$$V_{\text{inf}_i} = \sum_{j=1}^{J}\sum_{k=1}^{K}\gamma(p_i - sp_j)\begin{cases}1, & p_i > sp_j + op_k \vee (p_{max} > sp_j + op_k \wedge p_{min} > sp_j),\\ 0, & \text{otherwise},\end{cases}$$

$$V_{\text{def}_i} = \sum_{j=1}^{J}\sum_{k=1}^{K}\gamma(p_i - sp_j)\begin{cases}1, & p_i > sp_j + op_k \vee (p_{max} > sp_i + op_k \wedge p_i > sp_j),\\ 0, & \text{otherwise},\end{cases}$$

where:

$$\begin{aligned} p &= p_{min}, p_{min}+1, \ldots, p_{max},\\ sp &= -0.5, 0, \ldots, 14.5,\\ op &= op_{min}, op_{min}+1, \ldots, op_{max},\\ \gamma &= \frac{K \times V_{unit}}{1 + op_{max} - op_{min}}. \end{aligned}$$

The constant γ is introduced here to factor out common values. The number of units, K is given as 9000 by [17] and their individual volumes are $V_{unit} = 0.0002$. Opening pressures are given by op and range from op_{min} to op_{max}. Each lung compartment has a superimposed pressure sp, ranging from minimum to maximum as shown above, and with J compartments.

The pressure was varied from the lowest ventilator setting $p_{min} =$ PEEP to the maximum value of $p_{max} =$ PIP (Peek Inspiratory Pressure). Graphs of inflation and deflation can be plotted as shown in Figure 7 from (p_i, V_{inf_i}) and (p_i, V_{def_i}) with $i = 1, 2, \ldots, N$, where N is the size of the vector p.

Bates & Irvin's discrete rate-dependent model

In [6], Bates and Irvin developed a rate-dependent recruitment/derecruitment model based on an alveolus connected to a collapsible airway. If the airway remains open, the alveolar compartment will expand and contract as described by Salazer and Knowles' [33] expression:

$$V = A - Be^{-Kp}, \tag{11}$$

where A, B and K are constants and V is the alveolar compartment volume. If the airway closes, V will remain fixed, i.e. it retains the value it had at the closing pressure until the airway opens, where it will assume the value $V(p)$ from (11). The opening and closing of the airway is governed by $x(t)$ which is given by the following ODE :

$$\frac{dx}{dt} = (p - p_c)\begin{cases}s_{o,} & p > p_c\\ s_{c,} & p < p_c\end{cases},$$

where p_c is a critical pressure which is used alongside x, to determine if the airway is open $(x = 1)$ or closed $(x = 0)$. Note that x is constrained between these values:

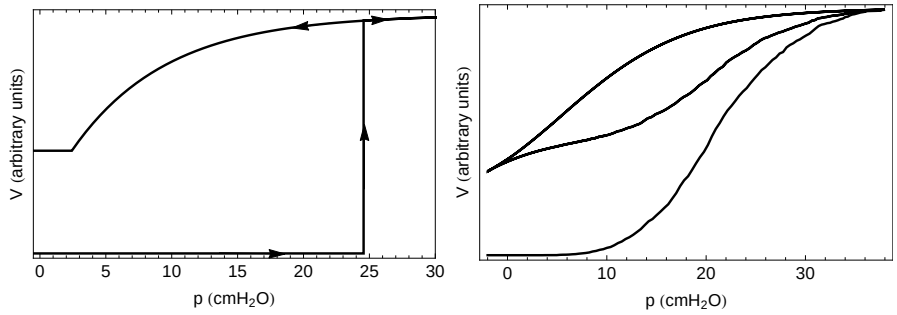

Figure 8: On the left: plot of Bates and Irvin's [6] single aleveolus-airway element. On the right: A plot of the parallel summation of alveolus airway elements, where each element has its own value of p_c, s_o and s_c.

$0 \leqslant x \leqslant 1$. The constants s_o and s_c control the rates at which x approaches opening or closing respectively. A plot of the P-V relationship it generates is shown on the left hand side of Figure 8.

To model the whole lung, they scale the model up by taking a parallel sum of an arbitrary number of these airway-alveolar units, and each unit has its own values of s_o, s_c and p_c, chosen randomly. The probability distribution chosen for p_c was the normal distribution, and s_o, s_c were given a hyperbolic distribution.

6. Preisach model

In the following the Preisach operator will be introduced and some of its properties will be illustrated.

6.1. The hysteron

One of the simplest hysteresis elements, or *hysteron*, is the non-ideal relay. It is characterised by its threshold values $\alpha < \beta$ and internal memory state $\eta(t)$. Its output $y(t)$ can take one of two values 0 or 1: at any moment the relay is either 'switched off' or 'switched on'. The dynamics of the relay are described by the picture in Figure 9.

The variable output $y(t)$

$$y(t) = R_{\alpha,\beta}[t_0, \eta_0]x(t), \qquad t \geqslant t_0, \tag{12}$$

depends on the variable input $x(t)$ $(t \geqslant t_0)$ and on the initial state η_0. Here the input is an arbitrary continuous scalar function; η_0 is either 0 or 1. The scalar function $y(t)$ has at most a finite number of jumps on any finite interval $t_0 \leqslant t \leqslant t_1$. The output behaves rather 'lazily': it prefers to be unchanged, as long as the phase pair $(x(t), y(t))$ belongs to the union of the bold lines in the picture above. The values of function (12) at a moment t are defined by the following explicit formula:

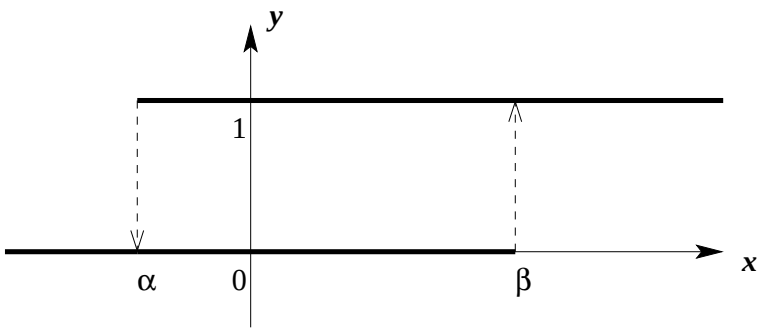

Figure 9: The non-ideal relay.

$$y(t) = R_{\alpha,\beta}[t_0,\eta_0]x(t) = \begin{cases} \eta_0, & \text{if } \alpha < x(\tau) < \beta \text{ for all } \tau \in [t_0,t]; \\ 1, & \text{if there exists } t_1 \in [t_0,t] \text{ such that} \\ & x(t_1) \geqslant \beta,\ x(\tau) > \alpha \text{ for all } \tau \in [t_1,t]; \\ 0, & \text{if there exists } t_1 \in [t_0,t] \text{ such that} \\ & x(t_1) \leqslant \alpha,\ x(\tau) < \beta \text{ for all } \tau \in [t_1,t]. \end{cases}$$

The equalities $y(t) = 1$ for $x(t) \geqslant \beta$ and $y(t) = 0$ for $x(t) \leqslant \alpha$ always hold for $t \geqslant t_0$.

This type of hysteron is one of the most frequently used in hysteresis models as it is the basis of the Preisach model.

6.2. Preisach operators

The main assumption made in the Preisach Model is that the system can be thought of as a parallel summation of a continuum of weighted non-ideal relays $R_{\alpha\beta}$, where the weighting of each relay is $\mu(\alpha,\beta)$. Such a summation can be uniquely represented as a collection of non-ideal relays as points on the two-dimensional half-plane $\Pi = \{(\alpha,\beta) : \beta > \alpha\}$ (see [23]), which is also known as the Preisach plane which is typically shown as in Figure 10. Here the colored area $S = S(t)$ is the set of the threshold values (α,β) for which the corresponding relays $R_{\alpha\beta}$ are in the "on" state at a given moment t. $L(t)$ (the so called staircase) is the interface between the relays, $R_{\alpha\beta}$, which are in the "on" or "off" states. This interface, $L(t)$, evolves according to the rules in section 6.3. The output of the Preisach Model is then represented by the following formula:

$$y(t) = \iint\limits_{\alpha<\beta} \rho(\alpha,\beta) R_{\alpha,\beta}[t_0,\eta_0(\alpha,\beta)]x(t)\, d\alpha d\beta = \iint\limits_{S(t)} \rho(\alpha,\beta)\, d\alpha d\beta. \tag{13}$$

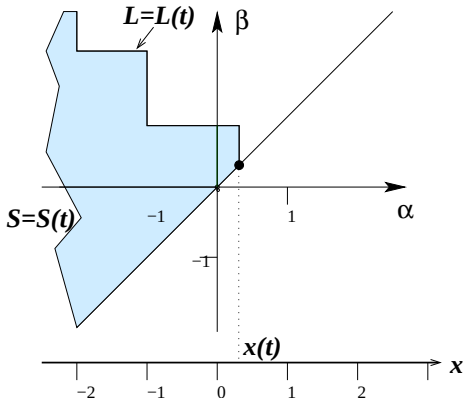

Figure 10: Typical state of a Preisach Plane.

Here $\rho(\alpha,\beta)$ is an integrable positive function in Π. This function is also called *the Preisach density*. We use the following notation to denote the Preisach operator

$$y(t) = (Px)(t).$$

As we see from (13), the output y depends on both the input and the initial values $\eta_0(\alpha,\beta)$ of all relays. Therefore, we sometimes use the more explicit notation

$$y(t) = (P[\eta_0]x)(t).$$

6.3. Geometrical description of the evolution rules

The evolution of the varying "on/off" states admits a simple geometrical interpretation, see Figures 11a and 11b. Here the input $x(t)$, moves along the horizontal scroll-bar, and controls the point on the diagonal $\alpha = \beta$ above itself. When moving toward the upper right corner, this point on the diagonal drags the *horizontal line*, and colors the domain below this line and above the diagonal. For instance, if, in Figure 11a, x increases from the value u to the value v, the colored area is increased by the yellow shaded triangle. When moving towards the bottom left corner in Figure 11b, the diagonal point drags the *vertical line*, and colors yellow everything to the right of this line and above the diagonal. The output $y(t)$ is the area of the blue domain with respect to the measure ρ.

7. Modelling the P-V relationship with the Preisach operator

PROPOSITION 1. *The integral of the Preisach density over any vertical line, $L(h)$ at some point p must equal the derivative $f'(p)$, where $V(p)$ is given by equation*

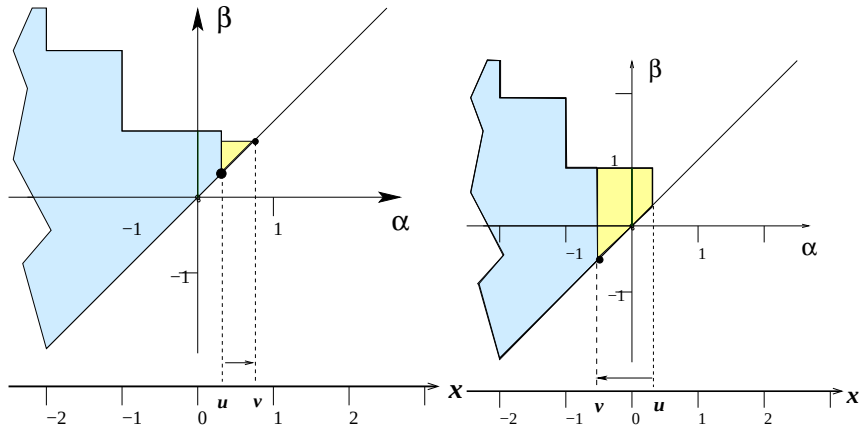

(a) Decreasing input (b) Increasing input

Figure 11: Dynamics of the Preisach Model.

(4) for the main deflation limb i.e.

$$\int_p^{\beta_{max}} \rho(p,\beta)\,d\beta = V'(p). \tag{14}$$

This density is distributed between $\beta = \alpha$ and $\beta = \beta_{max}$, where β_{max} is the maximum β threshold. Moreover, we suggest that the distribution is uniform within the fragment $[p, \beta_{max}]$ of any vertical lines of constant $\alpha \equiv p$. Using Proposition 1 we conclude that this density within this range is given by:

$$\rho(\alpha,\beta) = \frac{V'(\alpha)}{\beta_{max} - \alpha}.$$

We define this density as

$$\rho(\alpha,\beta) \quad = \quad \left(\frac{1}{\beta_{max} - \alpha}\right) \frac{d}{dp}\left(a + \frac{b}{\left(1 + e^{(p-c)/d}\right)}\right), \tag{15}$$

or more succinctly as:

$$\rho(\alpha,\beta) = \frac{b\,\mathrm{sech}^2\left(\frac{c-\alpha}{2d}\right)}{4d(\alpha - \beta_{\max})}. \tag{16}$$

This density is non-zero for $\alpha < \beta < \beta_{max}$, where $0 < \alpha < \beta < \beta_{max}$, and is zero otherwise.

The expression for the inflation curve after the first deflation is given by:

$$V_1(p) = V(p_1) + \int_{\alpha=p_1}^{\alpha=p} \int_{\beta=\alpha}^{\beta=p} \rho(\alpha,\beta)\,d\beta, \tag{17}$$

where p_1 is the pressure at which deflation stops and inflation begins. For convenience let us denote inflation curves with odd subscripts , i.e. by $V_1(p), V_3(p), V_5(p)$ and so on, and deflation curves (other than the main limb) by even subscripts $V_2(p), V_4(p), V_6(p)$ and so on. Since ρ is a function of α only, expression (17) can be reduced to:

$$V_1(p) = V(p_1) + \int_{\alpha=p_1}^{\alpha=p} \frac{b(p-\alpha)\mathrm{sech}^2\left(\frac{c-\alpha}{2d}\right)}{4d\,(\alpha-\beta_{\max})} d\beta. \tag{18}$$

7.1. Results of fitting

The data were extracted by means of specialised software [7] from published experiments. Three datasets were taken from Fig. 6 of Martin et al. [25]. These data, denoted datasets 1 to 3 in Table 2.1 were the measured P-V curves of mice who had lung damage. Dataset 4, was taken from Figure 2a in Koefoed et al. [22] and these data were measure P-V curves pigs lungs that were injured.

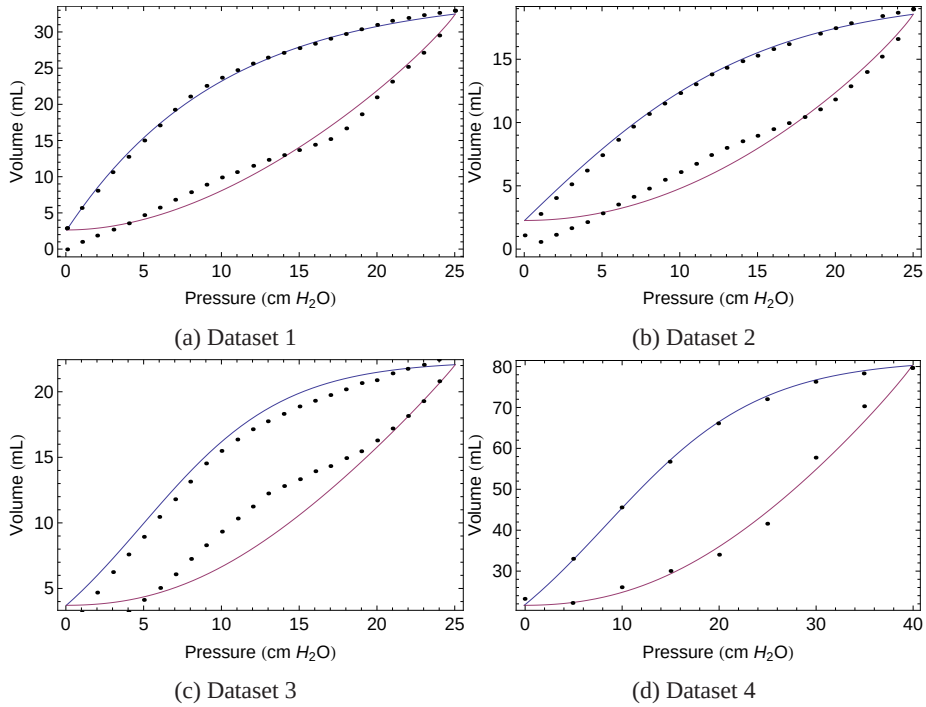

(a) Dataset 1 (b) Dataset 2

(c) Dataset 3 (d) Dataset 4

Figure 12: Results from fitting a Preisach model based on Venegas' equation.

The fitting of the data was done by global minimisation of an objective function

formed from the sum of squared residuals (SSEs):

$$g(a,b,c,d) = \sum_{i=1}^{N}(V(p_i) - V_i)^2 + \sum_{j=1}^{M}(V_1(p_j) - V_{1_j})^2, \tag{19}$$

where g is the objective function and a,b,c and d are the parameters of the model, which are treated like variables for the purposes of optimisation. The constants N and M denote the number of deflation and inflation data points respectively. The global optimisation method used was Differential Evolution [34]. The resulting SSE values and the parameters for each data set are shown in Table 2.1 and the plots are shown in Figure 12. Since the SSE was calculated for datasets whose volumes were not normalised, they cannot be used to compare the results of the fits. Instead an error term was added to Table 2.1 and was calculated as:

$$\frac{\sqrt{SSE}}{V_{max}},$$

where V_{max} is the maximum volume of an individual dataset.

Dataset	Data Source	SSE	Error	a	b	c	d
1	Martin et al. [25]	0.164	0.012	1.02	0.12	2.56	0.18
2	Martin et al.[25]	25.12	0.266	-18.12	38.02	-1.11	-7.91
3	Martin et al. [25]	131	0.502	-2.67	25.03	4.92	-4.56
4	Koefoed et al. [22]	47.1	0.086	0.904	80.87	8.38	-7.96

Table 2.1: Results from fitting P-V curves with the Preisach model.

8. Discussion and Conclusions

In this paper the author focused on several models of P-V relationship of the lungs. Earlier models such expression (2) in section 5.1, captured the P-V curve quite well when the lung was inside the body, where a full sigmoidal curve usually does not occur. This model was also used as the basis of more sophisticated models such as Bates and Irvin's in section 5.2. Later models, such as expressions (3) and (4) in section 5.1 captured the full sigmoidal behaviour, which occurs when the lung is outside the body. It is also possible to fit hysteresis loops with these models, however, the parameters are different for each part of the loop fitted.

Later models attempted to systematically capture the full hysteretic behaviour, these demonstrated that they could qualitatively predict the behaviour of P-V hysteresis loops. The approach in formulating these models is similar to the Preisach model, and further analysis of these may show that they can be reformulated as the Preisach model or a generalised version of it.

Also in this paper, a model was developed based on a similar approach as done for soil hydrology in [12], where a Preisach density was developed based on a function

that fit each branch of the curve successfully. The Preisach model that was developed here had no additional parameters but relied on the parameters of Venegas' function.

The results of the model's fit to the data, can be seen by comparing the error terms in table 2.1. Dataset 1 demonstrated the best fit, followed by datasets 4 and 2. The worst fit was to dataset 3. However, looking at the visual results in Figure 12, dataset 4 shows the best fit qualitatively, followed by datasets 1, 2 and 3.

From looking at Figure 12, it can be seen that the model only captures some of the qualitative behaviour. It does not reproduce the inflection points that can be seen in all the graphs, which is most pronounced in Figure 12c. That indicates that the model needs to be revised further. There are several approaches, firstly the Preisach density can have restrictions placed on it, this will add additional parameters which should improve the fits. Another possibility is to discretely measure the Preisach density using to procedure outlined in Mayergoyz [26]. Additionally the hysteresis models described in this paper may be adapted to develop a new Preisach operator.

The advantage of using hysteresis models such as the Preisach operator models in curve fitting, is that the number of parameters can be substantially reduced. As mentioned above, using earlier models that fit each limb of the hysteresis loop has to be fitted by n parameters, so for k loops you have $n \times k$ parameters in total. Whereas with the Preisach model, the maximum number of parameters required to fit the data would be same n parameters, plus m additional parameters to define the Preisach density. In total $n+m$ parameters could be used to fit any number of hysteresis loops generated from quasi-static P-V measurements. In addition, once the Preisach model has been calibrated it has the ability to predict further loops and thus can be incorporated into differential equations.

References

[1] AMATO M.B., BARBAS C.S., MEDEIROS D.M., SCHETTINO G.D.P., LORENZI FILHO G., KAIRALLA R.A., DEHEINZELIN D., MORAIS C., FERNANDES E.D.O. AND TAKAGAKI T.Y., *Beneficial effects of the "open lung approach" with low distending pressures in acute respiratory distress syndrome. a prospective randomized study on mechanical ventilation*, American Journal of Respiratory and Critical Care Medicine **152** (1995), 1835–1846.

[2] AMATO M.B.P., BARBAS C.S.V., MEDEIROS D.M., MAGALDI R.B., SCHETTINO G.P., LORENZI-FILHO G., KAIRALLA R.A., DEHEINZELIN D., MUNOZ C., OLIVEIRA R., ET AL., *Effect of a protective-ventilation strategy on mortality in the acute respiratory distress syndrome*, New England Journal of Medicine **338** (1998), 347–354.

[3] AMINI R., CREEDEN K. AND NARUSAWA U., *A mechanistic model for quasistatic pulmonary pressure-volume curves for inflation.*, Journal of biomechanical engineering **127** (2005), 619–629.

[4] BACHOFEN H., HILDEBRANDT J. AND BACHOFEN M., *Pressure-volume curves of air- and liquid-filled excised lungs-surface tension in situ.*, Journal of applied physiology **29** (1970), 422–431.

[5] BATES J.H., *Lung mechanics: an inverse modeling approach*, Cambridge University Press, Cambridge 2009.

[6] BATES J.H. AND IRVIN C.G., *Time dependence of recruitment and derecruitment in the lung: a theoretical model*, Journal of Applied Physiology **93** (2002), 705–713.

[7] BORMANN I. *Digitizeit version 1.5. 8b*, 2010.

[8] CARVALHO A. AND ZIN W., *Respiratory mechanics: Principles, utility and advances*, In *Anaesthesia, Pharmacology, Intensive Care and Emergency Medicine APICE*, Springer, Milan 2011, 33–46.

[9] CHASE J.G., YUTA T., MULLIGAN K.J., SHAW G.M. AND HORN B., *A novel mechanical lung model of pulmonary diseases to assist with teaching and training*, BMC pulmonary medicine **6** 21 (2006) 1–11.

[10] CHENG W., DELONG D., FRANZ G., PETSONK E. AND FRAZER D., *Contribution of opening and closing of lung units to lung hysteresis*, Respiration physiology **102** (1995), 205–215.

[11] CLOETTA M., *Untersuchungen über die elastizität der lunge und deren bedeutung für die zirkulation*, Pflüger's Archiv für die gesamte Physiologie des Menschen und der Tiere **152** (1913), 339–364.

[12] FLYNN D., MCNAMARA H., O'KANE P. AND POKROVSKII A., *Application of the Preisach model to Soil-Moisture Hysteresis*, Science of Hysteresis, vol. 3, Academic Press, Oxford 2005, (689–744).

[13] GANZERT S., KRAMER S. AND GUTTMANN J., *Predicting the lung compliance of mechanically ventilated patients via statistical modeling*, Physiological Measurement **33** (2012), 345–359.

[14] GREAVES I.A., HILDEBRANDT J. AND HOPPIN F.G., *Micromechanics of the lung*, Comprehensive Physiology (2011), 217–231

[15] HARRIS R.S., *Pressure-volume curves of the respiratory system*, Respiratory care **50** (2005), 78–99.

[16] HEROLD R., DEWITZ R., SCHÜRCH S. AND PISON U., *Pulmonary surfactant and biophysical function*, Studies in Interface Science **6** (1998), 433–474.

[17] HICKLING K.G., *The pressure–volume curve is greatly modified by recruitment: a mathematical model of ARDS lungs*, American journal of respiratory and critical care medicine **158** (1998), 194–202.

[18] HILDEBRANDT J., *Pressure-volume data of cat lung interpreted by a plastoelastic, linear viscoelastic model*, Journal of applied physiology **28** (1970), 365–372.

[19] HILLS B., *Contact-angle hysteresis induced by pulmonary surfactants*, Journal of Applied Physiology **54** (1983), 420–426.

[20] HUTCHINSON J. AND TODD R.B., *Cyclopedia of anatomy and physiology*, Thorax **4** (1849), 1016–1087.

[21] JONSON B. AND SVANTESSON C., *Elastic pressure–volume curves: what information do they convey?*, Thorax **54** (1999), 82–87.

[22] KOEFOED-NIELSEN J., ANDERSEN G., BARKLIN A., BACH A., LUNDE S., TØNNESEN E. AND LARSSON, A., *Maximal hysteresis: a new method to set positive end-expiratory pressure in acute lung injury?*, Acta Anaesthesiologica Scandinavica **52** (2008), 641–649.

[23] KRASNOSELSKII M.A. AND POKROVSKII A., *Systems with hysteresis*, Springer-Verlag, Berlin 1989.

[24] LIGAS J.R., *Lung tissue mechanics: Historical overview*, Respiratory Biomechanics, Springer, New York 1990, (3–18).

[25] MARTIN E.L., MCCAIG L.A., MOYER B.Z., PAPE M.C., LECO K.J., LEWIS J.F. AND VELDHUIZEN R.A., *Differential response of timp-3 null mice to the lung insults of sepsis, mechanical ventilation, and hyperoxia*, American Journal of Physiology-Lung Cellular and Molecular Physiology **289** (2005), 244–251.

[26] MAYERGOYZ I.D., *Mathematical models of hysteresis and their applications*, Academic Press, 2003.

[27] MEAD J., *Mechanical properties of lungs*, Physiological Reviews **41** (1961), 281–330.

[28] MILIC-EMILI J. AND D'ANGELO E., *Statics of the lung*, Physiologic basis of respiratory disease, BC Decker Incorporated 2005, (27–33).

[29] MOLS G., PRIEBE H.J. AND GUTTMANN J., *Alveolar recruitment in acute lung injury*, British journal of anaesthesia **96** (2006), 156–166.

[30] MURPHY B. AND ENGEL L., *Models of the pressure-volume relationship of the human lung*, Respiration physiology **32** (1978), 183–194.

[31] PETTY T.L., *The use, abuse, and mystique of positive end-expiratory pressure*, The American review of respiratory disease **138** (1988), 475–478.

[32] ROZANEK M. AND ROUBIK K., *Mathematical model of the respiratory system–comparison of the total lung impedance in the adult and neonatal lung*, Proceedings of the World Academy of Science, Engineering and Technology **24** (2007), 293–296.

[33] SALAZAR E. AND KNOWLES J.H., *An analysis of pressure-volume characteristics of the lungs*, Journal of Applied Physiology **19** (1964), 97–104.

[34] STORN R. AND PRICE K., *Differential evolution–a simple and efficient heuristic for global optimization over continuous spaces*, Journal of global optimization **11** (1997), 341–359.

[35] SUKI B., ANDRADE JR J.S., COUGHLIN M.F., STAMENOVIĆ D., STANLEY H.E., SUJEER M. AND ZAPPERI S., *Mathematical modeling of the first inflation of degassed lungs*, Annals of biomedical engineering **26** (1998), 608–617.

[36] SUKI B., BARABASI A.L., HANTOS Z., PETÁK F. AND STANLEY H.E., *Avalanches and power-law behaviour in lung inflation*, Nature **368** (1994), 615–618.

[37] SUKI B. AND BATES J.H., *Lung tissue mechanics as an emergent phenomenon*, Journal of Applied Physiology **110** (2011), 1111–1118.

[38] VON NEERGAARD K., *Neue auffassungen über einen grundbegriff der atemmechanik*, Research in Experimental Medicine **66** (1929), 373–394.

[39] VENEGAS J.G., HARRIS R.S. AND SIMON B.A., *A comprehensive equation for the pulmonary pressure-volume curve*, Journal of Applied Physiology **84** (1998), 389–395.

[40] WARE L.B. AND MATTHAY M.A., *The acute respiratory distress syndrome*, New England Journal of Medicine **342** (2000), 1334–1349.

AMS Subject Classification: 92C35, 76Z05, 92C50, 47J40

Denis FLYNN,
Centre of Excellence Telč
Batelovska 485, 486
588 56 Telč,
CZECH REPUBLIC
e-mail:flynn@itam.cas.cz

Lavoro pervenuto in redazione il 29.01.2015.

Rend. Sem. Mat. Univ. Politec. Torino
Vol. 72, 1–2 (2014), 37 – 55

D. Guidetti

SOME REMARKS ON OPERATORS PRESERVING OSCILLATIONS

Abstract. We prove some properties of nonlinear operators preserving oscillations. We consider the particular cases of Preisach operators and Generalized Plays, of which we give a short introduction.

1. Introduction

The aim of this paper is to state and prove some simple results, concerning nonlinear operators $\mathscr{W} : D(\mathscr{W}) \subseteq C([0,T]) \to C([0,T])$, preserving oscillations, in the sense that they satisfy the following conditions (AA1)-(AA2), for some $\alpha \in (0,1]$. We show that, in case $1 < p \leqslant \infty$ and $\frac{1}{p} < \beta < 1$, they map $D(\mathscr{W}) \cap W^{\beta,p}((0,T))$ into $W^{\alpha\beta,\frac{p}{\alpha}}((0,T))$. This result seems to be new. In case $\alpha = 1$, $\mathscr{W}$ preserves also the belonging to $W^{1,p}((0,T))$ $(1 \leqslant p \leqslant \infty)$ and to $BV((0,T))$. We are not aware of a general statement in this sense, although this result is certainly well known in the case of our two main examples, namely Preisach operators and Generalized Plays. In order to make the paper more or less self contained, we have written in Sections 3 and 4 short introductions to this classes of nonlinear operators, which are quite important in applications.

2. Nonlinear operators and oscillations

We begin by introducing some notations and conventions. We shall indicate with C a positive constant, which may be different from time to time. If we want to stress the fact che C depends on $\alpha, \beta, \dots$, we shall write $C(\alpha, \beta, \dots)$. We shall consider only real valued functions and we shall not precise this in the following.

Let $-\infty < a < b < \infty$. We shall indicate with $C([a,b])$ the Banach space of continuous functions with domain $[a,b]$, equipped with its natural norm $\|\cdot\|_{C([a,b])}$. If $s,t \in [a,b]$, we indicate with $os(f;s,t)$ the oscillation of f in $[\min\{s,t\}, \max\{s,t\}]$, defined as

$$os(f;s,t) := \sup\{|f(\sigma) - f(\tau)| : \sigma, \tau \in [\min\{s,t\}, \max\{s,t\}]\}. \tag{1}$$

Clearly, if $s,t \in [a,b]$,

$$|f(t) - f(s)| \leqslant os(f;s,t) \leqslant V_{\min\{s,t\}}^{\max\{s,t\}}(f),$$

with

$$V_{\min\{s,t\}}^{\max\{s,t\}}(f) := \sup\{\sum_{j=1}^{n} |f(t_j) - f(t_{j-1})| : n \in \mathbb{N}, \min\{s,t\} = t_0 < \dots < t_n = \max\{s,t\}\}.$$

We shall indicate with $BV([a,b])$ the class of real valued functions with bounded variation in $[a,b]$. If I is an open interval in $\mathbb{R}$ and $1 \leqslant p \leqslant \infty$, we shall indicate with $W^{1,p}(I)$ the class of elements f in $L^p(I)$ such that the derivative in the sense of distributions f' is in $L^p(I)$. This space will be equipped with its natural norm

$$\|f\|_{W^{1,p}(I)} := \|f\|_{L^p(I)} + \|f'\|_{L^p(I)} \tag{2}$$

If $p = 1$ and I is bounded, $W^{1,1}(I)$ coincides with the class $AC(I)$ of absolutely continuous functions in I, which means that, $\forall \varepsilon \in \mathbb{R}^+$, there exists $\delta(\varepsilon)$ in $\mathbb{R}^+$, such that, if $[a_k, b_k]$ $(1 \leqslant k \leqslant n,\ n \in \mathbb{N})$ are pairwise disjoint subintervals of I such that $\sum_{k=1}^n (b_k - a_k) \leqslant \delta(\varepsilon)$, then $\sum_{k=1}^n |f(b_k) - f(a_k)| \leqslant \varepsilon$.

If $p = \infty$, $W^{1,\infty}(I)$ coincides with the class of bounded, Lipschitz continuous functions with domain I. We observe that

$$\|f'\|_{L^\infty(I)} = [f]_{Lip(I)} := \sup_{s,t \in I, s \neq t} |t-s|^{-1} |f(t) - f(s)|.$$

Let I be an open interval in $\mathbb{R}$, $p \in [1,\infty]$, $\beta \in (0,1)$. We indicate with $W^{\beta,p}(I)$ the class of elements in $L^p(I)$ such that

$$[f]_{W^{\beta,p}(I)} < \infty, \tag{3}$$

with

$$[f]_{W^{\beta,p}(I)} := \begin{cases} \int_{I \times I} \frac{|f(t)-f(s)|^p}{|t-s|^{1+\beta p}} ds dt & \text{if } \ 1 \leqslant p < \infty, \\ \\ \sup_{t,s \in I, s \neq t} |t-s|^{-\beta} |f(t) - f(s)| & \text{if } \ p = \infty. \end{cases} \tag{4}$$

We set

$$\|f\|_{W^{\beta,p}(I)} := \|f\|_{L^p(I)} + [f]_{W^{\beta,p}(I)}. \tag{5}$$

We observe that $W^{\beta,\infty}(I)$ coincides with the class of bounded, Hölder continuous functions $C^\beta(I)$. In case $\beta > \frac{1}{p}$, $W^{\beta,p}(I)$ is continuously embedded into $BC(I)$, the class of real valued, continuous and bounded functions of domain I. For these definitions and embeddings, see [2], Chapters 3.4.2, 3.2.2, 2.7.1; in case $1 < p < \infty$ and $0 < \beta < 1$, $W^{\beta,p}(I)$ coincides with both the spaces $B^\beta_{p,p}(I)$ and $F^\beta_{p,p}(I)$, which are elements of the scales of (respectively) Besov and Triebel-Lizorkin spaces (see [2]). Obviously, we have also $W^{1,1}(I) \hookrightarrow BC(I)$.

The following fact will be important for us:

LEMMA 1. *Let $p \in (1,\infty)$, $\beta \in (\frac{1}{p}, 1)$. Then there exists $C \in \mathbb{R}^+$ such that, if $f \in W^{\beta,p}(\mathbb{R})$,*

$$\int_{\mathbb{R}\setminus\{0\}} \Big(\int_{\mathbb{R}} \sup_{|\rho| \leqslant h} |f(x+\rho) - f(x)|^p dx \Big) |h|^{-1-\beta p} dh \leqslant C(\beta, p) \|f\|^p_{W^{\beta,p}(I)}.$$

Proof. See [2], Chapter 2.5.10. □

As a simple consequence, we obtain the following

COROLLARY 1. *Let I be an open interval in $\mathbb{R}$ and $p \in (1,\infty]$. Let $\beta \in (\frac{1}{p},1)$. Then there exists $C = C(I,p,\beta)$ such that, $\forall f \in W^{\beta,p}(I)$,*

$$\int_{I\times I} \frac{os(f;s,t)^p}{|t-s|^{1+\beta p}} dsdt \leqslant C\|f\|^p_{W^{\beta,p}(I)}, \quad \text{if} \quad 1 < p < \infty,$$

$$\sup_{s,t\in I, s\neq t} os(f;s,t)(t-s)^{-\beta} \leqslant [f]_{W^{\beta,\infty}(I)}, \quad \text{if} \quad p = \infty.$$

Proof. The case $p = \infty$ is trivial. We assume $1 < p < \infty$. First, we observe that

$$os(f;s,t) \leqslant 2 \sup_{|\rho|\leqslant \frac{|t-s|}{2}} |f(\frac{s+t}{2}+\rho) - f(\frac{s+t}{2})|.$$

By Chapter 3.3.4 in [2], there exists a bounded linear extension operator E, mapping $W^{\beta,p}(I)$ into $W^{\beta,p}(\mathbb{R})$. So, if we set $\widetilde{f} := Ef$, we have

$$\int_{I\times I} \frac{os(f;s,t)^p}{|t-s|^{1+\beta p}} dsdt \leqslant \int_{\mathbb{R}\times\mathbb{R}} \frac{os(\widetilde{f};s,t)^p}{|t-s|^{1+\beta p}} dsdt \leqslant 2^p \int_{\mathbb{R}\times\mathbb{R}} \frac{\sup_{|\rho|\leqslant\frac{|t-s|}{2}} |\widetilde{f}(\frac{t+s}{2}+\rho) - \widetilde{f}(\frac{t+s}{2})|^p}{|t-s|^{1+\beta p}} dsdt$$

$$= 2^{-\beta p} \int_{\mathbb{R}\times\mathbb{R}} \frac{\sup_{|\rho|\leqslant|h|} |\widetilde{f}(x+\rho) - \widetilde{f}(x)|^p}{|h|^{1+\beta p}} dxdh \leqslant C(\beta,p)\|\widetilde{f}\|^p_{W^{\beta,p}(\mathbb{R})}$$

$$\leqslant C(\beta,p)\|E\|^p_{\mathscr{L}(W^{\beta,p}(I),W^{\beta,p}(\mathbb{R}))} \|f\|^p_{W^{\beta,p}(I)}.$$

□

Now we introduce a (nonlinear) operator $\mathscr{W} : D(\mathscr{W}) \to C([0,T])$, for some $T \in \mathbb{R}^+$. We shall assume that $\mathscr{W}$ satisfies the following conditions:

(AA1) $D(\mathscr{W}) \subseteq C([0,T])$;

(AA2) there exists $\alpha \in (0,1]$ such that, $\forall R \in \mathbb{R}^+$ there exists $C(R)$ in $\mathbb{R}^+$ so that, if $f \in D(\mathscr{W})$ and $\|f\|_{C([0,T])} \leqslant R$, $\forall s,t \in [0,T]$,

$$os(\mathscr{W}(f);s,t) \leqslant C(R) os(f;s,t)^\alpha.$$

THEOREM 1. *Let $\mathscr{W}$ satisfy (AA1)-(AA2). Let $p \in (1,\infty]$, $\beta \in (\frac{1}{p},1)$ and let $f \in D(\mathscr{W}) \cap W^{\beta,p}((0,T))$. Then $\mathscr{W}(f) \in W^{\alpha\beta,\frac{p}{\alpha}}((0,T))$. Moreover, $\forall R \in \mathbb{R}^+$, there exists $C(R) \in \mathbb{R}^+$ such that, if $f \in D(\mathscr{W}) \cap W^{\beta,p}((0,T))$ and $\|f\|_{C([0,T])} \leqslant R$,*

$$[\mathscr{W}(f)]_{W^{\alpha\beta,\frac{p}{\alpha}}((0,T))} \leqslant C(R)\|f\|^\alpha_{W^{\beta,p}((0,T))}.$$

Proof. In fact, by Corollary 1, we have, setting $I := (0,T)$,

$$[\mathscr{W}(f)]^{\frac{p}{\alpha}}_{W^{\alpha\beta,\frac{p}{\alpha}}((0,T))} \leqslant \int_{I\times I} \frac{os(\mathscr{W}(f);s,t)^{p/\alpha}}{|t-s|^{1+\beta p}}dtds$$

$$\leqslant C_0(R)\int_{I\times I}\frac{os(f;s,t)^p}{|t-s|^{1+\beta p}}dtds \leqslant C_1(R)\|f\|^p_{W^{\beta,p}((0,T))}.$$

□

In case $\alpha = 1$, we have also the following

THEOREM 2. *Assume that (AA1)-(AA2) hold, with $\alpha = 1$. Then:*
(I) $\forall p \in [1,\infty]$, $\mathscr{W}$ maps $D(\mathscr{W})\cap W^{1,p}((0,T))$ into $W^{1,p}((0,T))$;
(II) $|\mathscr{W}(f)'(t)| \leqslant C(|f\|_{C([0,T])})|f'(t)|$ a. e. in $(0,T)$.
(III) $\mathscr{W}$ maps $D(\mathscr{W})\cap BV((0,T))$ into $BV((0,T))$. Moreover, if $f \in D(\mathscr{W})\cap BV((0,T))$,

$$V_0^T(\mathscr{W}(f)) \leqslant C(\|f\|_{C([0,T])})V_0^T(f).$$

Proof. Assume that $f \in W^{1,1}([0,T])\cap D(\mathscr{W})$. Let $n \in \mathbb{N}$ and $0 \leqslant a_1 \leqslant b_1 \leqslant a_2 \leqslant b_2 \leqslant \cdots \leqslant a_n \leqslant b_n \leqslant T$. Then

$$\Sigma_{j=1}^n |\mathscr{W}(f)(b_j) - \mathscr{W}(f)(a_j)| \leqslant \Sigma_{j=1}^n os(\mathscr{W}(f);a_j,b_j)$$

$$\leqslant C(\|f\|_{C([0,T])})\Sigma_{j=1}^n os(f;a_j,b_j)$$

$$\leqslant C(\|f\|_{C([0,T])})\int_{\cup_{j=1}^n(a_j,b_j)}|f'(t)|dt \leqslant \varepsilon$$

if $\Sigma_{j=1}^n(b_j-a_j) \leqslant \delta(\varepsilon)$, by the absolute continuity of the integral. We deduce that $\mathscr{W}(f) \in AC((0,T)) = W^{1,1}([0,T])$ and so it is differentiable almost everywhere. Observe that, if f is differentiable in t and $t+h \in [0,T]$,

$$os(f;t,t+h) \leqslant |f'(t)||h| + o(|h|) \quad (h\to 0).$$

So, if f and $\mathscr{W}(f)$ are differentiable in t

$$|\tfrac{\mathscr{W}(f)(t+h)-\mathscr{W}(f)(t)}{h}| \leqslant |h|^{-1}os(\mathscr{W}(f);t,t+h)$$

$$\leqslant C(\|f\|_{C([0,T])})|h|^{-1}os(f;t,t+h) = C(\|f\|_{C([0,T])})(|f'(t)|+o(1)) \quad (h\to 0).$$

So (II) is proved and (I) follows easily.

Concerning (III), let $0 = t_0 < \cdots < t_n = T$. Then

$$\Sigma_{j=1}^n |\mathscr{W}(f)(t_j) - \mathscr{W}(f)(t_{j-1})| \leqslant \Sigma_{j=1}^n os(\mathscr{W}(f);t_{j-1},t_j)$$

$$\leqslant C(\|f\|_{C([0,T])})\Sigma_{j=1}^n os(f;t_{j-1},t_j)$$

$$\leqslant C(\|f\|_{C([0,T])})\Sigma_{j=1}^n V_{t_{j-1}}^{t_j}(f) = C(\|f\|_{C([0,T])})V_0^T(f)$$

□

3. Preisach operators

The first class of operators to which we apply the results of Section 2 is the class of Preisach operators, which were introduced by F. Preisach in 1935, in connection to problem in ferromagnetism (see [3], Historical Notes). Here we present an introduction to it, which seems simpler than the one in [3], Chapter IV.

Let $T \in \mathbb{R}^+$, $\rho := (\rho_1, \rho_2) \in \mathbb{R}^2$, with $\rho_1 < \rho_2$, $\xi \in \{-1, 1\}$. Given $u \in C([0,T])$, we set

$$A_t := \{s \in [0,t] : u(s) \in \{\rho_1, \rho_2\}\}. \tag{1}$$

and

$$h_\rho(u,\xi)(t) = \begin{cases} -1 & \text{if } A_t \neq \emptyset, u(\max A_t) = \rho_1, \text{ or } u(s) < \rho_1 \forall s \in [0,t] \\ & \text{or } \rho_1 < u(s) < \rho_2 \quad \forall s \in [0,t] \text{ and } \xi = -1, \\ 1 & \text{if } A_t \neq \emptyset, u(\max A_t) = \rho_2, \text{ or } u(s) > \rho_2 \forall s \in [0,t] \\ & \text{or } \rho_1 < u(s) < \rho_2 \quad \forall s \in [0,t] \text{ and } \xi = 1. \end{cases} \tag{2}$$

h_ρ is called *relay operator*. Roughly speaking we start from 1 if $u(0) \geqslant \rho_2$ or $u(0) > \rho_1$ and $\xi = 1$, from -1 if $u(0) \leqslant \rho_1$ or $u(0) < \rho_2$ and $\xi = -1$. Then, we pass from 1 to -1 whenever we meet t such that $u(t) = \rho_1$, we pass from -1 to 1 whenever we meet t such that $u(t) = \rho_2$. It is easily seen that, for fixed values of ρ and ξ, if $\delta \in \mathbb{R}^+$ is such that, whenever $|t-s| \leqslant \delta$, $|u(t) - u(s)| < \rho_2 - \rho_1$, $h_\rho(u,\xi)$ changes sign $[\frac{T}{\delta}] + 1$ times, at most.

In the following, we shall indicate with $\mathscr{P}$ the Preisach plane, defined as

$$\mathscr{P} := \{\rho = (\rho_1, \rho_2) \in \mathbb{R}^2 : \rho_1 < \rho_2\}. \tag{3}$$

The following properties are easy to prove and are left to the reader:

PROPOSITION 1. *Let $T \in \mathbb{R}^+$, $\xi \in \{-1,1\}$, $u, u_1, u_2 \in C([0,T])$, $\rho = (\rho_1, \rho_2)$, $\rho' = (\rho_1', \rho_2') \in \mathscr{P}$, $c \in \mathbb{R}$. Then:*
(I) if $t \in [0,T]$ and $u(t) \leqslant \rho_1$, then $h_\rho(u,\xi)(t) = -1$, if $u(t) \geqslant \rho_2$, $h_\rho(u,\xi)(t) = 1$;
(II) if $t \in [0,T]$ and $u_1(s) \leqslant u_2(s)$ $\forall s \in [0,t]$, then $h_\rho(u_1,\xi)(t) \leqslant h_\rho(u_2,\xi)(t)$;
(III) $\forall t \in [0,T]$, $h_\rho(u+c,\xi)(t) = h_{\rho_1 - c, \rho_2 - c}(u,\xi)(t)$;
(IV) if $\rho_1 \leqslant \rho_1'$ and $\rho_2 \leqslant \rho_2'$, $h_{\rho'}(u,\xi)(t) \leqslant h_\rho(u,\xi)(t)$ $\forall t \in [0,T]$;
(V) $\lim_{r \to \rho_1^+} h_{r,\rho_2}(u,\xi)(t) = h_\rho(u,\xi)(t) = lim_{r \to \rho_2^-} h_{\rho_1, r}(u,\xi)(t)$;
(VI) $h_{-\rho_2, -\rho_1}(-u, -\xi)(t) = -h_\rho(u,\xi)(t)$.
(VII) If $\phi : [0,T] \to [0,T]$ is an increasing homeomorphism of $[0,T]$ into itself, then $h_\rho(u \circ \phi, \xi) = h_\rho(u,\xi) \circ \phi$.
(VIII) If $u, v \in C([0,T])$ and, for some $t \in [0,T]$, $u_{|[0,t]} = v_{|[0,t]}$, then $h_\rho(u,\xi)_{|[0,t]} = h_\rho(v,\xi)_{|[0,t]}$.

REMARK 1. Property (VII) in Proposition 1 is known as the *rate independence property*. Property (VIII) in Proposition 1 is known as the *memory property*. Properties (VII) and (VIII) together characterise *hysteresis operators*.

Now we study the behaviour of $\rho \to h_\rho(u,\xi)(t)$, for fixed values of u, ξ, t.

LEMMA 2. *Let $u \in C([0,T])$, $\xi \in \{-1,1\}$, $t \in [0,T]$. Then:*
(I) if $\rho_1 \geqslant u(t)$, $h_{\rho_1,\rho_2}(u,\xi)(t) = -1$ $\forall \rho_2 \in (\rho_1,\infty)$;
(II) if $\rho_1 < \min_{[0,t]}(u)$, $h_{\rho_1,\rho_2}(u,1)(t) = 1$ $\forall \rho_2 \in (\rho_1,\infty)$;
(III) if $\rho_1 < u(t)$, there exists $\psi(\rho_1) \in (\rho_1,\infty)$, such that $h_{\rho_1,\rho_2}(u,-1)(t) = 1$ if $\rho_2 \in (\rho_1,\psi(\rho_1)]$, $h_{\rho_1,\rho_2}(u,-1)(t) = -1$ if $\rho_2 > \psi(\rho_1)$;
(IV) if $\min_{[0,t]}(u) \leqslant \rho_1 < u(t)$, there exists $\psi(\rho_1) \in (\rho_1,\infty)$, such that $h_{\rho_1,\rho_2}(u,1)(t) = 1$ if $\rho_2 \in (\rho_1,\psi(\rho_1)]$, $h_{\rho_1,\rho_2}(u,1)(t) = -1$ if $\rho_2 > \psi(\rho_1)$.
(V) The function ψ defined in (III) or (IV), the domain of which we indicate with $D(\psi)$, is non increasing; moreover, $\forall \rho_1 \in D(\psi)$ there exists $\delta \in \mathbb{R}^+$ such that $[\rho_1,\rho_1+\delta) \subseteq D(\psi)$ and ψ is constant in this interval.
(VI) As a consequence, ψ has an at most countable range and is right continuous.

Proof. The proof is elementary, employing Proposition 1 (IV)-(V).

□

Analogously, we have:

LEMMA 3. *Let $u \in C([0,T])$, $\xi \in \{-1,1\}$, $t \in [0,T]$. Then:*
(I) if $\rho_2 \leqslant u(t)$, $h_{\rho_1,\rho_2}(u,\xi)(t) = 1$ $\forall \rho_1 \in (\infty,\rho_2)$;
(II) If $\max_{[0,t]}(u) < \rho_2$, $h_{\rho_1,\rho_2}(u,-1)(t) = -1$ $\forall \rho_1 \in (\infty,\rho_2)$;
(III) if $u(t) < \rho_2 \leqslant max_{[0,t]}(u)$, there exists $\chi(\rho_2) \in (-\infty,\rho_2)$, such that $h_{\rho_1,\rho_2}(u,-1)(t) = 1$ if $\rho_1 \in (\infty,\chi(\rho_2))$, $h_{\rho_1,\rho_2}(u,-1)(t) = -1$ if $\chi(\rho_2) \leqslant \rho_1 < \rho_2$;
(IV) if $u(t) < \rho_2$, there exists $\chi(\rho_2) \in (-\infty,\rho_2)$, such that $h_{\rho_1,\rho_2}(u,1)(t) = 1$ if $\rho_1 \in (\infty,\chi(\rho_2))$, $h_{\rho_1,\rho_2}(u,1)(t) = -1$ if $\chi(\rho_2) \leqslant \rho_1 < \rho_2$;
(V) The function χ defined in (III) or (IV), the domain of which we indicate with $D(\chi)$, is non increasing; moreover, $\forall \rho_2 \in D(\chi)$ there exists $\delta \in \mathbb{R}^+$ such that $(\rho_2-\delta,\rho_2] \subseteq D(\chi)$ and χ is constant in this interval.
(VI) As a consequence, χ has an at most countable range and is left continuous.

REMARK 2. From Lemma 2 it is clear that, if $\rho_1 < \rho_2 < \rho_2'$ and $h_{\rho_1,\rho_2}(u,\xi)(t) \neq h_{\rho_1,\rho_2'}(u,\xi)(t)$, $\rho_1 \in D(\psi)$ and $\rho_2 \leqslant \psi(\rho_1) \leqslant \rho_2'$. Analogously, From Lemma 3 it follows that, if $\rho_1 < \rho_1' < \rho_2$ and $h_{\rho_1,\rho_2}(u,\xi)(t) \neq h_{\rho_1',\rho_2}(u,\xi)(t)$, $\rho_2 \in D(\chi)$ and $\rho_1 \leqslant \chi(\rho_2) \leqslant \rho_1'$.

Given $u \in C([0,T])$, $\xi \in \{-1,1\}$, $t \in [0,T]$, we get the functions $\psi = \psi(u,\xi,t)$ and $\chi = \chi(u,\xi,t)$ (which may have empty domain). Therefore we can consider the sets Ψ and X of the functions $\psi(u,\xi,t)$ and $\chi(u,\xi,t)$:

$$\Psi := \{\psi(u,\xi,t) : u \in C([0,t]), \xi \in \{-1,1\}, t \in [0,T]\}, \tag{4}$$

$$X := \{\chi(u,\xi,t) : u \in C([0,t]), \xi \in \{-1,1\}, t \in [0,T]\}. \tag{5}$$

If $\psi : D(\psi) \to \mathbb{R}$ is in Ψ and $\delta \in \mathbb{R}^+$, we set

$$\psi_\delta := \{(\rho_1, \rho_2) \in \mathscr{P} : \rho_1 \in D(\psi), \psi(\rho_1) - \delta \leqslant \rho_2 \leqslant \psi(\rho_1) + \delta\}. \tag{6}$$

Analogously, if $\chi : D(\chi) \to \mathbb{R}$ is in X and $\delta \in \mathbb{R}^+$, we set

$$\chi_\delta := \{(\rho_1, \rho_2) \in \mathscr{P} : \rho_2 \in D(\chi), \chi(\rho_2) - \delta \leqslant \rho_1 \leqslant \chi(\rho_2) + \delta\}. \tag{7}$$

REMARK 3. As example, we take $u : [0,T] \to \mathbb{R}$, $u(t) = c$, with $c \in \mathbb{R}$. We have $D(\psi(u,1,t)) = \emptyset$, $D(\psi(u,-1,t)) = (-\infty, c)$, $\psi(u,-1,t)(\rho_1) = c$, $D(\chi(u,1,t)) = (c,\infty)$, $\chi(u,1,t)(\rho_2) = c$, $D(\chi(u,-1,t)) = \emptyset$.

Now we fix in $\mathscr{P}$ a bounded positive Borel measure μ and a Borel measurable function ξ, with values in $\{-1,1\}$. Given $u \in C([0,T])$ and $t \in [0,T]$, the function $\rho \to h_\rho(u, \xi_\rho)(t)$ is Borel and bounded in $\mathscr{P}$. It follows that we can define the Preisach operator

$$\mathscr{H}(u,\xi)(t) := \int_{\mathscr{P}} h_\rho(u,\xi_\rho)(t) d\mu(\rho). \tag{8}$$

We set

$$\mathscr{P}_\pm := \{\rho \in \mathscr{P} : h_\rho = \pm 1\}. \tag{9}$$

Then

$$\mathscr{H}(u,\xi)(t) = \int_{\mathscr{P}^+} h_\rho(u,1)(t) d\mu(\rho) + \int_{\mathscr{P}^-} h_\rho(u,-1)(t) d\mu(\rho).$$

Clearly $\mathscr{H}(u,\xi)$ is bounded in $[0,T]$, as

$$|\mathscr{H}(u,\xi)(t)| \leqslant \mu(\mathscr{P}) \quad \forall t \in [0,T].$$

From Proposition 1 (VII)-(VIII), we immediately obtain:

PROPOSITION 2. *Let μ and ξ as above. Then:*
(I) If $\phi : [0,T] \to [0,T]$ is an increasing homeomorphism of $[0,T]$ into itself, then $\mathscr{H}(u \circ \phi, \xi) = \mathscr{H}_\rho(u,\xi) \circ \phi$.
(II) If $u, v \in C([0,T])$ and, for some $t \in [0,T]$, $u_{|[0,t]} = v_{|[0,t]}$, then $\mathscr{H}(u,\xi)_{|[0,t]} = \mathscr{H}(v,\xi)_{|[0,t]}$.

We show that, under suitable conditions, $\mathscr{H}(u,\xi) \in C([0,T])$ $\forall u \in C([0,T])$:

THEOREM 3. *Suppose that μ is such that, $\forall r \in \mathbb{R}$,*

$$\mu((\{r\} \times (r,\infty)) \cup ((-\infty, r) \times \{r\})) = 0. \tag{10}$$

Then $\mathscr{H}(\cdot,\xi)$ maps $C([0,T])$ into itself.

Proof. Let $u \in C([0,T])$. Clearly, if $t, t+h \in [0,T]$,

$$|\mathscr{H}(u,\xi)(t+h) - \mathscr{H}(u,\xi)(t)|$$

$$\leqslant \int_{\mathscr{P}} (|h_\rho(u,1)(t+h) - h_\rho(u,1)(t)| + |h_\rho(u,-1)(t+h) - h_\rho(u,-1)(t)|) d\mu(\rho)$$

If, for some $\rho \in \mathscr{P}$, $h_\rho(u,1)(t+h) \neq h_\rho(u,1)(t)$ or $h_\rho(u,-1)(t+h) \neq h_\rho(u,-1)(t)$, necessarily $u([t,t+h]) \cap \{\rho_1,\rho_2\} \neq \emptyset$. Let $\delta \in \mathbb{R}^+$, be such that $u([t,t+h]) \subseteq [u(t) - \delta, u(t) + \delta]$. Then

$$|\mathscr{H}(u,\xi)(t+h) - \mathscr{H}(u,\xi)(t)| \leqslant 4\mu\{(\rho_1,\rho_2) \in \mathscr{P} : [u(t)-\delta, u(t)+\delta] \cap \{\rho_1,\rho_2\} \neq \emptyset\}.$$

As

$$\bigcap_{\delta>0} \{(\rho_1,\rho_2) \in \mathscr{P} : [u(t)-\delta, u(t)+\delta] \cap \{\rho_1,\rho_2\} \neq \emptyset\}$$

$$= \{u(t)\} \times (u(t),\infty)) \cup ((-\infty, u(t)) \times \{u(t)\}),$$

from standard properties of measures, we deduce that

$$\lim_{\delta\to 0} \mu(\{(\rho_1,\rho_2) \in \mathscr{P} : [u(t)-\delta, u(t)+\delta] \cap \{\rho_1,\rho_2\} \neq \emptyset\})$$

$$= \mu(\{u(t)\} \times (u(t),\infty)) \cup ((-\infty, u(t)) \times \{u(t)\}) = 0,$$

which implies the conclusion. □

Now we give conditions ensuring that oscillations are "preserved".

THEOREM 4. *Suppose that μ is such that for certain $L \in \mathbb{R}^+$, $\alpha \in (0,1]$, $\forall r \in \mathbb{R}$, $\forall \delta \in \mathbb{R}^+$,*

$$\mu(\{(\rho_1,\rho_2) \in \mathscr{P} : \{\rho_1,\rho_2\} \cap [r-\delta, r+\delta] \neq \emptyset\}) \leqslant L\delta^\alpha. \tag{11}$$

Then, $\forall u \in C([0,T])$, $\forall a,b \in [0,T]$,

$$os(\mathscr{H}(u,\xi); a, b) \leqslant 4L \cdot os(u; a, b)^\alpha.$$

Proof. Let $a \leqslant s \leqslant t \leqslant b$. Then, as in the proof of Theorem 3,

$$|\mathscr{H}(u,\xi)(t) - \mathscr{H}(u,\xi)(s)|$$

$$\leqslant \int_{\mathscr{P}} (|h_\rho(u,1)(t) - h_\rho(u,1)(s)| + |h_\rho(u,-1)(t) - h_\rho(u,-1)(s)|) d\mu(\rho)$$

If, for some ρ, $|h_\rho(u,1)(t) - h_\rho(u,1)(s)| + |h_\rho(u,-1)(t) - h_\rho(u,-1)(s)| \neq 0$, necessarily $u([s,t]) \cap \{\rho_1,\rho_2\} \neq \emptyset$, so that, a fortiori, as $u([s,t]) \subseteq [u(a) - \delta, u(a) + \delta]$, with $\delta = os(u; a, b)$, we have

$$|\mathscr{H}(u,\xi)(t) - \mathscr{H}(u,\xi)(s)|$$

$$\leqslant 4\mu(\{(\rho_1,\rho_2) \in \mathscr{P} : \{\rho_1,\rho_2\} \cap [u(a)-\delta, u(a)+\delta] \neq \emptyset\}) \leqslant 4L\delta^\alpha.$$

The conclusion follows.

□

So from Theorems 1 and 2, we deduce the following

COROLLARY 2. *Assume that the assumptions of Theorem 6 are satisfied, for some* $\alpha \in (0,1]$. *Then*
(I) $\forall p \in (1,\infty]$, $\forall \beta \in (\frac{1}{p},1)$, $\mathscr{H}(\cdot,\xi)$ *maps* $W^{\beta,p}((0,T))$ *into* $W^{\alpha\beta,\frac{p}{\alpha}}((0,T))$*; moreover, there exists* $C \in \mathbb{R}^+$ *(depending on* μ, ξ, β, p, T*) such that*

$$[\mathscr{H}(u,\xi)]_{W^{\alpha\beta,\frac{p}{\alpha}}((0,T))} \leqslant C\|u\|^{\alpha}_{W^{\beta,p}((0,T))}.$$

In case $\alpha = 1$,
(II) $\forall p \in [1,\infty]$, $\mathscr{H}(\cdot,\xi)$ *maps* $W^{1,p}((0,T))$ *into itself;*
(III) $|\mathscr{H}(u,\xi)'(t)| \leqslant C|u'(t)|$ *a. e. in* $(0,T)$.
(IV) $\mathscr{H}(\cdot,\xi)$ *maps* $C([0,T]) \cap BV((0,T))$ *into itself. Moreover,*

$$V_0^T(\mathscr{H}(u,\xi)) \leqslant CV_0^T(u).$$

In applications, it is often important to know that a certain nonlinear operator enjoys certain regularity properties, one of which is the fact that it is Lipschitz continuous. So we exhibit a sufficient condition, in order that $\mathscr{H}(\cdot,\xi)$ is Lipschitz continuous in $C([0,T])$.

THEOREM 5. *Suppose that the measure* μ *is such that there exists* $L \in \mathbb{R}^+$, *so that, if* $\psi \in \Psi$, $\chi \in X$, $\delta \in \mathbb{R}^+$,

$$\mu(\psi_\delta \cup \chi_\delta) \leqslant L\delta. \tag{12}$$

Then $\mathscr{H}(\cdot,\xi)$ *is Lipschitz continuous from* $C([0,T])$ *into itself.*

Proof. By Remark 3, $\forall r \in \mathbb{R}$, $\forall k \in \mathbb{N}$,

$$\mu(\{(\rho_1,\rho_2) \in \mathscr{P} : r - 1/k \leqslant \rho_1 \leqslant r + 1/k, \rho_2 > r\}$$

$$\cup \{(\rho_1,\rho_2) \in \mathscr{P} : r - 1/k \leqslant \rho_2 \leqslant r + 1/k, \rho_1 < r\}) \leqslant Lk^{-1}.$$

Letting k go to ∞, we deduce that μ satisfies condition (10). So we know from Theorem 3 that $\mathscr{H}(\cdot,\xi)$ maps $C([0,T])$ into itself.

Next, let $u \in C([0,T])$ and let $\delta \in \mathbb{R}^+$. We estimate, for $t \in [0,T]$, $|\mathscr{H}(u+\delta,\xi)(t) - \mathscr{H}(u,\xi)(t)|$. By Proposition 1(III), we have

$$|\mathscr{H}(u+\delta,\xi)(t) - \mathscr{H}(u,\xi)(t)|$$

$$\leqslant \int_{\mathscr{P}} |h_{\rho_1-\delta,\rho_2-\delta}(u,1)(t) - h_{\rho_1-\delta,\rho_2}(u,1)(t)| d\mu(\rho)$$

$$+ \int_{\mathscr{P}} |h_{\rho_1-\delta,\rho_2}(u,1)(t) - h_{\rho_1,\rho_2}(u,1)(t)| d\mu(\rho)$$

$$+ \int_{\mathscr{P}} |h_{\rho_1-\delta,\rho_2-\delta}(u,-1)(t) - h_{\rho_1-\delta,\rho_2}(u,-1)(t)| d\mu(\rho)$$

$$+ \int_{\mathscr{P}} |h_{\rho_1-\delta,\rho_2}(u,-1)(t) - h_{\rho_1,\rho_2}(u,-1)(t)| d\mu(\rho).$$

Assume that

$$|h_{\rho_1-\delta,\rho_2-\delta}(u,1)(t)-h_{\rho_1-\delta,\rho_2}(u,1)(t)|$$

$$=|h_{\rho_1,\rho_2}(u+\delta,1)(t)-h_{\rho_1,\rho_2+\delta}(u+\delta,1)(t)|\neq 0.$$

Therefore,

$$\rho_2\leqslant\psi(u+\delta,1,t)(\rho_1)\leqslant\rho_2+\delta.$$

We deduce

$$\int_{\mathscr{P}}|h_{\rho_1-\delta,\rho_2-\delta}(u,1)(t)-h_{\rho_1-\delta,\rho_2}(u,1)(t)|d\mu(\rho)\leqslant 2L\delta.$$

Treating analogously the other summands, we obtain

$$|\mathscr{H}(u+\delta,\xi)(t)-\mathscr{H}(u,\xi)(t)|\leqslant 8L\delta,\quad\forall t\in[0,T].$$

Replacing u with $u-\delta$, we obtain also

$$|\mathscr{H}(u,\xi)(t)-\mathscr{H}(u-\delta,\xi)(t)|\leqslant 8L\delta,\quad\forall t\in[0,T].$$

Finally, let $v\in C([0,T])$. We set $\delta:=\|u-v\|_{C([0,T])}$. Then

$$u(t)-\delta\leqslant v(t)\leqslant u(t)+\delta\quad\forall t\in[0,T].$$

So, by Proposition 1(II), we have

$$|\mathscr{H}(u,\xi)(t)-\mathscr{H}(v,\xi)(t)|$$

$$\leqslant\mathscr{H}(u+\delta,\xi)(t)-\mathscr{H}(u-\delta,\xi)(t)$$

$$\leqslant|\mathscr{H}(u,\xi)(t)-\mathscr{H}(u-\delta,\xi)(t)|+|\mathscr{H}(u+\delta,\xi)(t)-\mathscr{H}(u,\xi)(t)|\leqslant 8L\delta$$

$$=8L\|u-v\|_{C([0,T])}.$$

The proof is complete.

□

REMARK 4. A sufficient condition implying (10) is $\mu=kd\rho$, with $k\in L^1(\mathscr{P})$. Assume, moreover, that, for some $p\in(1,\infty)$,

$$\int_{\mathbb{R}}\Big(\int_{(\rho_1,\infty)}k(\rho_1,\rho_2)^pd\rho_2\Big)^{1/p}d\rho_1+\int_{\mathbb{R}}\Big(\int_{(-\infty,\rho_2)}k(\rho_1,\rho_2)^pd\rho_1\Big)^{1/p}d\rho_2<\infty. \tag{13}$$

Let $r\in\mathbb{R}$, $\delta\in\mathbb{R}^+$. Then, identifying k with its trivial extension to $\mathbb{R}^2$, we have

$$\mu(\{(\rho_1,\rho_2)\in\mathscr{P}:\{\rho_1,\rho_2\}\cap[r-\delta,r+\delta]\neq\emptyset\})$$

$$\leqslant\int_{\mathbb{R}}\Big(\int_{r-\delta}^{r+\delta}k(\rho_1,\rho_2)d\rho_2\Big)d\rho_1+\int_{\mathbb{R}}\Big(\int_{r-\delta}^{r+\delta}k(\rho_1,\rho_2)d\rho_1\Big)d\rho_2$$

$$\leqslant\delta^\alpha 2^{1-1/p}\Big[\int_{\mathbb{R}}\Big(\int_{r-\delta}^{r+\delta}k(\rho_1,\rho_2)^pd\rho_2\Big)^{1-1/p}d\rho_1+\int_{\mathbb{R}}\Big(\int_{r-\delta}^{r+\delta}k(\rho_1,\rho_2)^pd\rho_1\Big)^{1-1/p}d\rho_2\Big],$$

with

$$\alpha = 1 - \frac{1}{p}. \tag{14}$$

So (11) holds.

Moreover, assume that there exist $K_1, K_2 \in L^1(\mathbb{R})$ such that

$$k(\rho_1, \rho_2) \leqslant \min\{K_1(\rho_1), K_2(\rho_2)\} \quad \text{a.e. in } \mathscr{P}. \tag{15}$$

Let $\psi \in \Psi$, $\delta \in \mathbb{R}^+$. Then

$$\psi_\delta \subseteq \cup_{j\in\mathbb{N}}(I_j \times [\beta_j - \delta, \beta_j + \delta]),$$

with $\{I_j : j \in \mathbb{N}\}$ pairwise disjoint intervals in $\mathbb{R}$, $\beta_j \in \mathbb{R}$. We deduce that

$$\mu(\psi_\delta) = \int_{\psi_\delta} k(\rho_1, \rho_2) d\rho_1 d\rho_2 \leqslant 2\delta \sum_{j\in\mathbb{N}} \int_{I_j} K_1(\rho_1) d\rho_1 \leqslant 2\delta \int_{\mathbb{R}} K_1(\rho_1) d\rho_1,$$

so that the assumptions of Theorem 5 are satisfied. We observe that (15) implies also the validity of (11) with $\alpha = 1$.

REMARK 5. We have assumed that μ is a real positive measure. We can replace this condition with the less restrictive assumption that μ is a real measure with bounded variation. Then Theorem 3, Theorem 6, Corollary 2, Theorem 5 can be extended to this more general situation, replacing the conditions (10), (11), (12) with corresponding conditions involving the variation measure $|\mu|$. The proofs can be easily adapted to this more general situation, employing Hahn's decomposition $\mu = \mu_+ - \mu_-$, with $\mu_\pm$ positive measures.

4. Generalized Plays

Another class of operators allowing applications of the results in Section 2 are Generalized Plays. The simplest case, with $\lambda_r(u) \equiv u$ and $\lambda_l(u) \equiv u + h$, with $h \in \mathbb{R}^+$, is known as "Ordinary Play" and models the interaction between the positions of a piston and of a cylinder (see [1], Chapter 1.2). Broader treatments of this class are given in [1], Chapter 2, and in [3], Chapter VI. We introduce the situation described in [3]. In [1] a slightly more general case is considered. So we introduce the assumption:

(AB) $\lambda_l, \lambda_r \in C(\mathbb{R})$, *they are nondecreasing and* $\lambda_r(u) \leqslant \lambda_l(u)$, $\forall u \in \mathbb{R}$.

We set

$$\Omega := \{(u, x) \in \mathbb{R}^2 : \lambda_r(u) \leqslant x \leqslant \lambda_l(u)\}. \tag{1}$$

Let $u \in C([a,b])$, monotonic, with $a, b \in \mathbb{R}$, $a \leqslant b$ and let $x_0 \in \mathbb{R}$ be such that $(u(a), x_0) \in \Omega$. Then, we set

$$W(a, x_0, u)(t) := \begin{cases} \max\{x_0, \lambda_r(u(t))\} & \text{if } u \text{ is nondecreasing,} \\ \\ \min\{x_0, \lambda_l(u(t))\} & \text{if } u \text{ is nonincreasing.} \end{cases} \tag{2}$$

REMARK 6. Observe that $(u(t),W(a,x_0,u)(t)) \in \Omega\ \forall t \in [a,b]$. In fact, this is obviously true if $W(a,x_0,u)(t) \in \{\lambda_r(u(t)),\lambda_l(u(t))\}$. Moreover, if, for example, u is nondecreasing, in case $W(a,x_0,u)(t)) = x_0$,

$$\lambda_r(u(t)) \leqslant x_0 \leqslant \lambda_l(u(a)) \leqslant \lambda_l(u(t)).$$

Observe also that, in case u is constant, from (2) we obtain

$$W(a,x_0,u)(t) = x_0, \quad \forall t \in [a,b].$$

In general, $W(a,x_0,u)$ is monotonic of the same type of u.

Next, we extend the previous definition to the case that $u \in C([a,b])$ and is piecewise monotonic. Assume that

$$a = t_0 < t_1 < \cdots < t_N = b,$$

and, for each $j \in \{1,\dots,N\}$, $u_{|[t_{j-1},t_j]}$ is monotonic. Then, if $x_0 \in \mathbb{R}$, and $(u(a),x_0) \in \Omega$, we can define $W(a,x_0,u)$ recursively in each interval $[t_{j-1},t_j]$, setting

$$W(a,x_0,u)(t) := \begin{cases} W(a,x_0,u_{|[t_0,t_1]})(t) & \text{if } t \in [t_0,t_1], \\ W(t_j,W(a,x_0,u)(t_j),u_{|[t_j,t_{j+1}]})(t) & \text{if } t \in [t_j,t_{j+1}], \\ & j \in \{1,\dots,N-1\}, \end{cases} \tag{3}$$

where, of course, we employ (2). Observe that $W(t_j,W(a,x_0,u)(t_j),u_{|[t_j,t_{j+1}]})(t)$ is well defined by Remark 6. We leave to the reader the following

PROPOSITION 3. *Let $-\infty < a \leqslant b < \infty$, $x_0 \in \mathbb{R}$, $u,v \in C([a,b])$, piecewise monotonic and such that $(u(a),x_0) \in \Omega$. Then:*
(I) $W(a,x_0,u)$, defined in (3), is independent of the choice of the decomposition $\{a = t_0 < t_1 < \cdots < t_N \leqslant b\}$;
(II) $W(a,x_0,u)([a,b]) \subseteq \{x_0\} \cup (\lambda_r \circ u)([a,b]) \cup (\lambda_l \circ u)([a,b])$.
(III)$W(a,x_0,u) \in C([a,b])$;
(IV) if $a \leqslant \tau \leqslant t \leqslant b$,

$$W(a,x_0,u)(t) = W(\tau,W(a,x_0,u)(\tau),u_{|[\tau,b]})(t).$$

(V) If $\phi : [a,b] \to [a,b]$ is an increasing homeomorphism of $[a,b]$ into itself, then $W(a,x_0,u\circ\phi) = W(a,x_0,u)\circ\phi$.
(VI) If $u,v \in C([a,b])$ and, for some $t \in [a,b]$, $u_{|[a,t]} = v_{|[a,t]}$, then $W(a,x_0,u)_{|[a,t]} = W(a,x_0,v)_{|[a,t]}$.

REMARK 7. (V) and (VI) together state that W is a hysteresis operator (see Remark 1).

PROPOSITION 4. *Let $-\infty < a < b < \infty$, $u, v \in C([a,b])$ piecewise monotonic, such that $u(t) \leqslant v(t)\ \forall t \in [a,b]$, $x_0, x_1 \in \mathbb{R}$, $x_0 \leqslant x_1$, so that $(u(a), x_0)$, $(v(a), x_1)$ are in Ω. Then*

$$W(a,x_0,u)(t) \leqslant W(a,x_1,v)(t), \quad \forall t \in [a,b]. \tag{4}$$

Proof. The core of the proof consists in showing that (4) holds in some right neighborhood of a in case u and v are monotonic. This is almost obvious, except in the case that $x_0 = x_1$, u is nondecreasing and v is nonincreasing. In this case, $W(a,x_0,u)(t) = W(a,x_1,v)(t) = x_0$ in some right neighborhood of a. We limit ourselves to show that $W(a,x_0,u)(t) = x_0$ in some right neighborhood of a. This is clear in case $\lambda_r(u(a)) < x_0$. So we assume that $\lambda_r(u(a)) = x_0$. If $u(a) = v(a)$, then $u(t) = v(t) = u(a)\ \forall t \in [a,b]$, so that $W(a,x_0,u)(t) = x_0\ \forall t \in [a,b]$. Finally, assume that $\lambda_r(u(a)) = x_0$ and $u(a) < v(a)$. Then, $u(t) \leqslant v(t) \leqslant v(a)\ \forall t \in [a,b]$. So

$$x_0 \leqslant \lambda_r(u(t)) \leqslant \lambda_r(v(a)) \leqslant x_0$$

because $(v(a), x_0) \in \Omega$. We conclude that $W(a,x_0,u)(t) = x_0$.

Now we prove the general statement. We set

$$A := \{t \in [a,b] : W(a,x_1,v)(t) < W(a,x_0,u)(t)\}.$$

We assume, by contradiction, that $A \neq \emptyset$ and we put $\tau := \inf(A)$. Then, clearly, by continuity, $a \leqslant \tau < b$, and, from $x_0 \leqslant x_1$, $W(a,x_0,u)(t) \leqslant W(a,x_1,v)(t)\ \forall t \in [a,\tau]$, $W(a,x_0,u)(\tau) = W(a,x_1,v)(\tau)$. By Proposition 3 (IV), we have, if $t \in [\tau,b]$,

$$W(a,x_0,u)(t) = W(\tau, W(a,x_0,u)(\tau),$$

$$u_{|[\tau,t]})(t), W(a,x_0,v)(t) = W(\tau, W(a,x_0,u)(\tau), v_{|[\tau,t]})(t).$$

So, from the first part of the proof, we deduce that $W(a,x_0,u)(t) \leqslant W(a,x_0,v)(t)$ for t in some right neighbourhood of τ, in contradiction with the definition of τ. □

Now we introduce the following notation: let I be an interval in $\mathbb{R}$, $f \in C(I)$, $\alpha, \beta \in I$, with $\alpha \leqslant \beta$, $\rho \in \mathbb{R}^+$. We set

$$\omega(f,\alpha,\beta,\rho) := \sup_{t,s \in [\alpha,\beta], |t-s| \leqslant \rho} |f(t) - f(s)|. \tag{5}$$

We have:

LEMMA 4. *Let $u \in C([a,b])$ be piecewise monotonic and let $\rho \geqslant 0$, $x_0, x_1 \in \mathbb{R}$, with $x_0 \leqslant x_1$, $(u(a), x_0)$ and $(u(a)+\rho, x_1)$ in Ω. Then, $\forall t \in [a,b]$,*

(6)

$$|W(a,x_1,u+\rho)(t) - W(a,x_0,u)(t)|$$

$$\leqslant \max\{x_1 - x_0, \omega(\lambda_r, \min_{[a,b]} u, \max_{[a,b]} u + \rho, \rho), \omega(\lambda_l, \min_{[a,b]} u, \max_{[a,b]} u + \rho, \rho)\}.$$

Proof. Let M be the second term in (6). We assume that $a = t_0 < t_1 < \cdots < t_N$ and u is monotonic in each interval $[t_0,t_1],\dots,[t_{N-1},t_N]$. We observe firstly that, by Proposition 4, $W(a,x_1,u+\rho)(t) - W(a,x_0,u)(t) \geqslant 0\ \forall t \in [a,b]$. We shall show that $W(a,x_1,u+\rho)(t) - W(a,x_0,u)(t) \leqslant M\ \forall t \in [a,b]$. We start by proving this inequality if $t \in [t_0,t_1]$, assuming (for example) that in this interval u is nondecreasing. Then, if $t \in [t_0,t_1]$,

$$W(a,x_1,u+\rho)(t) - W(a,x_0,u)(t) = \max\{x_1,\lambda_r(u(t)+\rho)\} - \max\{x_0,\lambda_r(u(t))\}$$

$$\leqslant \max\{x_1-x_0,\lambda_r(u(t)+\rho)-\lambda_r(u(t))\} \leqslant M.$$

We assume that (6) holds if $t \leqslant t_j$, with $1 \leqslant j < N$. Then, it $t \in [t_j,t_{j+1}]$ and u is (say) non increasing in this interval, then

$$W(a,x_1,u+\rho)(t) - W(a,x_0,u)(t)$$

$$= \min\{W(a,x_1,u+\rho)(t_j),\lambda_l(u(t)+\rho)\} - \min\{W(a,x_0,u)(t_j),\lambda_l(u(t))\}$$

$$\leqslant \max\{W(a,x_1,u+\rho)(t_j) - W(a,x_0,u)(t_j),\lambda_l(u(t)+\rho)-\lambda_l(u(t))\} \leqslant M.$$

□

REMARK 8. Employing Lemma 4 in case $\rho = 0$, we get

$$|W(a,x_1,u)(t) - W(a,x_0,u)(t)| \leqslant x_1 - x_0 \quad \forall t \in [a,b]. \tag{7}$$

We deduce the following

PROPOSITION 5. *Let $u,v \in C([a,b])$ be piecewise monotonic, $x_0,x_1 \in \mathbb{R}$, with $(u(a),x_0),(v(a),x_1) \in \Omega$. We set*

$$\rho := \|u-v\|_{C([a,b]}.$$

Then

$$\|W(a,x_1,v) - W(a,x_0,u)\|_{C([a,b])}$$

$$\leqslant 2\max\{|x_1-x_0|,\omega(\lambda_r,\min_{[a,b]} u-\rho,\max_{[a,b]} u+\rho,\rho),$$

$$\omega(\lambda_l,\min_{[a,b]} u-\rho,\max_{[a,b]} u+\rho,\rho)\}.$$

Proof. We set

$$x_2 := \max\{x_0,x_1,\lambda_r(u(a)+\rho)\},$$
$$x_3 := \min\{x_0,x_1,\lambda_l(u(a)-\rho)\}.$$

Then, $x_3 \leqslant x_2$, $(u(a)+\rho,x_2),(u(a)-\rho,x_3) \in \Omega$, as,

$$\lambda_r(u(a)+\rho) \leqslant x_2 \leqslant \max\{\lambda_l(u(a)),\lambda_l(v(a)),\lambda_r(u(a)+\rho)\} \leqslant \lambda_l(u(a)+\rho),$$

$$\lambda_r(u(a)-\rho) \leqslant \min\{\lambda_r(u(a)),\lambda_r(v(a)),\lambda_l(u(a)-\rho)\} \leqslant x_3 \leqslant \lambda_l(u(a)-\rho).$$

So, by Proposition 4 and Lemma 4, we have, $\forall t \in [a,b]$,

$$|W(a,x_1,v)(t) - W(a,x_0,u)(t)| \leqslant W(a,x_2,u+\rho)(t) - W(a,x_3,u-\rho)(t)$$

$$= [W(a,x_2,u+\rho)(t) - W(a,x_0,u)(t)] + [W(a,x_0,u)(t)] - W(a,x_3,u-\rho)(t)]$$

$$\leqslant \max\{x_2 - x_0, \omega(\lambda_r, \min_{[a,b]} u, \max_{[a,b]} u + \rho, \rho), \omega(\lambda_l, \min_{[a,b]} u, \max_{[a,b]} u + \rho, \rho)\}$$

$$+ \max\{x_0 - x_3, \omega(\lambda_r, \min_{[a,b]} u - \rho, \max_{[a,b]} u, \rho), \omega(\lambda_l, \min_{[a,b]} u - \rho, \max_{[a,b]} u, \rho)\}.$$

Moreover, in case $x_2 = \lambda_r(u(a)+\rho)$, we have

$$x_2 - x_0 \leqslant \lambda_r(u(a)+\rho) - \lambda_r(u(a)) \leqslant \omega(\lambda_r, \min_{[a,b]} u - \rho, \max_{[a,b]} u + \rho, \rho)$$

and, in case $x_3 = \lambda_l(u(a)-\rho)$,

$$x_0 - x_3 \leqslant \lambda_l(u(a)) - \lambda_l(u(a)-\rho) \leqslant \omega(\lambda_l, \min_{[a,b]} u - \rho, \max_{[a,b]} u + \rho, \rho).$$

The conclusion follows. □

COROLLARY 3. *Let $u \in C([a,b])$ and $x_0 \in \mathbb{R}$ be such that $(u(a),x_0) \in \Omega$. Let $(u_n)_{n\in\mathbb{N}}$ be a sequence of continuous and piecewise monotonic functions, uniformly converging to u and $(x_n)_{n\in\mathbb{N}}$ a sequence in $\mathbb{R}$, converging to x_0, and such that $(u_n(a),x_n) \in \Omega$ $\forall n \in \mathbb{N}$. Then the sequence $(W(a,x_n,u_n))_{n\in\mathbb{N}}$ converges uniformly in $[a,b]$. The limit depends only on u and x_0.*

Proof. Let α and β be real numbers, such that $\alpha \leqslant u_n(t) \leqslant \beta$ if (say) $n \geqslant n_0$. Let $\varepsilon \in \mathbb{R}^+$ and let $\rho \in (0,1]$, be such that

$$\max\{\omega(\lambda_r, \alpha-1, \beta+1, \rho), \omega(\lambda_l, \alpha-1, \beta+1, \rho)\} \leqslant \frac{\varepsilon}{2}.$$

The existence of ρ is a consequence of the local uniform continuity of λ_r and λ_l. Then, if $\min\{m,n\} \geqslant n_0$, by Proposition 5, in case $|x_n - x_m| \leqslant \frac{\varepsilon}{2}$., we have

$$\|W(a,x_n,u_n) - W(a,x_m,u_m)\|_{C([a,b])} \leqslant \varepsilon.$$

The conclusion follows easily. □

So we are able to state and prove the following

THEOREM 6. *Let $-\infty < a \leqslant b < \infty$, $x_0 \in \mathbb{R}$, $u \in C([a,b])$ and such that $(u(a),x_0)$ $\in \Omega$. Then:*

(I) there exists a sequence (x_n,u_n) in $\mathbb{R} \times C([a,b])$ such that $(u_n(a),x_n) \in \Omega$ $\forall n \in \mathbb{N}$, u_n is piecewise monotonic for every $n \in \mathbb{N}$ and $(x_n,u_n)_{n\in\mathbb{N}}$ converges to (x_0,u) in $\mathbb{R} \times C([a,b])$.

(II) The corresponding sequence $(W(a,x_n,u_n))_{n\in\mathbb{N}}$ *converges uniformly to an element* $W(a,x_0,u)$ *of* $C([a,b])$*. Such element does not depend on the sequence* $(x_n,u_n)_{n\in\mathbb{N}}$ *with the declared properties.*
(III) $\forall t\in[a,b]$, $W(a,x_0,u)(t)\in[\lambda_r(u(t)),\lambda_l(u(t))]$*;*
(IV) $W(a,x_0,u)([a,b])\subseteq\{x_0\}\cup(\lambda_r\circ u)([a,b])\cup(\lambda_l\circ u)([a,b])$*;*
(V) if $a\leqslant\tau\leqslant t\leqslant b$*,*

$$W(a,x_0,u)(t)=W(\tau,W(a,x_0,u)(\tau),u_{|[\tau,b]})(t);$$

(VI) let $v\in C([a,b])$ *be such that* $u(t)\leqslant v(t)$ $\forall t\in[a,b]$, $x_1\in\mathbb{R}$*, with* $x_0\leqslant x_1$ *and* $(v(a),x_1)$ *in* Ω*. Then*

$$W(a,x_0,u)(t)\leqslant W(a,x_1,v)(t),\quad\forall t\in[a,b].$$

(VII) If $\phi:[a,b]\to[a,b]$ *is an increasing homeomorphism of* $[a,b]$ *into itself, then* $W(a,x_0,u\circ\phi)=W(a,x_0,u)\circ\phi$*.*
(VIII) If $u,v\in C([a,b])$ *and, for some* $t\in[a,b]$, $u_{|[a,t]}=v_{|[a,t]}$*, then* $W(a,x_0,u)_{|[a,t]}=W(a,x_0,v)_{|[a,t]}$*.*
(IX) Let $u,v\in C([a,b])$, $x_0,x_1\in\mathbb{R}$*, with* $(u(a),x_0),(v(a),x_1)\in\Omega$*. We set*

$$\rho:=\|u-v\|_{C([a,b])}.$$

Then

$$\|W(a,x_1,v)-W(a,x_0,u)\|_{C([a,b])}$$

$$\leqslant 2\max\{|x_1-x_0|,\omega(\lambda_r,\min_{[a,b]}u-\rho,\max_{[a,b]}u+\rho,\rho),$$

$$\omega(\lambda_l,\min_{[a,b]}u-\rho,\max_{[a,b]}u+\rho,\rho)\}.$$

Proof. We prove only (I). The other statements can be proved passing to the limit in an appropriate sequence (x_n,u_n), with u_n piecewise monotonic. We take $z_n\in C([a,b])$, piecewise monotonic, such that $\|z_n-u\|_{C([a,b])}\leqslant\frac{1}{2n}$ and set $u_n:=z_n-\frac{1}{n}$, in such a way that, $\forall t\in[a,b]$,

$$u_n(t)=z_n(t)-\frac{1}{n}\leqslant u(t)+\frac{1}{2n}-\frac{1}{n}<u(t),$$

and $x_n:=\min\{x_0,\lambda_l(u_n(a))\}$, so that

$$\lambda_l(u_n(a))\geqslant x_n\geqslant\min\{\lambda_r(u(a)),\lambda_l(u_n(a))\}\geqslant\lambda_r(u_n(a))$$

and $(u_n(a),x_n)\in\Omega$. □

Now, we introduce the following assumption

(AC) Let $\alpha\in(0,1]$*. Then,* $\forall M\in\mathbb{R}^+$ *there exists* $\Gamma(M)\in\mathbb{R}^+$*, such that, if* $u,v\in\mathbb{R}$ *and* $\max\{|u|,|v|\}\leqslant M$*,*

$$\max\{|\lambda_r(u)-\lambda_r(v)|,|\lambda_l(u)-\lambda_l(v)|\}\leqslant\Gamma(M)|u-v|^\alpha.$$

From Theorem 6 and (AC), we immediately deduce the following

COROLLARY 4. *Assume that (AC) holds. Then, if* $u,v \in C([a,b])$, $x_0,x_1 \in \mathbb{R}$, $(u(a),x_0),(v(a),x_1) \in \Omega$ *and* $\|u\|_{C([a,b])} \leqslant M$,

$$\|W(a,x_1,v) - W(a,x_0,u)\|_{C([a,b])}$$

$$\leqslant 2max\{|x_1-x_0|, \Gamma(M+\|u-v\|_{C([a,b])})\|u-v\|^{\alpha}_{C([a,b])}\}.$$

Finally, we study how Generalized Plays modify oscillations. The following fact holds:

PROPOSITION 6. *(I) Assume that (AB) holds. Let* $u \in C([a,b])$ *and* $x_0 \in \mathbb{R}$ *be such that* $(u(a),x_0) \in \Omega$. *Then:*

$$os(W(a,x_0,u);a,b) \leqslant os(\lambda_r \circ u;a,b) + os(\lambda_l \circ u;a,b).$$

(III) Assume that (AC) holds. Then if $a \leqslant s \leqslant t \leqslant b$,

$$os(W(a,x_0,u);a,b) \leqslant C(\|u\|_{C([a,b])})os(u;s,t)^{\alpha}.$$

Proof. (I) If u is piecewise monotonic, it follows easily that, either $W(a,x_0,u)(t) = x_0$ $\forall t \in [a,b]$, or the range of $W(a,x_0,u)$ is contained in $(\lambda_r \circ u)([a,b]) \cup (\lambda_l \circ u)([a,b])$. Let $t \in [a,b)$, $h \in \mathbb{R}^+$ be such that $t < t+h \leqslant b$. Assume that $W(a,x_0,u)$ is not constant in $[t,t+h]$. We set

$$t_0 := \inf\{s \in [t,t+h] : W(a,x_0,u)(s) \neq W(a,x_0,u)(t)\},$$

$$t_1 := \sup\{s \in [t,t+h] : W(a,x_0,u)(s) \neq W(a,x_0,u)(t+h)\}.$$

Then, $t \leqslant t_0 < t_1 \leqslant t+h$, $W(a,x_0,u)(t) = W(a,x_0,u)(t_0)$,

$$W(a,x_0,u)(t+h) = W(a,x_0,u)(t_1)$$

and

$$W(a,x_0,u)(t_0) \in \{\lambda_r(u(t_0)),\lambda_l(u(t_0))\}, \quad W(a,x_0,u)(t_1) \in \{\lambda_r(u(t_1)),\lambda_l(u(t_1))\}.$$

Suppose that (for example)

$$W(a,x_0,u)(t_0) = \lambda_r(u(t_0)) \neq \lambda_l(u(t_0)), W(a,x_0,u)(t_1) = \lambda_l(u(t_1)) \neq \lambda_r(u(t_1)).$$

We set

$$t_2 := \sup\{s \in [t_0,t_1] : W(a,x_0,u)(s) = \lambda_r(u(s))\},$$

$$t_3 := \inf\{s \in [t_2,t_1] : W(a,x_0,u)(s) = \lambda_l(u(s))\}.$$

Then $W(a,x_0,u)(t_2)=\lambda_r(u(t_2))$, $W(a,x_0,u)(t_3)=\lambda_l(u(t_3))$, $t_0\leqslant t_2\leqslant t_3\leqslant t_1$. It is clear that $W(a,x_0,u)$ is constant in $[t_2,t_3]$ and so $\lambda_r(u(t_2))=\lambda_l(u(t_3))$. Therefore,

$$|W(a,x_0,u)(t+h)-W(a,x_0,u)(t)|=|W(a,x_0,u)(t_1)-W(a,x_0,u)(t_0)|$$

$$=|\lambda_l(u(t_1))-\lambda_r(u(t_0)|\leqslant|\lambda_l(u(t_1))-\lambda_l(u(t_3))|+|\lambda_r(u(t_2))-\lambda_l(u(t_0))|$$

$$\leqslant os(\lambda_r\circ u,a;b)+os(\lambda_l\circ u;a,b).$$

So the case of u piecewise monotonic is done. The general case follows by approximation.

Concerning (II), from (I) and Theorem 6(V) we have

$$os(W(a,x_0,u);s,t)\leqslant os(\lambda_r\circ u;s,t)+os(\lambda_l\circ u;s,t)\leqslant C(\|u\|_{C([a,b])})(t-s)^{\alpha}.$$

□

So from Theorems 1 and 2, we deduce the following

COROLLARY 5. *Assume that the assumptions (AB) and (AC) hold, for some* $\alpha\in(0,1]$. *Let* $x_0\in\mathbb{R}$. *Then*
(I) $\forall p\in(1,\infty]$, $\forall\beta\in(\frac{1}{p},1)$, $W(a,x_0,\cdot)$ *maps* $\{u\in W^{\beta,p}((0,T)):(u(a),x_0)\in\Omega\}$ *into* $W^{\alpha\beta,\frac{p}{\alpha}}((a,b))$*; moreover,*

$$[W(a,x_0,u)]_{W^{\alpha\beta,\frac{p}{\alpha}}((0,T))}\leqslant C(\|u\|_{C([a,b])})\|u\|^{\alpha}_{W^{\beta,p}((0,T))}.$$

In case $\alpha=1$,
(II) $\forall p\in[1,\infty]$, $W(a,x_0,\cdot)$ *maps* $\{u\in W^{1,p}((a,b)):(u(a),x_0)\in\Omega\}$ *into* $W^{1,p}((a,b))$*;*
(III) moreover, $|W(a,x_0,u)'(t)|\leqslant C(\|u\|_{C([a,b])})|u'(t)|$ *a. e. in* (a,b).
(IV) $W(a,x_0,\cdot)$ *maps* $\{u\in C([a,b])\cap BV((a,b)):(u(a),x_0)\in\Omega\}$ *into* $C([a,b])\cap BV((a,b))$. *Moreover,*

$$V_a^b(W(a,x_0,\cdot))\leqslant C(\|u\|_{C([a,b])})V_a^b(u).$$

References

[1] KRASNOSELSKII M., POKROVSKII A., *Systems with Hysteresis*, Springer-Verlag, 1980.

[2] TRIEBEL H., *Theory of Function Spaces*, Birkhäuser, 1983.

[3] VISINTIN A., *Differential Models for Hysteresis*, Applied Mathematical Sciences vol. 111, Springer-Verlag, 1994.

AMS Subject Classification: 47H30

Davide GUIDETTI,
Dipartimento di matematica, Università di Bologna
Piazza di Porta S.Donato 5, 40126 Bologna, ITALY
e-mail: davide.guidetti@unibo.it

Lavoro pervenuto in redazione il 29.01.2015.

Rend. Sem. Mat. Univ. Politec. Torino
Vol. 72, 1–2 (2014), 57 – 71

P. Nábělková

FLOW IN SOILS WITH HYSTERESIS

Abstract. Hysteresis in single–porosity flow through homogeneous unsaturated medium and in double–porosity model of Darcian flows through two distinct pore systems both treated as homogeneous media is here illustrated. Darcy's law and equation of continuity lead to nonlinear diffusion equation for single–porosity flow and to two coupled systems of nonlinear partial differential equations for double–porosity model. The effects of hysteresis in the relation between pressure and water content are represented by Preisach hysteresis operator. The existence results of the initial–boundary–value problems for both models with soil–moisture Preisach hysteresis term are summarized here.

1. Introduction

Unsaturated fluid flow through porous media is an important topic in hydrology, agronomy and soil physics. Fluid movement in unsaturated soil is subject to hysteresis. The soil–moisture hysteresis is observed in cycles of wetting–drying processes in soil. Thus hysteretic effects are in the relation between the volumetric water content and the pressure and are modeled by Preisach operator. Phenomenon of hysteresis has been investigated by different authors and for distinct applications. Already in 1930, Haines [12] had postulated that drying occurs at a higher value of pressure as the narrower section of the pores governs this process, while wetting happens at a lower pressure value originated by the wider section of the pores. This phenomenon has also been explained in these terms by using the concept of a "pore domain". The simplest version of the domain theory is the so called *independent domain theory*, where a domain consists of a unique pore of a given geometry acting independently from others, i.e., pores behave as if each one was directly connected to the outer boundary sample. This theory was conceived by Everett [7, 8, 9]. The independent domain model, which is essentially the Preisach model, was adopted by Poulovassilis [23], Mualem [20] and Parlange [22].

Concerning the single–porosity flow equation with excluded hysteresis relation, in [25], the authors proved the existence of a strong solution. There are papers devoted to this equation taking into consideration the hysteresis behaviour [2, 3, 14, 19]. In [2] existence result with hysteresis operator of Preisach type is established. Paper [3] deals with existence and asymptotic behaviour of solution. In paper [19] the wellposedness of the problem is shown. In [14] the existence of the solution to the single–porosity model of water flow with Preisach hysteresis operator was proved.

In [1], the author proved the global existence of weak solutions to the double–porosity (dual) model with mixed Dirichlet–Neumann boundary conditions. The existence and uniqueness of the solution to the dual water flow through porous media without hysteresis and with unilateral boundary conditions were obtained in [4]. In [15], the authors proved the existence of the solution to the model including dual approach, hysteresis as well as the unilateral boundary conditions.

The paper is organized as follows. In Section 2, we briefly review some basic

definitions in the unsaturated flow and recall some basic results concerning the hysteresis operators. In Section 3 we introduce the equations representing single–porosity and double–porosity flows through porous media. The existence of weak solutions to the model equations are summed up in Section 4.

2. Preliminaries

2.1. Soil structure. Soil–moisture hysteresis

A soil is a porous medium which consists of particles of varying sizes. These particles join together and the spacings among them are known as pore spaces (or voids), as shown in Figure 1.

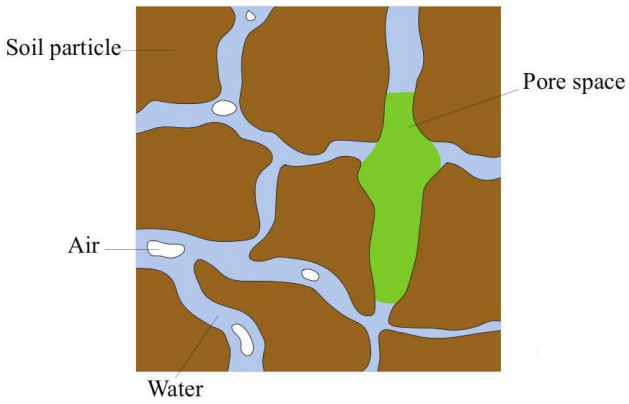

Figure 1: Schematic picture of the microstructure of a porous medium. Pore spaces can be either filled, partially filled or empty depending on the pressure head.

The soil is saturated if the pore spaces are completely filled with water. We call the water motion in this situation saturated flow. In the unsaturated case there are voids filled with air and the flow is said to be unsaturated. However, partially saturated zones may occur when all pores within them are filled with water. Then the interfaces between the saturated and unsaturated regions of the soil become free boundaries. The flow is termed saturated–unsaturated.

Water movement in unsaturated soil is subject to hysteresis, although its effects are often masked by heterogeneities. The hysteretic effect may be attributed to several factors [5, 13]:

1) the effects of nonhomogeneous pore size distribution, often referred as "ink–bottle effect",
2) entrapped air, which refers to the formation of closed air bubbles during wetting,

3) capillary condensation, which is related to adsorbed water films on the surfaces of fine–grained particles,

4) contact angle hysteresis, which is related to the difference between drying and wetting contact angles at the solid–water interface.

It was shown experimentally that there is hysteresis in the relationship between soil pressure and water content, see [12, 21, 24]. The hysteretic effect is observed in wetting–drying processes, i.e., is evident in the soil–water characteristic curve.

We can consider pore spaces as capillary tubes. The bulge in the centre of the tube can be considered as the pore. Now each pore is connected to a neighbouring pore by means of a pore throat with narrow end of the capillary tube (Figure 2). When an empty tube is placed into a water bath, water will rise up to a point above the waist of the tube until the water reaches its equilibrium state (wetting process). Likewise when a tube filled with water is placed into the same water bath, the water level will be moving down towards the waist until the water reaches its equilibrium state (drying process).

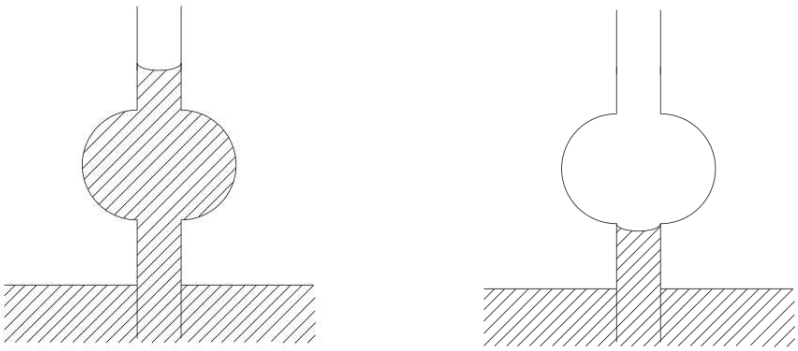

Figure 2: Simple model of the pore spaces represented by capillary tubes.

2.2. Hysteresis operators

The play operator

Now we briefly recall definition and properties of the play operator, the simplest example of continuous hysteresis operator. Let $r > 0$ be a given parameter. For a given input function $u \in C([0,T])$ and initial condition $x_r^0 \in [-r,r]$, we define the output $\xi := \mathscr{P}_r[x_r^0, u] \in C([0,T]) \cap BV(0,T)$ of the play operator

$$\mathscr{P}_r : [-r,r] \times C([0,T]) \to C([0,T]) \cap BV(0,T)$$

as the solution of the variational inequality in Stieltjes integral form

$$\begin{aligned}
&\int_0^T [u(t)-\xi(t)-y(t)]\,\mathrm{d}\xi(t) \geqslant 0, \quad \forall y \in C([0,T]),\ \max_{0\leqslant t\leqslant T}|y(t)| \leqslant r,\\
&|u(t)-\xi(t)| \leqslant r, \quad \forall t \in [0,T],\\
&\xi(0) = u(0) - x_r^0. \qquad (1)
\end{aligned}$$

In order to model a more complex hysteresis behavior, we consider the whole family of play operators $\mathscr{P}_r$ parametrized by $r > 0$, which can be interpreted as a memory variable. More precisely, following [16, Section II.2], we introduce the *configuration space* as well as its subspaces

$$\Lambda := \left\{ \lambda \in W^{1,\infty}(0,\infty); \left|\frac{d\lambda(r)}{dr}\right| \leqslant 1 \quad \text{a.e. in } (0,\infty) \right\}, \qquad (2)$$

$$\Lambda_K := \{\lambda \in \Lambda; \lambda(r) = 0 \quad \text{for } r \geqslant K\}, \quad \Lambda_0 := \bigcup_{K>0} \Lambda_K. \qquad (3)$$

The functions $\lambda \in \Lambda$ are called *memory configurations*. For a given $\lambda \in \Lambda$, we define the initial condition x_r^0 by formula $x_r^0 := Q_r(u(0) - \lambda(r))$, where $Q_r : \mathbb{R} \to [-r,r]$ is the projection

$$Q_r(x) := \operatorname{sign}(x) \min\{r, |x|\} = \min\{r, \max\{-r, x\}\}.$$

This implies that the initial configuration of the play system depends on λ and on $u(0)$. So we can introduce the following more convenient notation

$$p_r[\lambda, u] := \mathscr{P}_r[x_r^0, u], \qquad (4)$$

for any $\lambda \in \Lambda$, $u \in C([0,T])$ and $r > 0$.

The reason for introducing the space Λ is that for every fixed $t \in [0,T]$ and $\lambda \in \Lambda$, the state mapping $r \to p_r[\lambda,u](t)$ belongs to Λ.

In [18], the play operator is definied in the space $G_R(0,T)$ of right–continuous regulated functions. This is the space of functions $u : [0,T] \to \mathbb{R}$ which admits the left limit $u(t_-)$ at each point $t > 0$ and the right limit $u(t_+)$ exists and coincides with $u(t)$ at each point $t \geqslant 0$. The space $G_R(0,T)$ is endowed with the norm

$$\|u\|_{[0,T]} = \sup\{|u(\tau)|; \tau \in [0,T]\} \quad \text{for } u \in G_R(0,T), \qquad (5)$$

hence $G_R(0,T)$ is a Banach space. By [18, Theorem 2.1 and Proposition 2.4], this is Lipschitz continuous in the sense that

$$|p_r[\lambda,u](t) - p_r[\mu,v](t)| \leqslant \max\{|\lambda(r) - \mu(r)|, \|u - v\|_{[0,T]}\} \qquad (6)$$

for any $\lambda, \mu \in \Lambda$, $u, v \in G_R(0,T)$ and $t \in [0,T]$. For step functions $u \in G_R(0,T)$ of the form

$$u(t) = \sum_{n=1}^{m} u_m^{n-1} \chi_{[t_{n-1},t_n)}(t) + u_m^m \chi_{\{T\}}(t), \qquad (7)$$

where $0 = t_0 < t_1 < \ldots t_m = T$ is a given division of $[0,T]$, we have in particular

$$p_r[\lambda,u](t) = \sum_{n=1}^{m} \xi_m^{n-1}(r)\chi_{[t_{n-1},t_n)}(t) + \xi_m^m(r)\chi_{\{T\}}(t), \tag{8}$$

where $\chi_\omega(t)$ is the characteristic function of a set $\omega \subset [0,T]$, and

$$\xi_m^0(r) = P[\lambda, u_m^0](r), \quad \xi_m^n(r) = P[\xi_m^{n-1}, u_m^n](r), \tag{9}$$

with $P : \Lambda \times \mathbb{R} \to \Lambda$ defined as

$$P[\lambda,v](r) = \max\{v-r, \min\{v+r, \lambda(r)\}\}. \tag{10}$$

The Preisach operator

Now we briefly recall definition and some basic properties of the Preisach operator. Let us introduce the Preisach half–plane, defined as

$$\mathbb{R}^2_+ := \{(r,v) \in \mathbb{R}^2 : r > 0\} \tag{11}$$

and assume that a function $\psi \in L^1_{loc}(\mathbb{R}^2_+)$ (the Preisach density) is given with the following property.

ASSUMPTION 1. There exist $\beta_1 \in L^1_{loc}(0,\infty)$, such that

$$0 \leqslant \psi(r,v) \leqslant \beta_1(r) \quad \text{for a.e. } (r,v) \in \mathbb{R}^2_+.$$

We put

$$b_1(K) := \int_0^K \beta_1(r)\,\mathrm{d}r \quad \text{for } K > 0, \quad g(r,v) := \int_0^v \psi(r,x)\,\mathrm{d}x \quad \text{for } (r,v) \in \mathbb{R}^2_+ \tag{12}$$

and define the Preisach operator as follows.

DEFINITION 1. *Let $\psi \in L^1_{loc}(\mathbb{R}^2_+)$ be given and let g be as in* (12)*. Then the Preisach operator $\mathscr{W} : \Lambda_0 \times G_R(0,T) \to G_R(0,T)$ generated by the function g is defined by the formula*

$$\mathscr{W}[\lambda,u](t) := \int_0^\infty g(r, p_r[\lambda,u](t))\,\mathrm{d}r = \int_0^\infty \int_0^{p_r[\lambda,u](t)} \psi(r,x)\,\mathrm{d}x\,\mathrm{d}r \tag{13}$$

for $\lambda \in \Lambda_0$, $u \in G_R(0,T)$ and $t \in [0,T]$.

As a counterpart of [16, Section II.3, Proposition 3.11], we have the following

PROPOSITION 1. *Let Assumption 1 be satisfied and let $K > 0$ be given. Then for every $\lambda, \mu \in \Lambda_K$ and $u, v \in G_R(0,T)$ such that $\|u\|_{[0,T]}, \|v\|_{[0,T]} \leqslant K$, the Preisach operator (13) satisfies*

$$\|\mathscr{W}[\lambda,u] - \mathscr{W}[\mu,v]\|_{[0,T]} \leqslant \int_0^K |\lambda(r) - \mu(r)|\beta_1(r)\,\mathrm{d}r + b_1(K)\|u-v\|_{[0,T]} \quad \forall t \in [0,T].$$

We finally quote the Hilpert inequality which will be used to establish the uniqueness of the solution.

PROPOSITION 2. *Let $\mathscr{W}$ be a Preisach operator (13) satisfying Assumption 1. For given $u_1, u_2 \in W^{1,1}(0,T)$, $\lambda_1, \lambda_2 \in \Lambda_0$ put $\xi_r^i := p_r[\lambda, u]$, $w_i := \mathscr{W}[\lambda_i, u_i] = \int_0^\infty g(r, \xi_r^i)\,\mathrm{d}r$, $i = 1,2$. Then for a.e. $t \in (0,T)$ we have*

$$\frac{d}{dt}(w_1(t) - w_2(t))\; H(u_1(t) - u_2(t)) \geqslant \frac{d}{dt} \int_0^\infty (g(r, \xi_r^1(t)) - g(r, \xi_r^2(t))^+ \,\mathrm{d}r, \tag{14}$$

where H is the Heaviside function.

In our equation, both the input function and the initial memory configuration depend on the space variable x. If $\lambda(x,\cdot)$ belongs to Λ_0 and $u(x,\cdot)$ belongs to $C([0,T])$ for (almost) every x, then we can define

$$\mathscr{W}[\lambda, u](x,t) := \int_0^\infty g(r, p_r[\lambda(x,\cdot), u(x,\cdot)](t))\,\mathrm{d}r. \tag{15}$$

In the following we will often write $\mathscr{W}(u)$ instead of $\mathscr{W}[\lambda, u]$ for brevity or when λ is clear from the context.

We conclude this subsection with the convexification of the Preisach operator, i.e., that in a certain region, the convexity of the loops is satisfied (see [16, Section II.4, Proposition 4.22]).

Let $R > 0$ be fixed, set

$$\mathscr{D}_R := \{(r,v) \in \mathbb{R}^2_+ : |v| + r \leqslant R\}.$$

In addition to Assumption 1 we prescribe the following conditions.

ASSUMPTION 2.

1. $\frac{\partial \psi}{\partial v} \in L^\infty_{loc}(\mathbb{R}^2_+)$;
2. $A_R := \inf\{\psi(r,v); (r,v) \in \mathscr{D}_R\} > 0$.

Furthermore, denote

$$C_R := \sup\left\{ \left| \frac{\partial}{\partial v} \psi(r,v) \right| ; (r,v) \in \mathscr{D}_R \right\}.$$

Taking possibly a smaller $R > 0$, if necessary, we may assume that

$$K_R := \frac{1}{2} A_R - R C_R > 0. \tag{16}$$

We modify the density ψ outside $\mathscr{D}_R$ and set

$$\psi_R(r,v) = \begin{cases} \psi(r,v) & \text{if} \quad (r,v) \in \mathscr{D}_R, \\ \psi(r, -R + r) & \text{if} \quad v < -R + r,\ r \leqslant R, \\ \psi(r, R - r) & \text{if} \quad v > R - r,\ r \leqslant R, \\ \psi(R, 0) & \text{if} \quad r > R. \end{cases} \tag{17}$$

We define the convexified Preisach operator $\mathscr{W}_R$ by the formula

$$\mathscr{W}_R[\lambda,u](t)=\int_0^\infty\int_0^{p_r[\lambda,u](t)}\psi_R(r,v)\,\mathrm{d}v\,\mathrm{d}r \tag{18}$$

for $\lambda\in\Lambda_0$ and $u\in W^{1,1}(0,T)$. It has the property that all increasing trajectories of $\mathscr{W}_R$ are convex and all decreasing trajectories are concave, see [6]. This plays an important role in higher order energy inequalities.

2.3. Kirchhoff transformation

We apply the *Kirchhoff transformation*:

$$\mathscr{K}:p\mapsto u:=\int_0^p\widetilde{k}(s)\mathrm{d}s.$$

Since $\widetilde{k}(s)$ is positive, this transformation is one–to–one with $\mathscr{K}^{-1}$ Lipschitz continuous. We introduce a new variable, $u:=\mathscr{K}(p)$ and define

$$\nabla u=\nabla\mathscr{K}(p)=\widetilde{k}(p)\nabla p, \tag{19}$$

$$k(u)=\widetilde{k}(\mathscr{K}^{-1}(u)), \tag{20}$$

$$\theta=\widetilde{\mathscr{W}}[\lambda,\mathscr{K}^{-1}(u)]. \tag{21}$$

REMARK 1. By [17, Theorem 4.17], the mapping $u\mapsto\widetilde{\mathscr{W}}[\lambda,\mathscr{K}^{-1}(u)]$ is again a Preisach operator, $\mathscr{W}[\lambda,\cdot]=\widetilde{\mathscr{W}}[\lambda,\mathscr{K}^{-1}(\cdot)]$.

3. Model formulation

We assume that the porous medium is rigid, homogeneous and isotropic, that the fluid (water) is inviscid and incompressible. Let Ω be a bounded domain in $\mathbb{R}^n$, $n=1$, 2 or 3, with a Lipschitz boundary $\partial\Omega$, representing the region occupied by the porous medium, see Figure 3. The boundary of Ω is divided into three parts, namely Γ_1 the impervious part, Γ_2 the part in contact with water and Γ_3 the part in contact with open air. For a positive T we denote $Q=\Omega\times(0,T)$, $S_1=\Gamma_1\times(0,T)$, $S_2=\Gamma_2\times(0,T)$, $S_3=\Gamma_3\times(0,T)$, $S_T=\partial\Omega\times(0,T)$.

3.1. Single–porosity model

The law by which water flow through porous media can be described was found by Darcy experimentally. The law yields the following relation between the flux q of water inside the porous medium, pressure p and hydraulic conductivity $\widetilde{k}$

$$q=-\widetilde{k}\nabla(p+\rho gz), \tag{22}$$

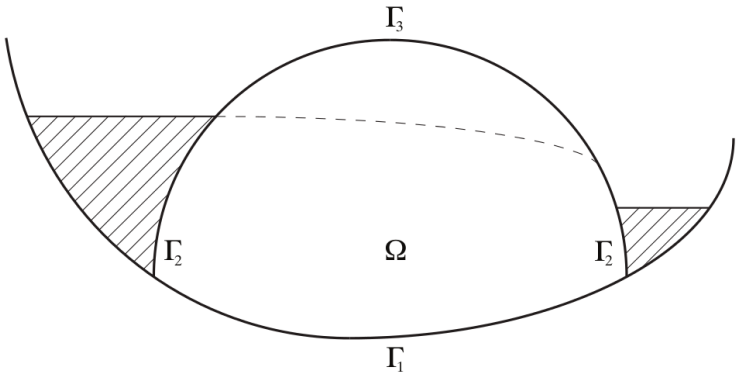

Figure 3: A porous dam with two reservoirs.

where z is upward oriented unit vertical vector, g is the gravity acceleration and ρ is the density of the water. Combining the Darcy's law with the equation of continuity, we obtain the equation

$$\partial_t \theta - \nabla \cdot [\widetilde{k} \nabla (p + \rho g z)] = f, \tag{23}$$

where f is water source term ($f > 0$), or sink term ($f < 0$) and θ is volumetric water content (or simply soil moisture). The lowest value that θ can take is θ_r, the residual moisture content, which is the quantity that remains in a soil after any drainage imposed by the gravitational forced has ceased, and θ_s is the saturation volumetric moisture content. When the soil matrix is perfectly dried then $\theta = 0$, when the matrix is fully saturated with water, then $\theta = \theta_s < 1$ and finally for in–between states the matrix contains both air and water. Hence θ is bounded between θ_r and θ_s, i.e., $0 < \theta_r \leqslant \theta \leqslant \theta_s < 1$.

The constitutive relation between the volumetric water content θ and the pressure p is typically represented by a relation of the form

$$\theta(x,t) \in h(p)(x,t), \tag{24}$$

where $h : \mathbb{R} \to [0,1]$ is a maximal monotone graph as in Figure 4.

The relation (24) is oversimplified. Porous media exhibit hysteresis for cycle of soil wetting–drying process. Hysteretic behaviour means that at any point x from the flow domain and any instant t, the soil moisture depends not only on the pressure, but also on the initial value of the soil moisture and on the previous evolution of the pressure at the same point.

Instead of relation (24) the hysteretic relation between volumetric water content θ and the pressure p is taken into account, i.e., $\theta(x,t) = \mathscr{W}(p)(x,t)$, see Figure 5. Hysteresis is here represented by the Preisach operator.

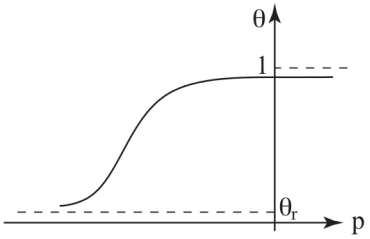

Figure 4: Water content versus pressure constitutive relation without hysteresis.

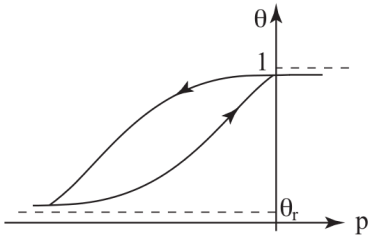

Figure 5: Water content versus pressure constitutive relation with hysteresis.

Suitable boundary conditions to equation (23) on the three boundary sets are considered:

$$-\widetilde{k}\nabla(p+\rho gz)\cdot\nu = 0 \qquad \text{on } S_1, \tag{25}$$

$$p = \widehat{p} \qquad \text{on } S_2, \tag{26}$$

$$\begin{cases} p \leqslant 0 \\ -\widetilde{k}\nabla(p+\rho gz)\cdot\nu \geqslant 0 \\ p[-\widetilde{k}\nabla(p+\rho gz)]\cdot\nu = 0 \end{cases} \qquad \text{on } S_3. \tag{27}$$

Here, ν denotes the outward normal unit vector. The condition (25) means that there is no flux through the impervious part. This condition may be replaced by a nonzero flux condition, for example $-\widetilde{k}\nabla(p+\rho gz)\cdot\nu = \mu(p-\widetilde{p})$, where $\mu > 0$ is constant and $\widetilde{p}$ is prescribed outer pressure. Hence, if the outer pressure $\widetilde{p}$ is higher than the inner pressure p, the fluid flows in and vice versa. The condition (26) is Dirichlet boundary condition, i.e., the case where p is prescribed equal to $\widehat{p}$ and $\widehat{p}$ is non–negative function defined on S_2. If $\widehat{p} = 0$, i.e., $p = 0$, the boundary is considered to be fully saturated. The condition (27) says that because of capillary force the pressure p is negative. In this case there is no flow across this part of the boundary. On the other hand where the pressure vanishes on S_3 water can only flow outward.

3.2. Dual porosity model

Flow in structured porous media is frequently described using dual porosity models. Such an approach assumes that the medium consists of two distinct pore homogeneous systems with separate hydraulic properties, the network of fractures and the matrix pore system. Variably saturated flow is considered for both, the fractures and the matrix pore system. The transfer of water across the fracture–matrix interface is described macroscopically using a first–order coupling term [10]. Darcian water flow in the dual porosity medium is governed by the following system of equations [10, 11]

$$\begin{cases} (\theta_1)_t &= \left(\widetilde{k}_1(p_1)(p_1)_z\right)_z + [\widetilde{k}_1(p_1)]_z - \alpha_w \frac{(p_1-p_2)}{\omega} + q_1, \\ (\theta_2)_t &= \left(\widetilde{k}_2(p_2)(p_2)_z\right)_z + [\widetilde{k}_2(p_2)]_z + \alpha_w \frac{(p_1-p_2)}{1-\omega} + q_2, \end{cases} \tag{28}$$

where the subscript 1 and 2, respectively, denotes the subsystem of fractures and matrix blocks, respectively, ω is a volume fraction, q_1 and q_2 are sink terms, α_w is the first order mass transfer coefficient, $\widetilde{k}_1$ and $\widetilde{k}_2$ are unsaturated hydraulic conductivities, z is a position coordinate measured vertically upwards. In (28) we assume a hysteretic relation described by the Preisach operator, i.e. $\theta_i(z,t) = \mathscr{W}_i[\lambda_i, p_i](z,t)$, where $i = 1,2$. Boundary conditions are determined analogously to the case of single–porosity model, i.e, boundary conditions of Dirichlet type ($z = 0$)

$$p_i = 0 \tag{29}$$

in the case of the fully–saturated boundary (water table). In the case of unsaturated–saturated flows, the unilateral boundary conditions ($z = \ell$, $\ell > 0$) are prescribed

$$\begin{cases} p_i \leqslant 0, \\ \widetilde{k}_i(p_i)(p_i + z)_z \leqslant 0, \\ p_i \left[\widetilde{k}_i(p_i)(p_i + z)_z\right] = 0. \end{cases} \tag{30}$$

If the boundary is unsaturated, (30) yields a no flow boundary condition, and in the saturated case it acts as the Dirichlet boundary of a zero pressure head.

4. Existence results

4.1. Single–porosity flow

Applying the Kirchhoff transformation to the equation (23) without sink term and using notation (19)–(21), we obtain the following equation

$$\partial_t \theta = \nabla \cdot [\nabla u + k(u)\rho g z]. \tag{31}$$

The paper [14] discusses equation (31) without gravity term, i.e,

$$\partial_t \theta = \nabla \cdot \nabla u, \tag{32}$$

and with the nonzero flux boundary condition

$$\nabla u \cdot \nu = \widetilde{u}, \tag{33}$$

on $\partial\Omega$, $\widetilde{u} \in L^\infty(\partial\Omega \times (0,T))$ is a given outer pressure.
The following problem is solved.

PROBLEM 1. Let us consider a Preisach hysteresis operator $w := \mathscr{W}[\lambda, u]$ and let $u_0 \in L^2(\Omega)$, $\lambda : \Omega \to \Lambda$ be given initial data. We search for a function u such that $u(x,0) = u_0(x)$ a.e. in Ω and for any $\phi \in H^1(\Omega)$, and for a.e. $t \in (0,T)$ we have

$$\int_\Omega \frac{\partial w}{\partial t}\phi \,\mathrm{d}x + \int_\Omega \nabla u \nabla \phi \,\mathrm{d}x = \int_{\partial\Omega} \widetilde{u}\phi \,\mathrm{d}\sigma \tag{34}$$

The result is stated as follows.

THEOREM 1. *Let us assume operator $\mathscr{W}$ be the Preisach hysteresis operator introduced in (15) and satisfying Assumptions 1 and 2. And let $R > 0$ be fixed as in Subsection 2.2. Let $K \in [0,R]$ and $\lambda : \Omega \to \Lambda_K$ be given. Moreover $\widetilde{u} \in L^\infty(\partial\Omega \times (0,T))$, $\widetilde{u}_t \in L^2(\partial\Omega \times (0,T))$, $u_0 \in H^1(\Omega)$, $w_0 \in L^2(\Omega)$ and compatibility condition*

$$\int_\Omega \nabla u_0(x)\nabla\phi(x)\mathrm{d}x - \int_{\partial\Omega} \widetilde{u}(x,0)\phi(x)\mathrm{d}\sigma = 0$$

holds for every $\phi \in H^1(\Omega)$. Set $\alpha := \max\{\|u_0\|_{H^1(\Omega)}, \|\widetilde{u}\|_{L^\infty(\partial\Omega\times(0,T))}, \|\widetilde{u}_t\|_{L^2(\partial\Omega\times(0,T))}\}$. Then there exists a constant $\beta > 0$ such that if $\alpha \leqslant \beta$, then Problem 1 has a unique solution such that

$$u \in C^0(Q),$$
$$u_t \in L^2(0,T;V_*),$$

where $V_* := \{u \in V : \int_\Omega u = 0\}$ is the space of functions with null average in Ω.

Proof. Existence of a solution is proved via time discretization, derivation of a priori estimates and using suitable energy inequalities, see [14]. To prove uniqueness we suppose that Problem 1 has two solutions u_1, u_2. We write equation (34) first for u_1, then for u_2. We substract the two equations and test by $\phi = H_m(u_1 - u_2)$, where H_m is an approximation of the Heaviside function defined as

$$H_m(\varepsilon) = \begin{cases} 1, & \varepsilon \geqslant m, \\ \frac{\varepsilon}{m}, & 0 < \varepsilon < m, \\ 0, & \varepsilon \leqslant 0. \end{cases}$$

We obtain

$$\int_\Omega \partial_t(w_1 - w_2)\, H_m(u_1 - u_2)\,\mathrm{d}x + \int_\Omega \nabla(u_1 - u_2)\,\nabla H_m(u_1 - u_2)\,\mathrm{d}x = 0.$$

Since H_m is nondecreasing, we have

$$\int_\Omega \nabla(u_1 - u_2)\,\nabla H_m(u_1 - u_2)\,\mathrm{d}x \geqslant 0,$$

thus

$$\int_\Omega \partial_t(w_1 - w_2)\, H_m(u_1 - u_2)\,\mathrm{d}x \leqslant 0.$$

Now let us pass to the limit for $m \to 0$ to obtain

$$\int_\Omega \partial_t(w_1 - w_2)\, H(u_1 - u_2)\,\mathrm{d}x \leqslant 0.$$

By Proposition 2 we have

$$\frac{d}{dt}\int_\Omega \int_0^\infty (g(r,\xi_r^1(t)) - g(r,\xi_r^2(t)))^+\,\mathrm{d}r\,\mathrm{d}x \leqslant 0.$$

Interchanging the roles of u_1 and u_2 we conclude that

$$0 \geqslant \frac{d}{dt}\int_\Omega \int_0^\infty (g(r,\xi_r^1(t)) - g(r,\xi_r^2(t))^+ \,\mathrm{d}r\,\mathrm{d}x + \frac{d}{dt}\int_\Omega \int_0^\infty (g(r,\xi_r^1(t)) - g(r,\xi_r^2(t))^- \,\mathrm{d}r\,\mathrm{d}x$$
$$= \frac{d}{dt}\int_\Omega \int_0^\infty |g(r,\xi_r^1(t)) - g(r,\xi_r^2(t)|\,\mathrm{d}r\,\mathrm{d}x.$$

Thus, the uniqueness of the weak solution follows, i.e., $u_1 = u_2$. □

4.2. Dual porosity flow

Let $T > 0$ and $\ell > 0$ be the fixed values, $\Omega = (0,\ell)$, $Q = \Omega \times (0,T)$. Applying the Kirchhoff transformation to the system (28)–(30), the resulting system we are going to solve consists of the following equations ($i = 1,2$):

$$(w_i)_t - (u_i)_{zz} - [k_i(u_i)]_z = F_i(\mathbf{u}) + q_i \qquad \text{in } Q, \tag{35}$$
$$u_i(0,t) = 0 \qquad \text{in } (0,T) \tag{36}$$

and

$$\left\{ \begin{array}{r|l} u_i \leqslant 0 & \\ (u_i)_z + k_i(u_i) \leqslant 0 & \Big|_{z=\ell} \\ u_i\,[(u_i)_z + k_i(u_i)] = 0 & \end{array} \right. \qquad \text{in } (0,T), \tag{37}$$

where

$$k_i(u_i) = \widetilde{k}_i(\kappa_i^{-1}(u_i)), \tag{38}$$
$$F_1(u_1,u_2) = -\alpha_w \frac{\kappa_2^{-1}(u_2) - \kappa_1^{-1}(u_1)}{\omega}, \tag{39}$$
$$F_2(u_1,u_2) = \alpha_w \frac{\kappa_2^{-1}(u_2) - \kappa_1^{-1}(u_1)}{1-\omega}, \tag{40}$$
$$w_i = \widetilde{\mathscr{W}_i}[\lambda_i, \kappa_i^{-1}(u_i)] \tag{41}$$

and $\mathbf{u} = [u_1,u_2]$. Here we suppose that all functions in (35)–(37) are smooth enough. We set c_k the Lipschitz constant of $\mathbf{k} = [k_1,k_2]$ and c_F the Lipschitz constant of $\mathbf{F} = [F_1,F_2]$. Let us define the closed and convex set

$$\mathscr{K} := \left\{\mathbf{v} \in \mathbb{V};\ v_j(\ell) \leqslant 0,\ j = 1,2\right\}, \tag{42}$$

where $\mathbb{V}$ be a closure of the space $\left\{\mathbf{v} \in C^\infty(\overline{\Omega})^2;\ \mathbf{v}(0) = \mathbf{0}\right\}$ in the norm of $W^{1,2}(\Omega)^2$.

The following existence result was stated and proved in [15]:

DEFINITION 2. *A vector function* $\mathbf{u} \in L^2((0,T);\mathscr{K})$, *such that* $\mathbf{u}_t \in L^2((0,T);\mathbb{V})$, *is a variational solution to the system* (35)–(37) *iff*

$$\int_0^T \langle \mathbf{w}_t, \varphi - \mathbf{u}\rangle \mathrm{d}t + \int_Q \mathbf{u}_z \cdot (\varphi - \mathbf{u})_z \,\mathrm{d}Q + \sum_{i=1}^{2} \int_Q k_i(u_i)(\varphi_i - u_i)_z \,\mathrm{d}Q \geqslant \int_Q \mathbf{F}(\mathbf{u}) \cdot (\varphi - \mathbf{u}) \,\mathrm{d}Q + \int_Q \mathbf{q}(z,t) \cdot (\varphi - \mathbf{u}) \,\mathrm{d}Q \tag{43}$$

holds for all $\varphi \in L^2((0,T);\mathscr{K})$, $\mathbf{u}(0) = \mathbf{u}^0$ *and* $\mathbf{w}(0) = \mathbf{w}^0$ *a.e. in* Ω.

THEOREM 2. *Let us assume* $w_i(z,t) = \mathscr{W}_i[\lambda_i, h_i](z,t)$ *is the Preisach hysteresis operator of the form (15) and satisfying Assumptions 1 and 2. And let* $R > 0$ *be fixed as in Subsection 2.2. Let* $K \in [0,R]$ *and* $\lambda : \Omega \to \Lambda_K$ *be given. Moreover* $q_1, q_2 \in W^{1,2}(Q)$, $\mathbf{u}_0 \in \mathbb{V}$ *and the following compatibility condition*

$$\int_\Omega \mathbf{u}_z^0(z) \cdot (\mathbf{v}(z))_z \,\mathrm{d}z + \sum_{i=1}^{2} \int_\Omega k_i(u_i^0(z))(v_i(z))_z \,\mathrm{d}z - \int_\Omega \mathbf{F}(\mathbf{u}^0(z)) \cdot \mathbf{v}(z) \,\mathrm{d}z + \int_\Omega \mathbf{q}(z,0) \cdot \mathbf{v}(z) \,\mathrm{d}z = 0 \tag{44}$$

holds for every $\mathbf{v} \in \mathbb{V}$. *Set* $\gamma := \max\{\|\mathbf{u}^0\|_{\mathbb{V}}, \|\mathbf{q}\|_{L^2(Q)^2}, \|\mathbf{q}_t\|_{L^2(Q)^2}, c_F, c_K\}$. *Then there exists* $\gamma_1 > 0$, *such that provided* $\gamma \leqslant \gamma_1$ *there exists the variational solution* $\mathbf{u} \in L^2((0,T);\mathscr{K})$ *to the system* (35)–(37), *such that* $\mathbf{u}_t \in L^2((0,T);\mathbb{V})$.

References

[1] ALT H. W. AND LUCKHAUS S., *Quasilinear Elliptic-Parabolic Differential Equations*, Mathematische Zeitschrift **183** 3 (1983), 311–341.

[2] BAGAGIOLO F. AND VISINTIN A., *Hysteresis in Filtration Through Porous Media*, Journal for Analysis and its Applications **19** 4 (2000), 977–997.

[3] BAGAGIOLO F. AND VISINTIN A., *Porous Media Filtration with Hysteresis*, Advances in Mathematical Sciences and Applications **14** 2 (2004), 379-403.

[4] BENEŠ M., *A note on Doubly Nonlinear Parabolic Systems with Unilateral Constraint*, Results in Mathematics **63** 1–2 (2011), 47–62.

[5] DE GENNES P-G., BROCHARD-WYART F. AND QUERE D., *Capillarity and Wetting Phenomena*, Springer, New York 2004.

[6] ELEUTERI M.,KOPFOVÁ J. AND KREJČÍ P., *Magnetohydrodynamic Flow with Hysteresis*, Siam Journal on Mathematical Analysis **41** 2 (2009), 435–464.

[7] EVERETT D. H. AND WHITTON W. I., *A General Approach to Hysteresis*, Transactions of the Faraday Society **48** 8 (1952), 749–757.

[8] EVERETT D. H. AND WHITTON W. I., *A General Approach to Hysteresis. Part 2: Development of the Domain Theory*, Transactions of the Faraday Society **50** 2 (1954), 187–197.

[9] EVERETT D. H., *A General Approach to Hysteresis. Part3. –A Formal Treatment of the Independent Domain Model of Hysteresis.*, Transactions of the Faraday Society **50** 10 (1954), 1077– 1096.

[10] GERKE H. H. AND VAN GENUCHTEN M.T., *A Dual-Porosity Model for Simulating the Preferential Movement of Water and Solutes in Structured Porous Media*, Water Resources Research **29** 2 (1993), 305–319.

[11] GERKE H. H. AND VAN GENUCHTEN M. T. , *Evaluation of a First-Order Water Transfer Term for Variably Saturated Dual-Porosity Flow Models*, Water Resources Research **29** 4 (1993), 1225–1238.

[12] HAINES W. B., *Studies in the Physical Properties of Soil. V. the Hysteresis Effect in Capillary Properties, and the Modes of Moisture Distribution Associated therewith*, Journal of Agricultural Science (1930), 97–116.

[13] HILLEL D., *Introduction to soil physics*, Academic Press, Inc., New York 1982.

[14] KORDULOVÁ P., *Hysteresis in Flow Through Porous Media*, Journal of Physics Conference Series **268** (2011), 012014.

[15] KORDULOVÁ P. AND BENEŠ M., *Solutions to the Seepage Face Model for Dual Porosity Flows with Hysteresis*, Nonlinear Analysis **75** 18 (2012), 6473–6484.

[16] KREJČÍ P., *Hysteresis, convexity and dissipation in hyperbolic equations*, Gakkotosho, Tokyo 1996.

[17] KREJČÍ P., *Hysteresis Memory Preserving Operators*, Applications of Mathematics **36** 4 (1991), 305–326.

[18] KREJČÍ P., *The Kurzweil Integral and Hysteresis*, Journal of Physics Conference Series, **55** (2006), 144–154.

[19] MARINOSCHI G, *The Diffusive Form of Richards' Equation with Hysteresis*, Nonlinear Analysis. Real World Application **9** 2 (2008), 518–535.

[20] MUALEM Y., *Modified Approach to Capillary Hysteresis Based on a Similarity Hypothesis*, Water Resources Research **9** 5 (1973), 1324–1331.

[21] MUALEM Y., *A modified dependent-domain theory of hysteresis*, Soil Science **137** (1984), 283–291.

[22] PARLANGE J. Y., *Capillary Hysteresis and Relationship Between Drying and Wetting Curves*, Water Resources Research **12** 2 (1976), 224–228.

[23] POULOVASSILIS A., *Hysteresis of Pore Water, an Application of the Concept of Independent Domains*, Soil Science **93** (1962), 405–412.

[24] POULOVASSILIS A. AND CHILDS E.C., *Hysteresis of pore water-nonindependence of domain*, Soil Science **112** (1971), 301–312.

[25] MERZ W. AND RYBKA P., *Strong Solutions to the Richards Equation in the Unsaturated Zone*, Journal of Mathematical Analysis and Applications **371** 2 (2010), 741–749.

AMS Subject Classification: 76S05, 47J40

Petra NÁBĚLKOVÁ,
Mathematical Institute, Silesian University in Opava
Na Rybníčku 1, 74601 Opava, CZECH REPUBLIC
e-mail: Petra.Nabelkova@math.slu.cz

Lavoro pervenuto in redazione il 29.01.2015.

Rend. Sem. Mat. Univ. Politec. Torino
Vol. 72, 1–2 (2014), 73 – 117

A. Bermúdez, D. Gómez, R. Rodríguez and P. Venegas

MATHEMATICAL ANALYSIS AND NUMERICAL SOLUTION OF AXISYMMETRIC EDDY-CURRENT PROBLEMS WITH PREISACH HYSTERESIS MODEL

Abstract. This paper deals with the mathematical analysis and the computation of transient electromagnetic fields in nonlinear magnetic media with hysteresis. This work complements the results obtained previously by the authors, where existence of the solution has been proved under fairly general assumptions on the H-B curve, namely, the nonlinear constitutive relation between the magnetic field H and the magnetic induction B. In our case, the constitutive relation between H and B is given by a hysteresis operator, i.e., the values of magnetic field not only depends on the present values of magnetic induction but also on the past history. We assume axisymmetry of the fields and then consider two kinds of boundary conditions. First the magnetic flux through a meridian plane is given, leading to a non-standard boundary-value problem. Secondly, the magnetic field is given on the boundary (Dirichlet boundary condition). For both problems, under suitable assumptions, an existence result is achieved. For the numerical solution, we consider the Preisach model as hysteresis operator, a finite element discretization by piecewise linear functions, and the backward Euler time-discretization. Finally, we report a numerical test.

1. Introduction

This work deals with the mathematical analysis and the numerical computation of transient electromagnetic fields in nonlinear magnetic media with hysteresis.

The phenomenon of hysteresis has been observed for a long time in many different areas of science and engineering and, in particular, in the area of magnetism. Many ferromagnetic materials present this behavior which essentially means that the magnetic induction at each particular point depends not only on its present magnetic intensity, but also on the past magnetic history of the volume element under consideration. Thus, building a mathematical model of the magnetic constitutive law is a very difficult task and numerical simulation of devices involving ferromagnetic materials is still quite a challenge.

From the physical point of view one must distinguish between scalar hysteresis models and vector hysteresis models. Scalar models correspond to the cases where magnetic induction and magnetic field are aligned at any position and at any time. However, in some cases, the magnetic field and the magnetic induction may be non-collinear so it can no longer be modeled by a scalar hysteresis model and a vector model must be considered. One possibility (see [28, 27, 44, 10, 24, 25]) consists in assuming that the hysteresis operator can be expressed as the integral on the unit sphere of a scalar function operating on the projection of the magnetic field on each space direction times the corresponding unit direction vector. In this work we will restrict ourselves to scalar hysteresis models.

The results presented in this work complement those in [3, 4], where the mathematical and numerical analysis of a two-dimensional (2D) nonlinear axisymmetric eddy current model was performed under fairly general assumptions on the H-B curve, but without considering hysteresis effects. Now, the constitutive relation between H and B is given by a rather general hysteresis operator. Like in [3, 4], we assume axisymmetry of the fields and in view of applications we also consider that the source inputs are current intensities or voltage drops. With this in mind, two source terms are considered: either the magnetic field on the boundary (Dirichlet condition) or the magnetic flux across a meridian section of the device (magnetic flux condition) are given. These source terms are physically realistic in the sense that there are many real applications where they can be readily obtained from measurable quantities (see [11, 1, 2, 29, 26, 37]). Moreover, we consider a time and space dependent electrical conductivity, an important issue because this quantity is typically a function of temperature which, in its turn, is a time dependent field. For both problems, an existence result is achieved under suitable assumptions.

For the numerical solution, we consider the classical Preisach model as hysteresis operator, a finite element discretization by piecewise linear functions on triangular meshes, and the backward Euler scheme for time discretization; all these results can be found in [39].

In the context of parabolic equations with hysteresis there are several publications devoted to the mathematical analysis of the problem (see, [42, 43, 44, 47, 19, 34] and more recently [12, 16, 13]). In particular, [16] deals with an abstract parabolic equation motivated by a 2D eddy current model with hysteresis, but the numerical analysis and computer implementation of the problem are not considered. Numerical approximation of parabolic problems with hysteresis are considered, for instance, in [40, 41]. In the context of the computational methods for 2D eddy current models with hysteresis we mention [37, 38]. However, to the best of the authors' knowledge, the parabolic problem presented in [37] has not been mathematically analyzed yet.

In the present work, by using appropriate weighted two-dimensional Sobolev spaces for axisymmetric problems, we prove the existence of solution to a weak formulation in terms of the magnetic field. The method used for this purpose is the Rothe's method that consists of introducing an implicit time discretization, obtaining a priori estimates and then passing to the limit as the time-step goes to zero (see [32]). This approximation procedure is often used in the analysis of equations including a memory operator (see, for instance, [13, 44]) because at each time step we deal with a stationary problem where the memory operator is reduced to a nonlinear operator of the unknown field at this time step. In particular, we base our proof on arguments given in [44] where existence of solution to a homogeneous Dirichlet problem is achieved. Let us remark that, to the best of the author's knowledge, the problems addressed in this paper do not fit in this or other existing results because, on the one hand, in our case the coefficients depend on time and, on the other hand, different boundary conditions are considered.

The outline of this work is as follows: in Section 2 and Section 3 we recall, respectively, some basic principles of magnetic hysteresis and the properties of hysteresis operators that will be used in the mathematical analysis of the problem. To make the

document self-contained, in Section 4 we include a detailed description of the classical Preisach model following Mayergoyz [27]. In particular, we recall the method to identify, for a particular magnetic material, the function defining the associated Preisach operator.

Next, in Section 5, we introduce the transient eddy current model with hysteresis to be analyzed. The axisymmetric case is considered and the two alternative types of source terms are introduced. In Section 6, after recalling some analytical tools, weak formulations are obtained. Then, existence of solution is proved for both formulations. Section 7 is devoted to the numerical implementation of the fully-discrete problem arising from backward Euler time-discretization and a finite element method for space discretization. Finally, in Section 8, a numerical test is reported.

2. Magnetic hysteresis

Ferromagnetic materials are very sensitive to be magnetized. These materials are made up of small regions in the material structure, known as *magnetic domains*, where all the dipoles are paralleled in the same direction. In each domain, all of the atomic dipoles are coupled together in a preferential direction (see Figure 1 (left)). In other words, the domains are like small permanent magnets oriented randomly in the material.

Ferromagnetic materials become magnetized when the magnetic domains within the material are aligned (see Figure 1 (right)). This can be done by subjecting the material to a strong external magnetic field or by passing electrical current through it. Then, some or all of the domains can become aligned. The more the aligned domains, the stronger the magnetic field in the material. When all of the domains are aligned, the material is said to be magnetically saturated. This means that no additional amount of external magnetization force will cause an increase in its internal level of magnetization. After removing this external field, most of the domains come back to random positions, but a few of them still remain in their changed position. Because of these unchanged domains, the substance becomes slightly magnetized permanently. The phenomenon which causes B to lag behind H, so that the magnetization curve for increasing and decreasing fields is not the same, is called hysteresis and the loop traced out by the magnetization curve is called a *hysteresis cycle* or *hysteresis loop*.

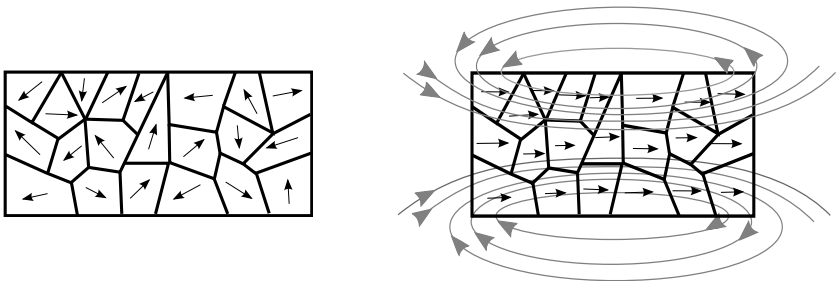

Figure 1: Randomly oriented domains (left) and aligned domains (right).

Figure 2 shows an example of a hysteresis loop. In this loop we represent the relationship between the induced magnetic flux density B and the magnetizing field H. It is often referred to as the B-H loop.

The loop is generated by measuring the magnetic flux of a ferromagnetic material while the magnetic field is changing. We start at the *virginal* state, that is when the material has never been previously magnetized or has been thoroughly demagnetized, and we subject it to a monotonically increasing magnetic field starting from zero. Then, the couples $(H(t),B(t))$ describe the curve labelled 1 shown in Figure 2. Thus, the magnetic induction also increases up to a maximum value B_m at which *saturation* is attained. This curve is called *initial* (or *normal*) magnetization curve.

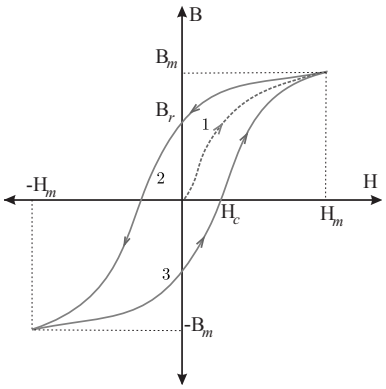

Figure 2: Magnetic hysteresis.

Next, we decrease *monotonically* the magnetic field from the saturation value H_m to the opposite saturation value $-\mathrm{H}_m$. Then, points $(\mathrm{H}(t),\mathrm{B}(t))$ do not trace back the above initial curve but follow curve labelled 2 until the magnetic field attains the value $-\mathrm{H}_m$. If we increase again the magnetic field, then points $(\mathrm{H}(t),\mathrm{B}(t))$ describe curve labelled 3. More generally, if the magnetic field oscillates between two extreme and opposite values H_m and $-\mathrm{H}_m$ monotonically (i.e., $\mathrm{H}(t)$ does not have any local extrema apart from the global ones) then the couples $(\mathrm{H}(t),\mathrm{B}(t))$ follow alternatively curves 2 and 3 in the indicated sense, i.e., they travel along the so-called hysteresis *major loop*.

Two important quantities are related with ferromagnetic materials: the *remanence* and the *coercive fields*. Remanence represents the magnetization after applying a large magnetic field and then removing it. Thus, it corresponds to the remanent magnetic induction denoted by B_r in Figure 2. In its turn, the coercive field is the intensity of the magnetic field needed to bring the magnetization from the remanent value to zero, i.e., the value H_c in Figure 2. According to these parameters, ferromagnetic materials can be classified in *soft* and *hard* magnetic materials. Soft magnetic materials have small coercive fields, so they are easy to magnetize and their hysteresis loops are thin. On the contrary, hard magnetic materials have large coercive fields and they tend

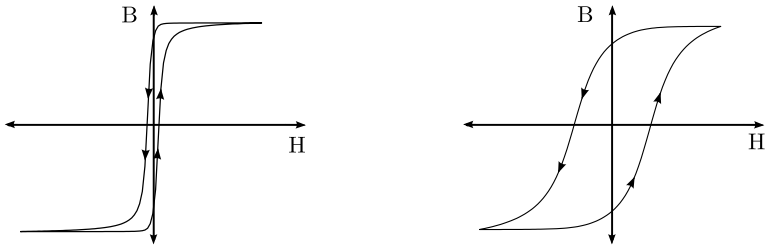

Figure 3: Hysteresis loops for soft (left) and hard (right) magnetic materials.

to stay magnetized, while soft materials do not (see Figure 3).

3. Hysteresis operators

3.1. Basic properties

The hysteresis phenomenon is present not only in electromagnetism but also in different areas of science such as mechanics, among others. Hysteresis modelling early work date back to 1935 and was proposed by the physicist F. Preisach [30] in the context of ferromagnetism (see [44] for some comments on this and further references). From the mathematical point of view, first of all we refer to the pioneering work of Krasnosel'skiĭ and Pokrovskiĭ [22], who introduced the fundamental concept of hysteresis operator and conducted a systematic analysis of the mathematical properties of these objects. In recent years, research on models of hysteresis as well as their coupling with partial differential equations has been progressing; see among others the books by Visintin [44], Krejčí [23] and Brokate and Sprekels [8], for a more mathematically oriented character, and Mayergoyz and Bertotti [27, 6, 7] and Della Torre [9], for a physical point of view.

In this section, we recall some basic background material on hysteresis operators based on the description given in [44], which will be used in the sequel.

Let us start by considering a simple setting, namely, a system whose state is characterized by two scalar variables, u and w, both of them depending on time t. Let us suppose that the evolution of w is determined by the one of u.

For instance, in Figure 4, if u increases from u_1 to u_2, the pair (u,w) moves along the monotone curve *abc*. Conversely, if u decreases from u_2 to u_1, then (u,w) moves along a different monotone curve *cda*. Moreover, if u inverts its motion when $u_1 < u(t) < u_2$, then (u,w) moves inside of the hysteresis region, namely, the part of the (u,w)-plane that is bounded by the major loop *abcd*. Here we assume that pair (u,w) moves along continuous curves so we speak of continuous hysteresis. Although most typical examples of hysteresis phenomena exhibit hysteresis loops, the occurrence of loops should not be regarded as an essential feature of hysteresis.

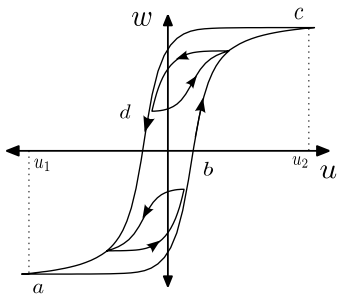

Figure 4: Hysteresis loop.

According to [44], we can distinguish two main characteristics of hysteresis phenomena: the *memory effect* and the *rate independence*.

To illustrate these concepts, we consider the (u,w) relation introduced above. The *memory effect* means that, at any instant t, the value of $w(t)$ depends on the previous evolution of u rather than only on $u(t)$. On the other hand, *rate independence* means that, at any instant t, $w(t)$ depends just on the range of function $u:[0,t]\to\mathbb{R}$ and on the order in which the values of u before t have been attained. In other words, w does not depend on the *velocity* of u.

We notice that, even in most typical hysteresis phenomena, like ferromagnetism, ferroelectricity or plasticity, memory effects are not purely rate independent, since hysteresis is coupled with viscous-type effects. However, in several cases the rate independent component prevails, provided that evolution is not too fast.

In order to introduce a functional setting for hysteresis operators, we first notice that, at any instant t, $w(t)$ will depend not only on the previous evolution of u (i.e., on $u|_{[0,t]}$) but also on the "initial state" of the system. Due to the memory dependence of hysteresis processes, additional information is needed to make up for the lack of history when the process begins. This initial information must represent the "history" of function u before $t=0$. Hence, not only the standard initial value $(u(0),w(0))$ must be provided. In general, we consider a variable ξ containing all the information about the "initial state". For instance, we express this as follows:

$$\begin{aligned}\widetilde{\mathscr{F}}:C([0,T])\times Y &\to C([0,T])\\ (u,\xi) &\to w=\widetilde{\mathscr{F}}(u,\xi)\end{aligned}$$

with Y a suitable metric space. Thus, $\widetilde{\mathscr{F}}(\cdot,\xi)$ represents an operator between spaces of time-dependent functions, for each fixed ξ.

REMARK 1. Sometimes the standard initial value itself is enough to determine the whole history of the system.This is the case of play and stop operators (see [44],

for instance). In these cases, the state of the system can be described by an operator of the following type:

$$(u, w^0) \to w(t) = [\widetilde{\mathscr{F}}(u, w^0)](t).$$

We introduce the following definitions related to the previous discussion.

- *Causality*: An operator $\widetilde{\mathscr{F}}(\cdot, \xi)$ is said to be *causal* if for any $t \in [0,T]$, the output $w(t) = [\widetilde{\mathscr{F}}(u,\xi)](t)$ is independent of $u|_{[t,T]}$, i.e.,

$$\begin{aligned} &\forall (u_1,\xi),(u_2,\xi) \in \mathrm{Dom}(\widetilde{\mathscr{F}}), \\ &u_1|_{[0,t]} = u_2|_{[0,t]} \Rightarrow [\widetilde{\mathscr{F}}(u_1,\xi)](t) = [\widetilde{\mathscr{F}}(u_2,\xi)](t) \quad \forall t \in (0,T]. \end{aligned} \tag{1}$$

- *Rate-independence*: $\widetilde{\mathscr{F}}$ is said *rate independent* if the path of the pair (u,w) is invariant with respect to any increasing diffeomorphism $\varphi : [0,T] \to [0,T]$, i.e.,

$$\begin{aligned} &\forall (u,\xi) \in \mathrm{Dom}(\widetilde{\mathscr{F}}), \\ &\widetilde{\mathscr{F}}(u \circ \varphi, \xi) = \widetilde{\mathscr{F}}(u,\xi) \circ \varphi \ \text{ in } [0,T]. \end{aligned} \tag{2}$$

This means that at any instant t, $w(t)$ only depends on $u|_{[0,t]}$ and on the order in which the values of u have been attained before t.

We characterize a *hysteresis operator* as a causal and rate independent operator.

In what follows we shall deal with hysteresis operators that are continuous and monotone in the following sense:

- *Strong continuity*

$$\begin{aligned} &\forall \left\{ (u_n,\xi_n), \in \mathrm{Dom}(\widetilde{\mathscr{F}}) \right\}_{n\in\mathbb{N}}, \\ &\text{if } \ u_n \to u \text{ uniformly in } [0,T] \text{ and } \xi_n \to \xi \text{ in } \ Y, \\ &\text{then } \widetilde{\mathscr{F}}(u_n,\xi_n) \to \widetilde{\mathscr{F}}(u,\xi) \text{ uniformly in } [0,T]. \end{aligned} \tag{3}$$

- *Piecewise monotonicity*

$$\begin{aligned} &\forall (u,\xi) \in \mathrm{Dom}(\widetilde{\mathscr{F}}), \forall [t_1,t_2] \subset [0,T], \\ &\quad \text{if } u \text{ is either nondecreasing or nonincreasing in } [t_1,t_2], \text{ then so is } \widetilde{\mathscr{F}}(u,\xi). \end{aligned} \tag{4}$$

Another property which may be fulfilled by hysteresis operators is *order preservation*, that is,

$$\begin{aligned} &\forall (u_1,\xi_1),(u_2,\xi_2), \in \mathrm{Dom}(\widetilde{\mathscr{F}}), \text{ if } u_1 \leqslant u_2 \text{ and } \xi_1 \leqslant \xi_2, \\ &\text{then } |[\widetilde{\mathscr{F}}(u_1,\xi_1)](t)| \leqslant |[\widetilde{\mathscr{F}}(u_2,\xi_2)](t)| \quad \forall t \in (0,T]. \end{aligned}$$

We notice that the classical L^2-monotonicity property

$$\int_0^T \left([\widetilde{\mathscr{F}}(u_1,\xi)](t) - [\widetilde{\mathscr{F}}(u_2,\xi)](t) \right) (u_1(t)-u_2(t))\, dt \geqslant 0 \qquad \forall u_1, u_2 \in \mathrm{Dom}(\widetilde{\mathscr{F}})$$

is a too strong requirement for hysteresis operators. Actually, a rate independent operator is monotone with respect to the usual scalar product of $L^2(0,T)$ only if it is of the form $\widetilde{\mathscr{F}}(u,\xi) = \varphi \circ u$ for some function $\varphi : \mathbb{R} \to \mathbb{R}$ (see [7, Chapter I]).

3.2. Space and time dependence

The hysteresis operators introduced in the above section work between spaces of continuous functions, i.e.,

$$\widetilde{\mathscr{F}} : C([0,T]) \times Y \to C([0,T]),$$

where we recall that Y is a suitable metric space containing all the information about the desired "initial state" needed to compute $\widetilde{\mathscr{F}}$ (including eventually its history). These operators are usually employed in problems in which time is the only independent variable, like in the case of ordinary differential equations. In the case of partial differential equations, these operators cannot be directly applied and it is necessary to define a suitable operator $\mathscr{F}$ acting between function spaces involving the space variable.

To begin with, we first define appropriate Lebesgue spaces that will be used for the mathematical analysis of the problem (see [44, Section XII.2]).

Let Q be a Banach space and $\widehat{\Omega}$ an open subset of $\mathbb{R}^N (N \geqslant 1)$ with Lipschitz continuous boundary. We define $\mathscr{S}(\widehat{\Omega};Q)$ to be the family of *simple functions* $\widehat{\Omega} \to Q$, namely, functions with finite range such that the inverse image of any element of Q is measurable. Then, we introduce the space of strongly measurable functions:

$$\mathscr{M}(\widehat{\Omega};Q) := \Big\{ v : \widehat{\Omega} \to Q : \exists \left\{ v_n \in \mathscr{S}(\widehat{\Omega};Q) \right\}_{n\in\mathbb{N}} \text{ such that } v_n \to v \text{ strongly in } Q \text{ a.e. in } \widehat{\Omega} \Big\}.$$

Now, we are in a position to introduce a space-time hysteresis operator. Given a hysteresis operator $\widetilde{\mathscr{F}}$, we introduce, for any $u : \widehat{\Omega} \times [0,T] \to \mathbb{R}$ such that $u(x,\cdot) \in C([0,T])$ and any $\xi : \widehat{\Omega} \to Y$, the corresponding space dependent operator $\mathscr{F} : \mathscr{M}(\widehat{\Omega};C([0,T]) \times Y) \to \mathscr{M}(\widehat{\Omega};C([0,T]))$ as follows

$$[\mathscr{F}(u,\xi)](x,t) := [\widetilde{\mathscr{F}}(u(x,\cdot),\xi(x))](t), \qquad \forall t \in [0,T], \text{ a.e in } \widehat{\Omega}.$$

We notice that operator $\widetilde{\mathscr{F}}$ is here applied at each point $x \in \widehat{\Omega}$ independently, hence, the output $[\mathscr{F}(u,\xi)](x,t)$ depends on $u(x,\cdot)|_{[0,t]}$, but not on $u(y,\cdot)|_{[0,t]}$ for $y \neq x$.

We conclude by summarizing some properties that will be useful in the following sections. Given an "initial state" ξ, we list the following properties of $\mathscr{F}(.,\xi)$, which are the direct extension a.e. in $\widehat{\Omega}$ of the same properties for $\widetilde{\mathscr{F}}(.,\xi)$:

- *Causality*

(5) $\forall v_1, v_2 \in \mathscr{M}(\widehat{\Omega}; C([0,T])),$ if $v_1 = v_2$ in $[0,t]$ a.e. in $\widehat{\Omega}$,
then $[\mathscr{F}(v_1,\xi)](\cdot,t) = [\mathscr{F}(v_2,\xi)](\cdot,t) \quad \forall t \in [0,T],$ a.e. in $\widehat{\Omega}$.

- *Rate-independence*

(6) For any increasing diffeomorphism $\varphi : [0,T] \to [0,T]$
$\forall v \in \mathscr{M}(\widehat{\Omega}; C([0,T])), \ [\mathscr{F}(v \circ \varphi, \xi)](\cdot,t) = [\mathscr{F}(v,\xi)] \circ \varphi(\cdot,t)$
$\forall t \in [0,T],$ a.e. in $\widehat{\Omega}$.

- *Strong continuity*

(7) $\forall \left\{ v_n \in \mathscr{M}(\widehat{\Omega}; C([0,T])) \right\}_{n\in\mathbb{N}}$, if $v_n \to v$ uniformly in $[0,T]$ a.e. in $\widehat{\Omega}$,
then $\mathscr{F}(v_n,\xi) \to \mathscr{F}(v,\xi)$ uniformly in $[0,T]$ a.e. in $\widehat{\Omega}$.

- *Piecewise monotonicity*

(8) $\forall v \in \mathscr{M}(\widehat{\Omega}; C([0,T])), \forall [t_1,t_2] \subset [0,T],$
if $v(x,\cdot)$ is affine in $[t_1,t_2]$ a.e. in $\widehat{\Omega}$, then
$([\mathscr{F}(v,\xi)](x,t_2) - [\mathscr{F}(v,\xi)](x,t_1))\,(v(x,t_2) - v(x,t_1) \geqslant 0$ a.e. in $\widehat{\Omega}$.

4. The Preisach scalar hysteresis model

Different models have been proposed to represent the magnetic hysteresis phenomenon. At the macroscopic level, the most popular is the classical Preisach model [31]. This model is based on some hypotheses concerning the physical mechanisms of magnetization, and for this reason was primarily known in the area of magnetics. Nowadays it is recognized as a fundamental tool for describing a wide range of hysteresis phenomena in different subjects as electromagnetism and mechanics, in particular plasticity, phase transitions, soil hydrology, magnetohydrodynamics, material fatigue, among others. As mentioned in the introduction, in this section we briefly recall the classical definition and some properties of this operator following the works of Mayergoyz and Visintin (see [27, 44]).

4.1. Mathematical definition and properties

The classical Preisach model is constructed from an infinite set of hysteresis operators called *relay operators*. A relay operator is represented by elementary rectangular loops with "up" and "down" switching values. Given any couple $\rho = (\rho_1, \rho_2) \in \mathbb{R}^2$, with $\rho_1 <$

ρ_2, the corresponding relay operator h_ρ, depicted in Figure 5, is defined as follows: for any $u \in C([0,T])$ and $\eta \in \{1,-1\}$, $h_\rho(u,\eta)$ is a function from $[0,T]$ to $\mathbb{R}$ such that,

$$h_\rho(u,\eta)(0) := \begin{cases} -1 & \text{if } u(0) \leqslant \rho_1, \\ \eta & \text{if } \rho_1 < u(0) < \rho_2, \\ 1 & \text{if } u(0) \geqslant \rho_2. \end{cases}$$

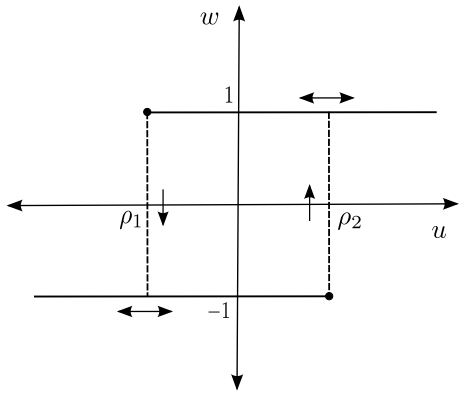

Figure 5: Scalar relay.

Then, for any $t \in (0,T]$, let us set $X_u(t) := \{\tau \in (0,t] : u(\tau) \in \{\rho_1,\rho_2\}\}$ and define

$$h_\rho(u,\eta)(t) := \begin{cases} h_\rho(u,\eta)(0) & \text{if } X_u(t) = \emptyset, \\ -1 & \text{if } X_u(t) \neq \emptyset \text{ and } u(\max X_u(t)) = \rho_1, \\ 1 & \text{if } X_u(t) \neq \emptyset \text{ and } u(\max X_u(t)) = \rho_2. \end{cases}$$

We notice that $h_\rho = \pm 1$ with "switch-up" and "switch-down" values at ρ_2 and ρ_1, respectively. The value of the relay operator remains at the last value (± 1) until u takes the value of one opposite switch, that is, switch to value $+1$ when u attains the value ρ_2 from below, and to -1 when it attains ρ_1 from above. This operator is the simplest model of discontinuous hysteresis.

Now, given $\rho_0 > 0$, let us introduce the *Preisach triangle* $\mathscr{T} := \{\rho = (\rho_1,\rho_2) \in \mathbb{R}^2 : -\rho_0 \leqslant \rho_1 \leqslant \rho_2 \leqslant \rho_0\}$ (see Figure 6 (left)). Let us denote by Y the family of Borel measurable functions $\mathscr{T} \to \{-1,1\}$ and by ξ a generic element of Y. Let us define the following *Preisach operator*

$$\begin{aligned} &\widetilde{\mathscr{F}_p} : C([0,T]) \times Y \longrightarrow C([0,T]), \\ &(u,\xi) \longmapsto [\widetilde{\mathscr{F}_p}(u,\xi)](t) = \int_{\mathscr{T}} [h_\rho(u,\xi(\rho))](t) p(\rho)\, d\rho, \end{aligned} \tag{9}$$

where $p \in \mathrm{L}^1(\mathscr{T})$ with $p > 0$ is known as the *Preisach density function*. The Preisach model can be understood as the "sum" of a family of relays, distributed with a certain density p.

REMARK 2. The definition of the Preisach operator is more general. The domain of the integral is not the Preisach triangle but the Preisach half-plane

$$\mathscr{P} := \{\rho = (\rho_1, \rho_2) \in \mathbb{R}^2 : \rho_1 < \rho_2\}$$

Moreover, any finite (signed) Borel measure can be used in (9) instead of one absolutely continuous with respect to the Lebesgue measure (see [44, Section IV]). In fact, the results that follow are actually true for such general Preisach operators, under appropriate assumptions about the measure. However, we prefer to restrict ourselves to the particular case (9), which turns to be useful when dealing with the numerical implementation of the Preisach model.

From the above definition of the hysteresis operator and [44, Section IV, Theorems 1.2 and 3.2] we have the following result:

LEMMA 1. *Given $\xi \in Y$, the Preisach operator $\widetilde{\mathscr{F}}_p(\cdot,\xi) : C([0,T]) \to C([0,T])$ is a hysteresis operator, namely, is causal and rate independent (cf.* (1), (2)*). Moreover is strongly continuous, piecewise monotone (cf.* (3), (4)*) and satisfies*

$$\left|[\widetilde{\mathscr{F}}_p(u,\xi)](t)\right| \leqslant \int_{\mathscr{T}} p(\rho)\, d\rho \qquad \forall u \in C([0,T]).$$

As in Section 3.2 it is possible to define the operator $\mathscr{F}_p : \mathscr{M}(\widehat{\Omega}; C([0,T]) \times Y) \to \mathscr{M}(\widehat{\Omega}; C([0,T]))$ as follows: given $(u,\xi) \in \mathscr{M}(\widehat{\Omega}; C([0,T]) \times Y)$

$$[\mathscr{F}_p(u,\xi)](r,z,t) := [\widetilde{\mathscr{F}}_p(u(x),\xi(x))](t) \qquad \forall t \in [0,T], \text{ a.e. in } \widehat{\Omega} \subset \mathbb{R}^N. \tag{10}$$

Then, from Propositions 3.1 in [44, Section XII.3], we obtain the following result:

LEMMA 2. *Let $\xi : \widehat{\Omega} \to Y$ be an "initial state". Then, the operator $\mathscr{F}_p(\cdot,\xi) : \mathscr{M}(\widehat{\Omega}; C([0,T])) \to \mathscr{M}(\widehat{\Omega}; C([0,T]))$ is causal, rate independent, strongly continuous, piecewise monotone (cf.* (5), (6), (7), (8)*, respectively) and satisfies*

$$\forall v \in \mathscr{M}(\widehat{\Omega}; C([0,T])), \quad \|[\mathscr{F}_p(v,\xi)](x,\cdot)\|_{C([0,T])} \leqslant \int_{\mathscr{T}} p(\rho)\, d\rho \quad \text{a.e. in } \widehat{\Omega}. \tag{11}$$

4.2. Geometric interpretation

The understanding of the Preisach operator is considerably facilitated by its geometric interpretation which is based on the fact that there is a one-to-one correspondence between relay operators h_ρ and points (ρ_1, ρ_2) of the Preisach triangle $\mathscr{T}$.

We notice that, given $u \in C([0,T])$ and ξ, each relay $h_\rho(u, \xi(\rho))$ is such that, for any $t \in [0,T]$,

$$h_\rho(u,\xi(\rho))(t) := \begin{cases} 1 & \text{if } u(t) \leqslant \rho_1, \\ -1 & \text{if } u(t) \geqslant \rho_2, \\ \pm 1 & \text{if } \rho_2 < u(t) < \rho_1, \end{cases} \tag{12}$$

and the choice of the sign above depends on $u|_{[0,t]}$ and $\xi(\rho)$. Therefore, for a given $u(t)$, all the relays h_ρ such that $\rho_1 \geqslant u(t)$ are "switched down". Similarly the relays h_ρ such that $\rho_2 \leqslant u(t)$ are "switched up" (see Figure 6 (right)).

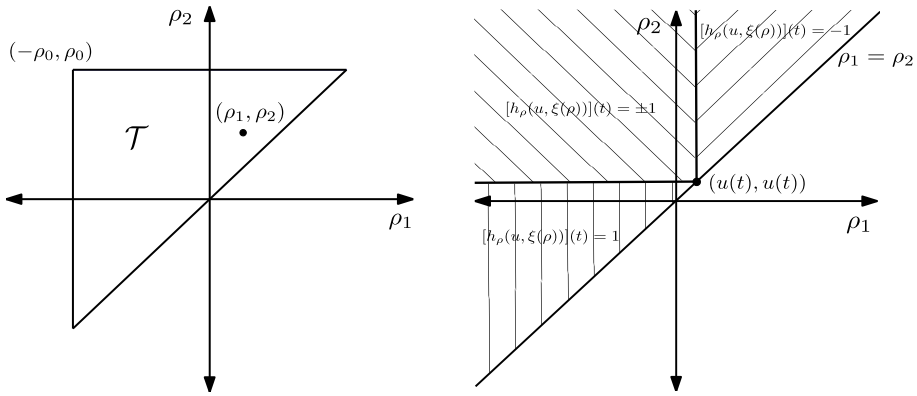

Figure 6: Preisach triangle (left) and Preisach domain (right).

Now, to understand the geometrical interpretation of the Preisach operator, we consider a simple setting and proceed in the same way as described by Mayergoyz in [27]. From now on and throughout the rest of the paper $t^0 < t^1 < \ldots < t^n$, $n \in \mathbb{N}$ denote different times (and not powers of t). First we consider a function $u(t) \in C([0,T])$ as the one shown in Figure 7 such that at some time t^0, $u(t^0) < -\rho_0$. Notice that, because of this particular choice of u, all the relays are well defined in $\mathscr{T}$ for $t > t^0$ without the need of giving an "initial state" ξ. Therefore, to simplify the notation, from now on, we drop out ξ and write $[h_\rho(u)](t) := [h_\rho(u,\xi)](t)$. Given that, $u(t^0) \leqslant -\rho_0 \leqslant \rho_1$ for all $(\rho_1,\rho_2) \in \mathscr{T}$, then from (12) it follows that all the relay operators $[h_\rho(u)](t^0) = -1$ in $\mathscr{T}$. Now, since u increases monotonically for $t \in [t^0, t^1]$, from the definition of the relay operator, the relays can only change to a positive state. Thus, at each time $t \geqslant t^0$, triangle $\mathscr{T}$ is subdivided into two sets (one possibly empty):

$$
\begin{aligned}
S_u^-(t) &:= \left\{(\rho_1,\rho_2) \in \mathscr{T} : [h_\rho(u)](t) = -1\right\}, \\
S_u^+(t) &:= \left\{(\rho_1,\rho_2) \in \mathscr{T} : [h_\rho(u)](t) = 1\right\}.
\end{aligned} \tag{13}
$$

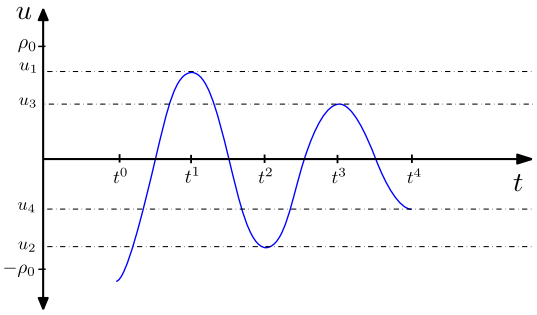

Figure 7: Continuous function u.

Since the change to a positive state of the relay h_ρ depends only on the value of ρ_2, we obtain that the interface $L_u(t)$ between these two subsets is the line $\rho_2 = u(t)$ (see Figure 8 (left)) which moves up as u increases in time. We consider a particular case in which function u increases until it reaches some maximum value u_1 ($-\rho_0 < u_1 < \rho_0$) at time t^1 (see Figure 7)

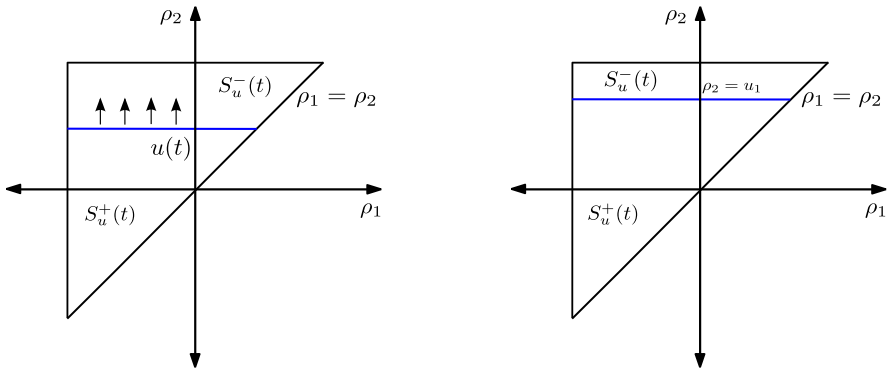

Figure 8: $L_u(t)$: $u(t)$ is increasing (left) and attains a maximum at u_1 (right).

Next, $u(t)$ decreases monotonically for $t \in [t^1, t^2]$. Then, the relays can only change to a negative state. Since changing to a negative state of the relay h_ρ depends only on the value of ρ_1, we obtain that the line $\rho_1 = u(t)$ moves from right to left (see Figure 9 (left)). Function u decreases until it reaches, at time t^2, some value $u_2 > -\rho_0$. At this point, the interface $L_u(t)$ between $S_u^+(t)$ and $S_u^-(t)$ has now two segments, the horizontal and vertical ones depicted in Figure 9 (right).

Next, $u(t)$ increases again until it reaches at time t^3 some maximum value $u_3 < u_1$. Geometrically, this increment produces a new horizontal segment in $L_u(t)$ which moves up. This motion ends when the maximum u_3 is reached. This is shown in

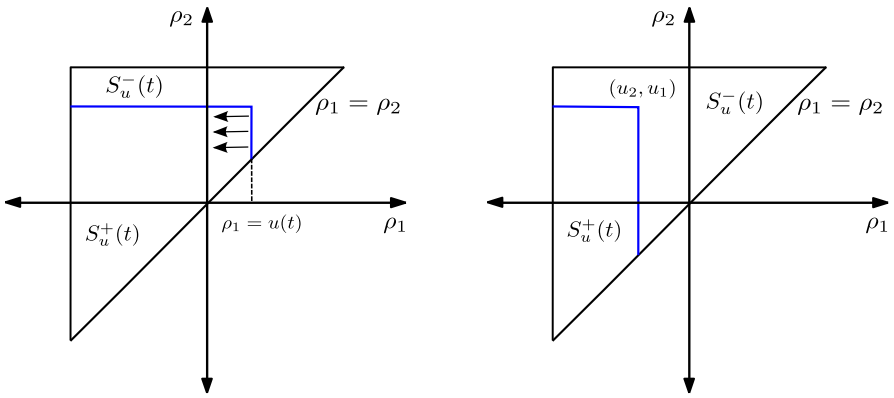

Figure 9: $L_u(t)$: $u(t)$ is decreasing from u_1 (left) and attains a minimum at u_2 (right).

Figure 10 (left). Finally $u(t)$ decreases until it reaches, at time t^4, some minimum value $u_4 > u_2$. This variation results in a new vertical segment in $L_u(t)$ that moves from right to left as it is shown in Figure 10 (right). As shown in this figure, at this point, $L_u(t)$ has two vertices (u_2, u_1) and (u_4, u_3).

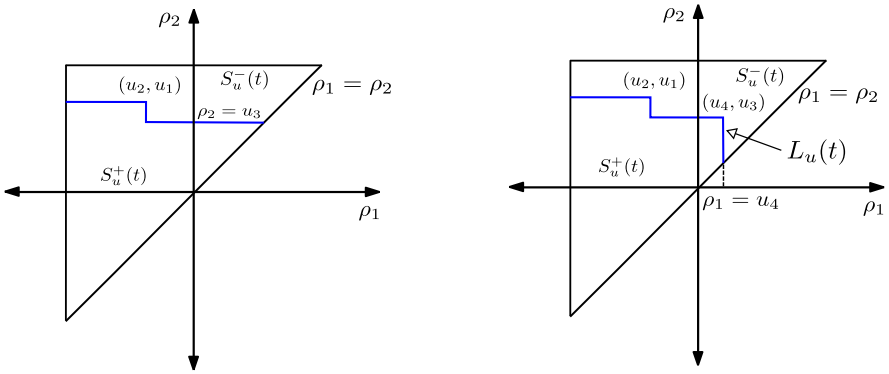

Figure 10: $L_u(t)$: $u(t)$ attains a maximum at u_3 (left) and attains a minimum at u_4 (right).

REMARK 3. A similar figure is obtained if we consider another function $v \in C([0,T])$ such that, at some time t^0, $v(t^0) > \rho_0$. We assume that $v(t)$ decreases to $v_1 > -\rho_0$, then increases to $v_2 \leqslant \rho_0$, next decreases to $v_3 > v_1$ and finally increases to $v_4 < v_2$, as depicted in Figure 11 (left). $L_v(t)$ is illustrated in Figure 11 (right).

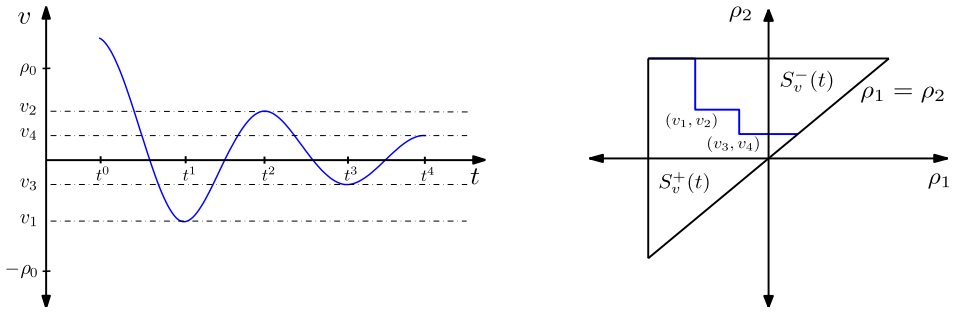

Figure 11: Input $v(t)$ (left) and staircase line $L_v(t)$ (right).

We can summarize the above analysis as follows; for a given $u \in C([0,T])$ as the one shown in Figure 7 and any time t, the triangle $\mathscr{T}$ is subdivided into two sets: $S_u^+(t)$ consisting of points (ρ_1,ρ_2) for which the corresponding relay operators $h_\rho(u)$ are positive, and $S_u^-(t)$ consisting of points (ρ_1,ρ_2) for which the corresponding relay operators $h_\rho(u)$ are negative. The interface $L_u(t)$ between $S_u^+(t)$ and $S_u^-(t)$ is a staircase line whose vertices have coordinates (ρ_1,ρ_2) coinciding respectively with the local minimum and maximum values of u at previous instants of time. At time t, the staircase line $L_u(t)$ intersects the line $\rho_1 = \rho_2$ at $(u(t),u(t))$. $L_u(t)$ moves up as $u(t)$ increases and it moves from right to left as $u(t)$ decreases (see Figure 12).

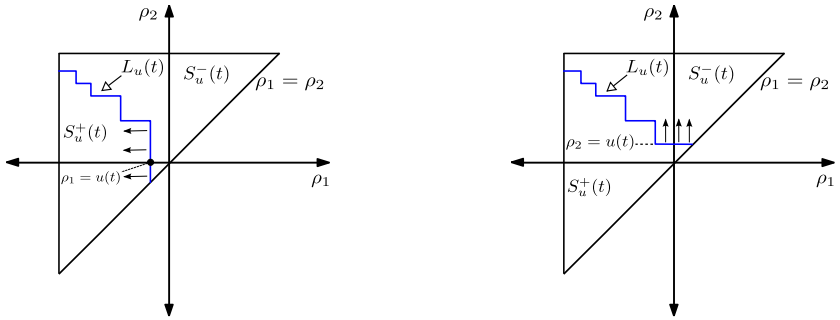

Figure 12: Staircase line $L_u(t)$ moving right to left (left) and moving up (right).

Hence, from the latter we notice that, at any time t, the integral in (9) can be subdivided into two integrals, over $S_u^+(t)$ and $S_u^-(t)$, respectively:

$$\begin{aligned} w_u(t) := [\widetilde{\mathscr{F}_p}(u)](t) &= \int_{\mathscr{T}} [h_\rho(u)](t)\,p(\rho)\,d\rho \\ &= \int_{S_u^+(t)} [h_\rho(u)](t)\,p(\rho)\,d\rho + \int_{S_u^-(t)} [h_\rho(u)](t)\,p(\rho)\,d\rho. \end{aligned}$$

(We recall that, because of the particular choice of the values of u we do not need an

"initial state" ξ.) Moreover, because of (13) and the latter equality we obtain that

$$w_u(t) = \int_{S_u^+(t)} p(\rho)\, d\rho - \int_{S_u^-(t)} p(\rho)\, d\rho. \tag{14}$$

REMARK 4. To compute the Preisach model in $(t^0, T]$, in general it is enough to know $u(t^0)$, the Preisach density function p and the history of u represented by $S_u^+(t)$ and $S_u^-(t)$, which contain the least amount of information to compute (14).

From (14), it follows that $[\widetilde{\mathscr{F}_p}(u)](t)$ depends on the particular subdivision of the limiting triangle $\mathscr{T}$ into $S_u^+(t)$ and $S_u^-(t)$. Therefore, it depends on the shape of the interface $L_u(t)$, which in its turn is determined by the extremum values of $u(t)$ at previous time. It turns out that not all extremal input values are needed. In fact, given the dependence on the staircase line $L_u(t)$, we can see that the Preisach operator has a *wiping-out property*. This property states that each time the input reaches a local maximum $u(t)$, $L_u(t)$ erases, or "wipes out" the previous vertices of the staircase whose ρ_2 value is lower than the value $u(t)$. Similarly, each time an input reaches a local minimum $u(t)$, the memory curve erases all previous vertices whose ρ_1 value is higher than the $u(t)$ value.

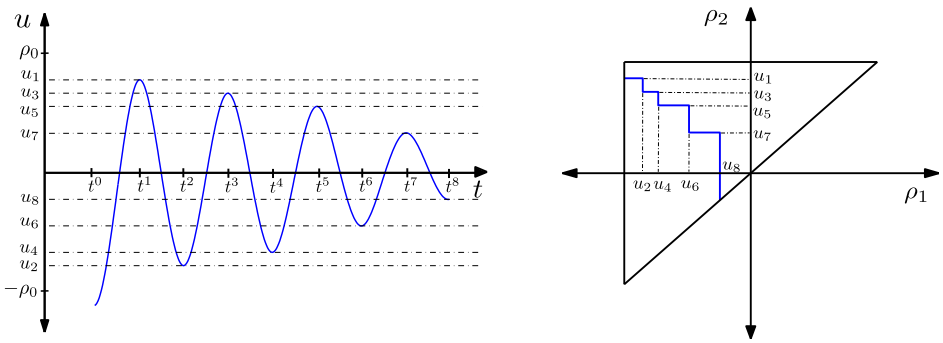

Figure 13: Function u (left) and initial staircase line L_u (right).

To illustrate this property, we consider a simple setting. Let $u \in C([0,T])$ be characterized by a finite decreasing sequence $\{u_1, u_3, u_5, u_7\}$ of local maxima and an increasing sequence $\{u_2, u_4, u_6, u_8\}$ of local minima, with $-\rho_0 < u_i < \rho_0$, $i = 1, \ldots, 8$ (see Figure 13). Now, let us assume that $u(t)$ is monotonically increasing until it reaches u_9, such that $u_3 < u_9 < u_1$. This increase of $u(t)$ results in the formation of a new line in $L_u(t)$ which intersects the line $\rho_1 = \rho_2$ horizontally and moves up until the maximum value u_9 is reached. Then we obtain a modified staircase line $L_u(t)$ where all vertices whose ρ_2-coordinates are below u_9 have been wiped out (see Figure 14).

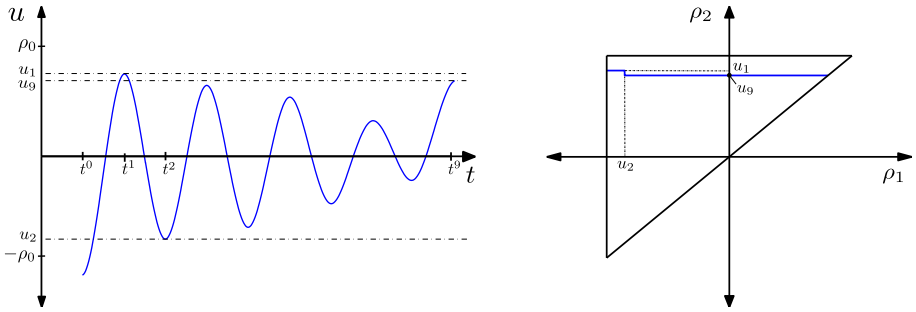

Figure 14: Function u (left) and L_u for increasing u until u_9 (right). This represents the wiping out property.

Similarly, instead of assuming that $u(t)$ is monotonically increasing, let us suppose that it decreases until it reaches u_9, such that $u_2 < u_9 < u_4$. Function u and the corresponding staircase line $L_u(t)$ are depicted in Figure 15.

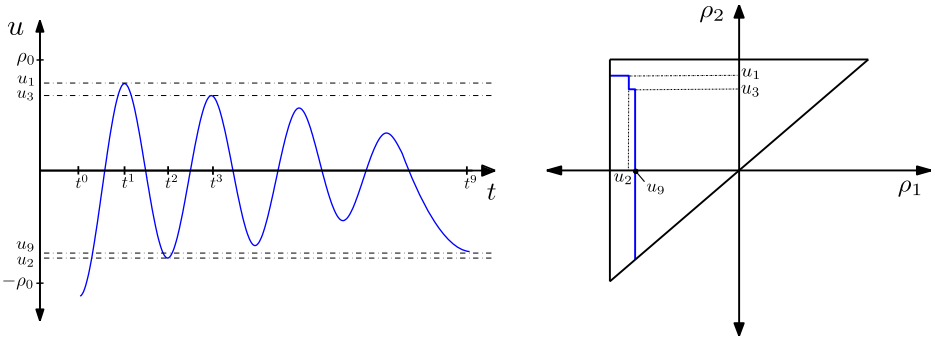

Figure 15: Function u (left) and L_u for decreasing u until u_9 (right). This represents the wiping out property.

Another important property of the Preisach operator is referred to as the *congruency property*. This property states that, as the input is cycled between two extremum values, the minor loop traced will have the same shape, independently of history. However, the position of the minor loop along the output axis will be determined by the history of past input variations (see Figure 16, for further details, see [27]).

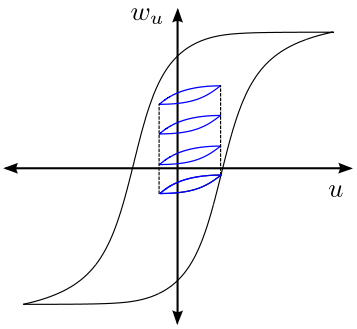

Figure 16: Congruency property.

In general the loops of the Preisach model are not globally convex (as it is the case of some other operators, for instance the Prandtl-Ishlinskiĭ operator), but it may be proved (see [23, Sect. II.3 and II.4]) that small amplitude minor loops of the Preisach model are convex and this property can be conveniently used in connection of well-posedness of systems of partial differential equations in several fields, for instance in magnetohydrodynamics [14] or soil hydrology [21].

4.3. Computation of the Preisach model

Once we have the distribution function and an "initial state", given $u \in C([0,T])$ we can compute $w_u(t) := [\widetilde{\mathscr{F}_p}(u)](t)$ by means of (9). Based on this feature, Mayergoyz [27] developed an approach for the computation of the Preisach model that does not require the Preisach density function p but the so-called *Everett function* which describes the effect of p on the hysteresis operator. In what follows, for the sake of completeness, we describe the approach proposed by Mayergoyz in [27].

To obtain the Everett function, the so-called first order transition curves are required. To define such a curve, first we consider a function $u \in C([0,T])$, such that at time t^0, $u(t^0) \leqslant -\rho_0$. Then, u increases monotonically until it reaches some value ρ_2' at time t^1 (see Figure 18 (left)). We denote $w_{\rho_2'} := w_u(t^1)$. A first order transition curve is formed by the above monotonic increase of u followed by a subsequent monotonic decrease, namely, from ρ_2', u decreases monotonically until it reaches some value $\rho_1' < \rho_2'$ at time t^2; we denote $w_{\rho_2',\rho_1'} := w_u(t^2)$ (see Figures 17 and 18).

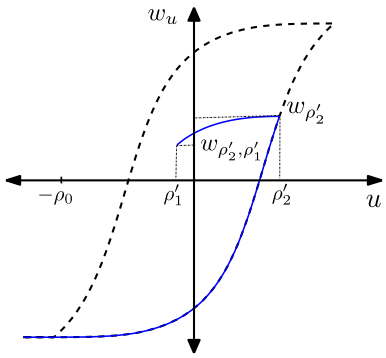

Figure 17: First order transition curve.

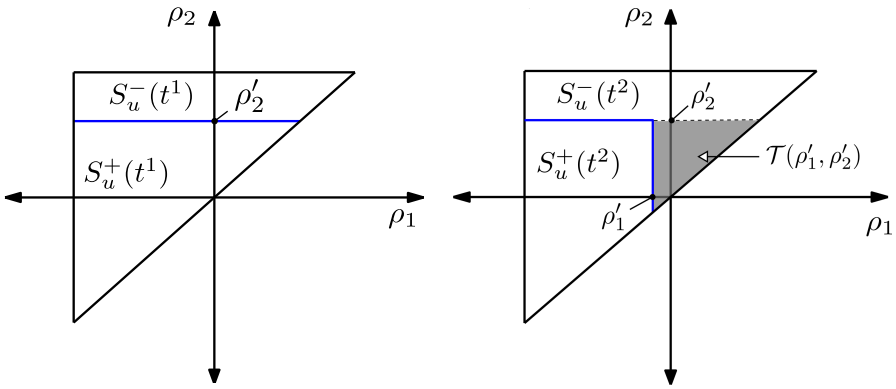

Figure 18: Staircase line $L_u(t)$ at time t^1 (left) and at time t^2 (right).

We define the Everett function $E : \mathscr{T} \to \mathbb{R}$ by

$$E(\rho_1',\rho_2') := \frac{w_{\rho_2'} - w_{\rho_2',\rho_1'}}{2}. \tag{15}$$

From (14), we notice that

$$\begin{aligned} w_{\rho_2',\rho_1'} - w_{\rho_2'} &= \left(\int_{S_u^+(t^2)} p(\rho)\,d\rho - \int_{S_u^-(t^2)} p(\rho)\,d\rho\right) - \left(\int_{S_u^+(t^1)} p(\rho)\,d\rho - \int_{S_u^-(t^1)} p(\rho)\,d\rho\right) \\ &= -2\int_{\mathscr{T}(\rho_1',\rho_2')} p(\rho)\,d\rho, \end{aligned}$$

with $\mathscr{T}(\rho_1',\rho_2')$ the triangle shown in Figure 18 (right) with the vertex of the right angle at (ρ_1',ρ_2'). This is so because $S_u^+(t^2) = S_u^+(t^1) \setminus \mathscr{T}(\rho_1',\rho_2')$ and $S_u^-(t^2) = S_u^-(t^1) \cup$

$\mathscr{T}(\rho_1',\rho_2')$ (see Figure 18 (right)). Therefore, we obtain the following relation between the Preisach density function p and the Everett function E:

$$E(\rho_1,\rho_2)=\int_{\mathscr{T}(\rho_1,\rho_2)} p(\rho)\,d\rho \qquad \forall(\rho_1,\rho_2)\in\mathscr{T}. \tag{16}$$

To take into account this relation in the computation of the Preisach operator, first we rewrite (14), by adding and subtracting the integral of p over $S_u^+(t)$ as follows:

$$w_u(t)=2\int_{S_u^+(t)} p(\rho)\,d\rho-\int_{\mathscr{T}} p(\rho)\,d\rho,$$

where $\mathscr{T}$ is the Preisach triangle. Moreover, from (16) and the definition of the Preisach triangle $\mathscr{T}=\mathscr{T}(-\rho_0,\rho_0)$ (cf. Figure 6 (left)) it follows that,

$$w_u(t)=2\int_{S_u^+(t)} p(\rho)\,d\rho-E(-\rho_0,\rho_0). \tag{17}$$

Provided that the Preisach density function p is known, to obtain $w_u(t)$ we can compute the both terms on the right-hand side of (17). For this purpose we further assume that u is piecewise monotonic and distinguish two cases: u monotonically increasing and u monotonically decreasing in an interval (t',t) for some $t'<t$. For decreasing u, we subdivide $S_u^+(t)$ into n trapezoids $Q_k(t)$ (see Figure 19 (left)). We can perform this subdivision because, for decreasing arguments, the staircase line $L_u(t)$ intersects the line $\rho_1=\rho_2$ vertically. Then we have

$$\int_{S_u^+(t)} p(\rho)\,d\rho=\sum_{k=1}^{n(t)}\int_{Q_k(t)} p(\rho)\,d\rho, \tag{18}$$

where $n(t)$ is the number of local maxima of u up to time t that have not been wiped-out (recall the wipe-out process as it has been illustrated in Figure 15, for u monotonically decreasing)

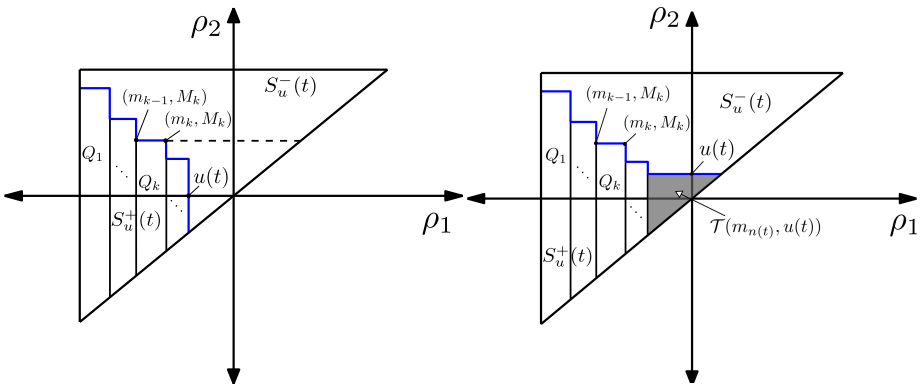

Figure 19: Staircase line for a decreasing input (left) and a increasing input (right).

Each trapezoid $Q_k(t)$ depends on the local maximum M_k and on the local minima m_k and m_{k-1}. Notice that, for $k=1$, $m_0=-\rho_0$. Moreover, each trapezoid can be represented as the set difference of two triangles $\mathscr{T}(m_{k-1},M_k)$ and $\mathscr{T}(m_k,M_k)$:

$$\int_{Q_k(t)} p(\rho)\,d\rho = \int_{\mathscr{T}(m_{k-1},M_k)} p(\rho)\,d\rho - \int_{\mathscr{T}(m_k,M_k)} p(\rho)\,d\rho. \tag{19}$$

Now, from (16), it follows that

$$\int_{S_u^+(t)} p(\rho)\,d\rho = \sum_{k=1}^{n(t)} \left(E(m_{k-1},M_k) - E(m_k,M_k)\right). \tag{20}$$

Finally, from (20) and (17), we obtain

$$w_u(t) = 2\sum_{k=1}^{n(t)} \left(E(m_{k-1},M_k) - E(m_k,M_k)\right) - E(-\rho_0,\rho_0).$$

Since we consider u monotonically decreasing in (t',t), we obtain that the last minimum value $m_{n(t)}$ is equal to the current value of u, namely, $m_{n(t)}=u(t)$. Then

$$w_u(t) = -E(-\rho_0,\rho_0) + 2\sum_{k=1}^{n(t)-1} \left(E(m_{k-1},M_k) - E(m_k,M_k)\right) \tag{21}$$

$$+\,2\left(E(m_{n(t)-1},M_{n(t)}) - E(u(t),M_{n(t)})\right). \tag{22}$$

Because of the decomposition of S_u^+ into trapezoids (see Figure 19), this expression is valid only for u being monotonically decreasing in (t',t). If $u(t)$ is monotonically increasing, then the staircase line $L_u(t)$ intersects the line $\rho_1=\rho_2$ horizontally. Hence, we may decompose S_u^+ into trapezoids and a triangle (see Figure 19 (right)). It follows that

$$\int_{S_u^+(t)} p(\rho)\,d\rho = \sum_{k=1}^{n(t)-1} \left(E(m_{k-1},M_k) - E(m_k,M_k)\right) + E(m_{n(t)-1},M_{n(t)}). \tag{23}$$

In this case, the last maximum value $M_{n(t)}$ is equal to the current value of u, namely, $M_{n(t)}=u(t)$. Hence, from (23) we write (17) for a monotonically increasing u in (t',t) as follows:

$$w_u(t) = -E(-\rho_0,\rho_0) + 2\sum_{k=1}^{n(t)-1} \left(E(m_{k-1},M_k) - E(m_k,M_k)\right) + 2E(m_{n(t)-1},u(t)). \tag{24}$$

From (21) and (24) we obtain the following expression to compute the Preisach operator in terms of the Everett function

$$w_u(t) := \begin{cases} -E(-\rho_0,\rho_0) + 2\displaystyle\sum_{k=1}^{n(t)-1} \left(E(m_{k-1},M_k) - E(m_k,M_k)\right) \\ \qquad\qquad + 2\left(E(m_{n(t)-1},M_{n(t)}) - E(u(t),M_{n(t)})\right) & \text{for } u \text{ decreasing,} \\ -E(-\rho_0,\rho_0) + 2\displaystyle\sum_{k=1}^{n(t)-1} \left(E(m_{k-1},M_k) - E(m_k,M_k)\right) \\ \qquad\qquad + 2E(m_{n(t)-1},u(t)) & \text{for } u \text{ increasing.} \end{cases}$$

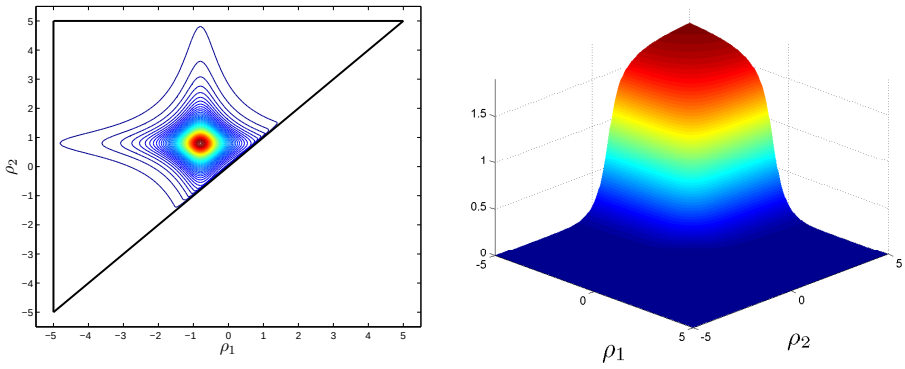

Figure 20: Factorized-Lorentzian distribution function p (left) and corresponding Everett function (right).

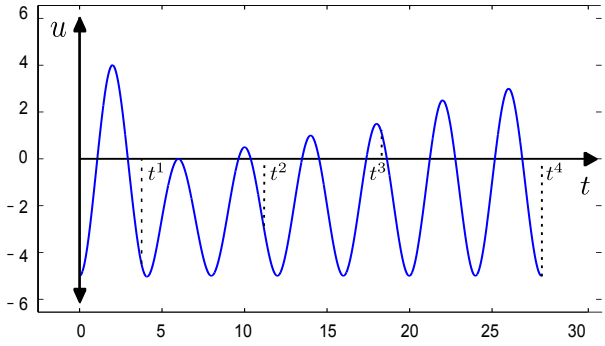

Figure 21: Function $u(t)$.

As an example, we compute $w_u(t)$ by using the Preisach density function p given by the Factorized-Lorentzian distribution (see [6]):

$$p(\rho_1,\rho_2) := N\left(\left(1+\left(\frac{\rho_2-\omega}{\gamma\omega}\right)^2\right)\left(1+\left(\frac{\rho_1+\omega}{\gamma\omega}\right)^2\right)\right)^{-1} \tag{25}$$

with parameters $N=1, \omega=0.8$ and $\gamma=0.6$ (see Figure 20). The Preisach triangle $\mathscr{T}$ is characterized by $\rho_0=5$. We compute the w_u-u loop in two cases. First we consider the input function $u(t)$ shown in Figure 21. The evolution of the corresponding w_u-u loop are shown in Figure 22 at times t^1,t^2,t^3 and t^4. Finally we consider the input function $u(t)$ shown in Figure 23. In this case we present in Figure 24 the final staircase line and the complete w_u-u loop.

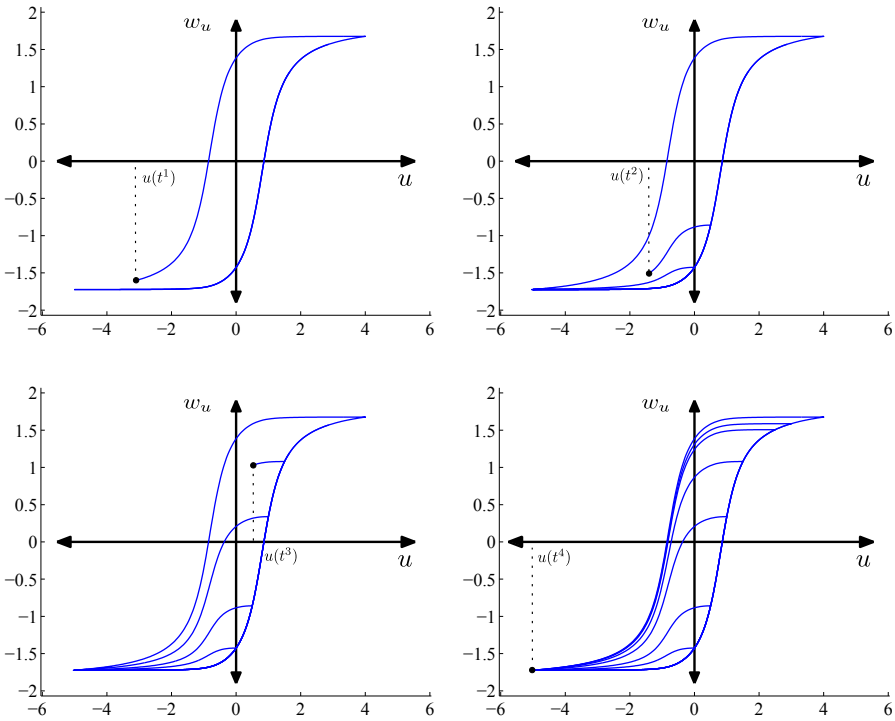

Figure 22: $w_u - u$ curve at time t^1, t^2, t^3 and t^4.

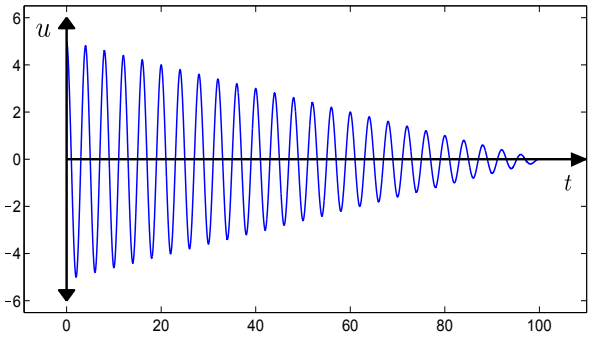

Figure 23: Function $u(t)$.

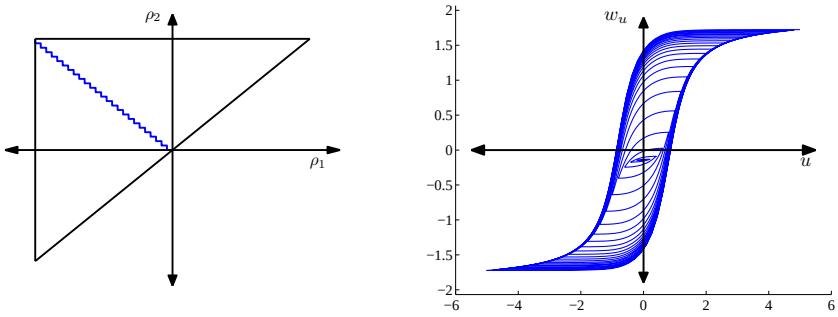

Figure 24: Staircase function (left) and $w_u - u$ curve (right).

REMARK 5. In the previous examples we consider different inputs u, such that $u(t^0) \geqslant \rho_0$ or $u(t^0) \leqslant -\rho_0$. Clearly, in both cases $S_u^+(t^0)$ and $S_u^-(t^0)$ are determined and because of that, there is no need to consider additional information to compute $w_u(t)$, $t \geqslant t^0$. In particular, we have $w_u(t^0) = E(-\rho_0, \rho_0)$ if $u(t^0) \geqslant \rho_0$, and $-E(-\rho_0, \rho_0)$ if $u(t^0) \leqslant -\rho_0$. However, in the case of $-\rho_0 < u(t^0) < \rho_0$, to compute $w_u(t^0)$ we must have an "initial state". To illustrate this we consider three different previous "histories" of u as shown in the curves $u_1(t), u_2(t)$ and $u_3(t)$ in Figure 25. The curves u_1 and u_3 are extreme cases in which:

$$u_1(t) \leqslant u_1(t^0) = u_0 \qquad \forall t \leqslant t^0$$
$$u_3(t) \geqslant u_3(t^0) = u_0 \qquad \forall t \leqslant t^0.$$

Instead, u_2 takes values large and smaller that u_0 for $t < t^0$.

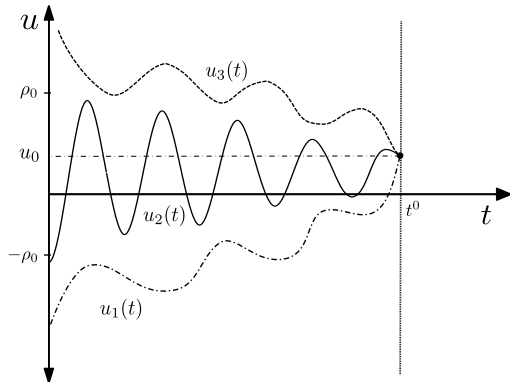

Figure 25: Functions $u_1(t), u_2(t)$ and $u_3(t)$.

We show in Figure 26 (left) the corresponding staircase lines L_{u_1}, L_{u_2} and L_{u_3}

and in Figure 26 (right) the corresponding values of $w_u(u_1)$, $w_u(u_2)$ and $w_u(u_3)$ at time $t = t^0$ (w_u^1, w_u^2 and w_u^3, respectively). Notice that the three values are different; w_u^1 and w_u^3 lie on the major loop, whereas w_u^2 lies in the interval (w_u^1, w_u^3).

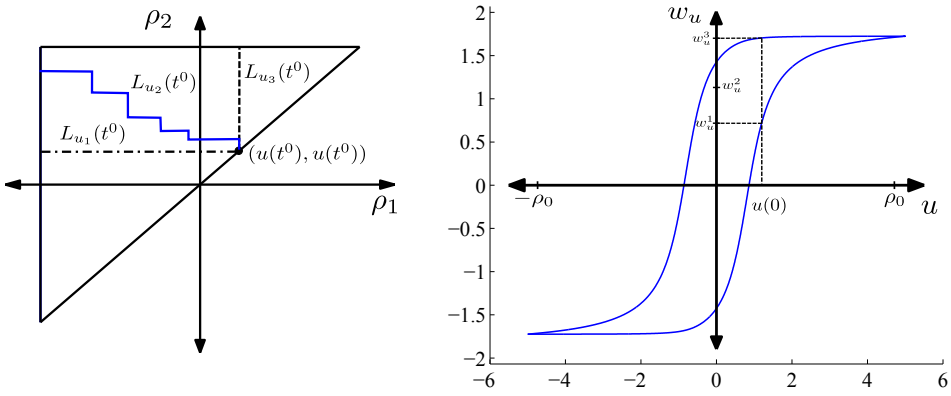

Figure 26: Staircase function (left) $w_u - u$ curve (right).

In what follows, we will take into account the previous discussion to study a particular transient eddy current problem where hysteresis effects are considered.

5. The transient eddy current model with hysteresis

Eddy currents are modeled by the so-called low-frequency Maxwell's equations:

$$\begin{aligned} \mathbf{curl}\, H &= J, \\ \frac{\partial B}{\partial t} + \mathbf{curl}\, E &= 0, \\ \operatorname{div} B &= 0, \end{aligned}$$

where we have used the standard notation in electromagnetism: E is the electric field, B the magnetic induction, H the magnetic field and J the current density.

In order to obtain a closed system we need constitutive laws. We have the Ohm's law in conductors,

$$J = \sigma E,$$

where σ is the electrical conductivity and we consider the constitutive equation

$$B = \mu_0 (H + M),$$

where M is the magnetization and μ_0 is the magnetic permeability in vacuum. In ferromagnetic and ferrimagnetic materials, where hysteresis phenomena may occur, the

dependence between M and H exhibits a history-dependent behavior and must be represented by a suitable constitutive law accounting for hysteresis. We synthetically represent this dependence in the form

$$M = \mathscr{F}(H),$$

where $\mathscr{F}$ is a vector *hysteresis operator* (see [28, 27, 45, 46, 36, 35]). This dependence is nonlocal in time but pointwise in space. We notice that a real ferromagnetic material may exhibit also rate dependent memory effects but they will not be considered in this analysis.

From the above equations we can easily obtain the following vector partial differential equation in conductors:

$$\frac{\partial B}{\partial t} + \mathbf{curl}\left(\frac{1}{\sigma}\,\mathbf{curl}\, H\right) = 0, \tag{26}$$

which has to be solved together the constitutive equation

$$B = \mu_0\,(H + \mathscr{F}(H)) \tag{27}$$

in a conducting domain $\widetilde{\Omega} \subset \mathbb{R}^3$.

5.1. Axisymmetric eddy current model

In many applications the computational domain $\widetilde{\Omega}$ has cylindrical symmetry and all fields are independent of the angular variable θ. In such a case, in order to reduce the dimension and thereby the computational effort, it is convenient to consider a cylindrical coordinate system (r,θ,z).

Let us denote by $\mathbf{e}_r$, $\mathbf{e}_\theta$ and $\mathbf{e}_z$ the corresponding unit vectors of the local orthonormal basis. Moreover, let us assume the magnetic field has only azimuthal component, i.e., it is of the form,

$$H(r,z,t) = H(r,z,t)\mathbf{e}_\theta. \tag{28}$$

If we also assume that the materials composing the domain have an isotropic behavior, then B has only azimuthal component too:

$$B(r,z,t) = B(r,z,t)\mathbf{e}_\theta. \tag{29}$$

We notice that any field of the form (29) is divergence–free.

According to (28),

$$\mathbf{curl}\, H(r,z,t) = -\frac{\partial}{\partial z}H(r,z,t)\mathbf{e}_\theta + \frac{1}{r}\frac{\partial}{\partial r}(rH)(r,z,t)\mathbf{e}_z, \tag{30}$$

and then equation (26) reads

$$\frac{\partial B}{\partial t} - \frac{\partial}{\partial r}\left(\frac{1}{\sigma r}\frac{\partial (rH)}{\partial r}\right) - \frac{\partial}{\partial z}\left(\frac{1}{\sigma}\frac{\partial H}{\partial z}\right) = 0.$$

This equation holds in a meridian section Ω of $\widetilde{\Omega}$, for all time $t \in [0,T]$.

In order to write a well-posed problem we must add an initial condition

$$B(r,z,0) = B_0(r,z) \quad \text{in } \Omega, \tag{31}$$

and appropriate source terms. In view of applications, we will consider alternatively the two following cases:

- Non-homogeneous Dirichlet condition:

$$H(r,z,t) = g(r,z,t) \qquad \text{on } \Gamma,$$

where g is a given function and $\Gamma := \partial\Omega$. For applications of this model, we refer for instance to [1, 2, 20], where a Dirichlet problem arises in the simulation of metallurgical electrodes, or the computation of current losses in a toroidal laminated core [26, 29]. In this case, the Dirichlet boundary data g can be obtained from the current intensity.

- Magnetic flux condition:

$$\int_\Omega B(r,z,t)\, drdz = b(t), \tag{32}$$

$$rH|_\Gamma = \psi(t) \qquad \text{on } \Gamma, \tag{33}$$

where b is a given function but ψ is unknown; the meaning of the last condition is just that at each time t, rH is constant on Γ. The above integral in (32) represents the magnetic flux $b(t)$ through a meridian section Ω of the domain. Such a condition holds, for instance, in toroidal transformers when a voltage drop between the ends of the coil is applied (see, for instance, [37]).

Finally, taking into account that now the involved fields are scalar, relation (27) can be described as

$$B(r,z,t) = \mu_0 \left(H(r,z,t) + [\mathscr{F}(H)](r,z,t)\right), \tag{34}$$

where $\mathscr{F}$ is a scalar hysteresis operator.

All together, the two resulting axisymmetric problems read:

PROBLEM 2. Find $H_N(r,z,t)$, $B_N(r,z,t)$ and $\psi(t)$ such that

$$\frac{\partial B_N}{\partial t} - \frac{\partial}{\partial r}\left(\frac{1}{\sigma r}\frac{\partial (rH_N)}{\partial r}\right) - \frac{\partial}{\partial z}\left(\frac{1}{\sigma}\frac{\partial H_N}{\partial z}\right) = f \qquad \text{in } \Omega \times (0,T), \tag{35}$$

$$B_N = \mu_0 \left(H_N + \mathscr{F}(H_N, \xi)\right) \qquad \text{in } \Omega \times (0,T), \tag{36}$$

$$rH_N(r,z,t) = \psi(t) \qquad \text{on } \Gamma \times (0,T), \tag{37}$$

$$\int_\Omega B_N(r,z,t)\, drdz = b(t) \qquad \text{in } (0,T), \tag{38}$$

$$B_N|_{t=0} = B_{N0} \qquad \text{in } \Omega. \tag{39}$$

PROBLEM 3. Find $H_D(r,z,t)$ and $B_D(r,z,t)$ such that

$$\frac{\partial B_D}{\partial t} - \frac{\partial}{\partial r}\left(\frac{1}{\sigma r}\frac{\partial (rH_D)}{\partial r}\right) - \frac{\partial}{\partial z}\left(\frac{1}{\sigma}\frac{\partial H_D}{\partial z}\right) = f \qquad \text{in } \Omega\times(0,T), \tag{40}$$

$$B_D = \mu_0\,(H_D + \mathscr{F}(H_D,\xi)) \qquad \text{in } \Omega\times(0,T), \tag{41}$$

$$H_D = g \qquad \text{on } \Gamma\times(0,T), \tag{42}$$

$$B_D|_{t=0} = B_{D0} \qquad \text{in } \Omega. \tag{43}$$

In both problems $\sigma(r,z,t)$, $f(r,z,t)$, $g(r,z,t)$, $b(t)$, $\xi(r,z)$, $B_{D0}(r,z)$ and $B_{N0}(r,z)$ are given functions.

REMARK 6. For the sake of completeness, in (40) and (35) we have considered a general right-hand side f. Moreover, we consider a space and time dependent electrical conductivity σ because, in practical applications, σ is a function of temperature which, in its turn, is a time dependent field.

REMARK 7. Notice that, in order to compute the hysteresis operator $[\mathscr{F}(H)]$ a.e. in $\Omega\times[0,T]$, we need to provide an appropriate "initial state". From a practical point of view, a typical initial condition (cf. (43) and (39)) is the so-called demagnetized or virginal state of the material, namely, $(B,H)|_{t=0} = (0,0)$. The demagnetized state can be achieved, for instance, by heating the material above its Curie temperature. Another method that returns the material to a nearly demagnetized state is to apply a magnetic field with a direction that changes back and forth, while at the same time its amplitude reduces to zero.

6. Mathematical analysis

In this section, we derive weak formulations for Problems 2 and 3, and prove that they are well-posed. The techniques used for this purpose are based on [44, Chapter IX], where the existence of solution to a similar 2D problem in standard Sobolev spaces with homogeneous Dirichlet condition is proved (for a homogeneous Neumann condition we refer to [15, 41]).

The presence of time dependent coefficients, the different source terms (cf. (42) and (38)) and the fact that the problems are posed on weighted Sobolev spaces because of the cylindrical symmetry assumption brings some technical complications to the analysis with respect to previous works on the subject. In particular, (37)–(38) yield a non-classical boundary condition for the resulting non-linear parabolic problem. Such a condition and the fact of having a time dependent conductivity (cf. Remark 6), lead us to deal with a time dependent bilinear form which, instead of being elliptic, satisfies a Gårding's inequality (see (47) below). On the other hand, with respect to Problem 3, in order to deal with condition (42) we have to introduce a *lifting* of the boundary data which brings additional complications in the mathematical analysis.

First, we introduce some preliminary results.

6.1. Functional spaces and preliminary results

We define appropriate weighted Sobolev spaces that will be used for the mathematical analysis of the problem and recall some of their properties. For the sake of simplicity, in this paragraph the partial derivatives will be denoted by ∂_r and ∂_z.

Let $\Omega \subset \{(r,z) \in \mathbb{R}^2 : r > 0\}$ be a bounded connected two-dimensional open set with a connected Lipschitz boundary Γ. Let $\mathrm{L}^2_r(\Omega)$ denote the weighted Lebesgue space of all measurable functions u defined in Ω for which

$$\|u\|^2_{\mathrm{L}^2_r(\Omega)} := \int_\Omega |u|^2 r \, drdz < \infty.$$

The weighted Sobolev space $\mathrm{H}^1_r(\Omega)$ consists of all functions in $\mathrm{L}^2_r(\Omega)$ whose first derivatives are also in $\mathrm{L}^2_r(\Omega)$. We define the norms and semi-norms in the standard way; in particular,

$$|u|^2_{\mathrm{H}^1_r(\Omega)} := \int_\Omega \left(|\partial_r u|^2 + |\partial_z u|^2\right) r \, drdz.$$

Let $\widetilde{\mathrm{H}}^1_r(\Omega) := \mathrm{H}^1_r(\Omega) \cap \mathrm{L}^2_{1/r}(\Omega)$, where $\mathrm{L}^2_{1/r}(\Omega)$ denotes the set of all measurable functions u defined in Ω for which

$$\|u\|^2_{\mathrm{L}^2_{1/r}(\Omega)} := \int_\Omega \frac{|u|^2}{r} \, drdz < \infty.$$

$\widetilde{\mathrm{H}}^1_r(\Omega)$ is a Hilbert space with the norm

$$\|u\|^2_{\widetilde{\mathrm{H}}^1_r(\Omega)} := \|u\|^2_{\mathrm{H}^1_r(\Omega)} + \|u\|^2_{\mathrm{L}^2_{1/r}(\Omega)}.$$

We recall from [18, Section 3] that functions in $\widetilde{\mathrm{H}}^1_r(\Omega)$ have traces on Γ. We denote

$$\widetilde{\mathrm{H}}^{1/2}_r(\Gamma) := \left\{ v|_\Gamma : v \in \widetilde{\mathrm{H}}^1_r(\Omega) \right\}$$

endowed with the norm

$$\|g\|_{\widetilde{\mathrm{H}}^{1/2}_r(\Gamma)} := \inf \left\{ \|v\|_{\widetilde{\mathrm{H}}^1_r(\Omega)} : v \in \widetilde{\mathrm{H}}^1_r(\Omega), v|_\Gamma = g \right\}$$

which makes the trace operator $v \to v|_\Gamma$ continuous.

Also, let us introduce the function space $\widehat{\mathrm{H}}^1_r(\Omega)$ defined by

$$\widehat{\mathrm{H}}^1_r(\Omega) := \left\{ u \in \mathrm{L}^2_r(\Omega) : \partial_r(ru) \in \mathrm{L}^2_{1/r}(\Omega), \partial_z u \in \mathrm{L}^2_r(\Omega) \right\}$$

which is a Hilbert space with the norm

$$\|u\|^2_{\widehat{\mathrm{H}}^1_r(\Omega)} := \left(\|u\|^2_{\mathrm{L}^2_r(\Omega)} + \|\partial_r(ru)\|^2_{\mathrm{L}^2_{1/r}(\Omega)} + \|\partial_z u\|^2_{\mathrm{L}^2_r(\Omega)} \right)^{1/2}.$$

Clearly $\widetilde{\mathrm{H}}^1_r(\Omega) \subset \widehat{\mathrm{H}}^1_r(\Omega)$.

Finally, given a Banach space Q, we introduce the space $\mathrm{L}^2_r(\Omega;Q)$ of all function $u:\Omega\to Q$ such that

$$\|u\|^2_{\mathrm{L}^2_r(\Omega;Q)} := \int_\Omega \|u(r,z)\|^2_Q\, r\, drdz < \infty.$$

REMARK 8. For Ω being a meridian section of a 3D axisymmetric domain $\widetilde{\Omega}$, the space $\widehat{\mathrm{H}}^1_r(\Omega)$ can be considered as an axisymmetric version of the 3D space $\mathbf{H}(\mathbf{curl},\widetilde{\Omega}) := \{\mathbf{u}\in \mathrm{L}^2(\widetilde{\Omega})^3 : \mathbf{curl}\,\mathbf{u}\in \mathrm{L}^2(\widetilde{\Omega})^3\}$. In fact, it is easy to see that $G(r,z)\in \widehat{\mathrm{H}}^1_r(\Omega)$ if and only if $\mathbf{G}(r,z,\theta)=G(r,z)\mathbf{e}_\theta(\theta)\in\mathbf{H}(\mathbf{curl},\widetilde{\Omega})$. Similarly, we deduce that $G(r,z)\in\widetilde{\mathrm{H}}^1_r(\Omega)$ if and only if $\mathbf{G}(r,z,\theta)=G(r,z)\mathbf{e}_\theta(\theta)\in\mathrm{H}^1(\widetilde{\Omega})^3$.

Moreover, given $\mathbf{G}$ of the form $\mathbf{G}(r,z,\theta)=G(r,z)\mathbf{e}_\theta(\theta)$, then $\mathrm{div}\,\mathbf{G}=0$ and $\mathbf{G}\cdot n=0$ on $\partial\widetilde{\Omega}$, i.e., $\mathbf{G}$ belong to $\mathbf{H}_0(\mathrm{div}^0;\widetilde{\Omega}) := \{\mathbf{u}\in \mathrm{L}^2(\widetilde{\Omega})^3 : \mathrm{div}\,\mathbf{u}=0, \mathbf{u}\cdot n = 0\}$. Thus $\widehat{\mathrm{H}}^1_r(\Omega)$ can be identified with a closed subspace of $\mathbf{H}(\mathbf{curl},\widetilde{\Omega})\cap\mathbf{H}_0(\mathrm{div}^0;\widetilde{\Omega})$ continuously included in $\mathrm{H}^s(\widetilde{\Omega})^3$ for $s>1/2$, which, in turn, is compactly included in $\mathrm{L}^2(\widetilde{\Omega})^3$ (see [17, Theorem I.1.3]). Then,

$$\widehat{\mathrm{H}}^1_r(\Omega)\subset \mathrm{L}^2_r(\Omega)$$

with compact inclusion and, hence, $\widetilde{\mathrm{H}}^1_r(\Omega)$ is also compactly included in $\mathrm{L}^2_r(\Omega)$.

6.2. Weak formulation

In order to give a weak formulation of the above problems, let us define the closed subspaces of $\widetilde{\mathrm{H}}^1_r(\Omega)$ and $\widehat{\mathrm{H}}^1_r(\Omega)$

$$\mathscr{U} := \left\{ G\in \widetilde{\mathrm{H}}^1_r(\Omega) :\ G|_\Gamma = 0 \right\},$$

$$\mathscr{W} := \left\{ G\in \widehat{\mathrm{H}}^1_r(\Omega) :\ rG|_\Gamma \ \text{ is constant} \right\},$$

respectively.

Before stating a weak formulation of Problem 2, we notice that if the boundary of Ω intersects the symmetry axis ($r=0$), then $\psi(t)$ should be identically zero because r vanishes there. In that case, (37) would become a homogeneous Dirichlet boundary condition and Problem 2 without condition (38) would be exactly Problem 3 with $g=0$, so there is no reason for (38) to hold for a given $b(t)$. However, this does not happen in the application that motivates this problem in which the domain does not intersect the symmetry axis (see [37]). This is the reason why, from now on, when dealing with Problem 2, we will assume that

$$\inf\{r>0 : (r,z)\in\Omega\} > 0 \tag{44}$$

and, hence, $\mathrm{L}^2_r(\Omega)$ and $\mathrm{L}^2_{1/r}(\Omega)$ are both identical to $\mathrm{L}^2(\Omega)$. Similarly, $\widehat{\mathrm{H}}^1_r(\Omega)$ is identical to $\mathrm{H}^1(\Omega)$. Straightforward computations lead to the following weak formulation for Problem 2 (see [3]):

PROBLEM 4. Given $b \in \mathrm{H}^2(0,T)$, $f \in \mathrm{H}^1(0,T;\mathscr{W}')$, $B_{N0} \in \mathrm{L}^2_r(\Omega)$ and $\xi : \Omega \to Y$, find $H_N \in \mathrm{H}^1(0,T;\,\mathrm{L}^2_r(\Omega)) \cap \mathrm{L}^\infty(0,T;\mathscr{W})$ and $B_N \in \mathrm{L}^2(0,T;\mathrm{L}^2_r(\Omega))$ with $\partial_t B_N \in \mathrm{L}^2(0,T;\mathscr{W}')$, such that

$$\begin{aligned}\left\langle \frac{\partial B_N}{\partial t}, G \right\rangle_{\mathscr{W},\mathscr{W}'} + \int_\Omega \frac{1}{\sigma r}\left(\frac{\partial (rH_N)}{\partial r}\frac{\partial (rG)}{\partial r} + \frac{\partial (rH_N)}{\partial z}\frac{\partial (rG)}{\partial r}\right) dr dz & \\ = \langle f, G\rangle_{\mathscr{W},\mathscr{W}'} + \left(b'(t) - \langle f, r^{-1}\rangle_{\mathscr{W},\mathscr{W}'}\right)(rG)\,|_\Gamma \quad & \forall G \in \mathscr{W},\ \text{a.e. in } (0,T], \\ B_N = \mu_0\,(H_N + \mathscr{F}(H_N,\xi)) \quad & \text{in } \Omega\times(0,T), \\ B_N|_{t=0} = B_{N0} \quad & \text{in } \Omega.\end{aligned}$$

On the other hand, for each $t \in [0,T]$ a weak formulation of Problem 3 is given by:

PROBLEM 5. Given $g \in \mathrm{H}^2(0,T;\widetilde{\mathrm{H}}^{1/2}_r(\Gamma))$, $f \in \mathrm{H}^1(0,T;\mathscr{U}')$, $B_{D0} \in \mathrm{L}^2_r(\Omega)$, and $\xi : \Omega \to Y$, find $H_D \in \mathrm{L}^2(0,T;\widetilde{\mathrm{H}}^1_r(\Omega)) \cap \mathrm{L}^\infty(0,T;\mathrm{L}^2_r(\Omega))$ and $B_D \in \mathrm{L}^2(0,T;\mathrm{L}^2_r(\Omega))$ with $\partial_t B_D \in \mathrm{L}^2(0,T;\mathscr{U}')$, such that

$$\begin{aligned}\left\langle \frac{\partial B_D}{\partial t}, G \right\rangle_{\mathscr{U},\mathscr{U}'} + \int_\Omega \frac{1}{\sigma r}\left(\frac{\partial (rH_D)}{\partial r}\frac{\partial (rG)}{\partial r} + \frac{\partial (rH_D)}{\partial z}\frac{\partial (rG)}{\partial z}\right) dr dz & \\ = \langle f, G\rangle_{\mathscr{U},\mathscr{U}'} \quad & \forall G \in \mathscr{U},\ \text{a.e. in } (0,T], \\ B_D = \mu_0\,(H_D + \mathscr{F}(H_D,\xi)) \quad & \text{in } \Omega\times(0,T), \\ H_D = g \quad & \text{on } \Gamma\times(0,T), \\ B_D|_{t=0} = B_{D0} \quad & \text{in } \Omega.\end{aligned}$$

We use the classical notation $\langle\cdot,\cdot\rangle_{\mathscr{U},\mathscr{U}'}$ for the duality product between $\mathscr{U}$ and its dual space $\mathscr{U}'$.

We introduce the following assumptions that will be used to prove the existence of a solution to Problem 4 and Problem 5:

H.1 $\mathscr{F} : \mathscr{M}(\Omega;C([0,T])\times Y) \to \mathscr{M}(\Omega;C([0,T]))$ is causal, strongly continuous and piecewise monotone (cf. (5)–(8)). We also assume that $\mathscr{F}$ is *affinely bounded*, namely,

$$\begin{aligned}&\exists L_{\mathscr{F}} > 0, \exists \tau \in \mathrm{L}^2_r(\Omega) : \forall v \in \mathrm{L}^2_r(\Omega;C([0,T])), \\ &\|[\mathscr{F}(v,\xi)](r,z,\cdot)\|_{C([0,T])} \leqslant L_{\mathscr{F}}\,\|v(r,z,\cdot)\|_{C([0,T])} + \tau(r,z) \quad \text{a.e. in } \Omega. \qquad (45)\end{aligned}$$

H.2 $\sigma : (0,T)\times\Omega \to \mathbb{R}$ belongs to $\mathrm{W}^{1,\infty}(0,T;\mathrm{L}^\infty(\Omega))$ and there exist non-negative constants σ_* and σ^* such that

$$\sigma_* \leqslant \sigma(r,z,t) \leqslant \sigma^* \quad \forall t \in [0,T],\ \text{a.e. in } \Omega.$$

H.3 There exist $(H_{0D}, W_{0D}) \in \widetilde{\mathrm{H}}^1_r(\Omega) \times \mathrm{L}^2_r(\Omega)$ or $(H_{0N}, W_{0N}) \in \mathscr{W} \times \mathrm{L}^2_r(\Omega)$, such that

$$B_{D0}(r,z) = \mu_0\,(H_{0D} + W_{0D})\,(r,z) \quad \text{and} \quad B_{N0}(r,z) = \mu_0\,(H_{0N} + W_{0N})\,(r,z)\ \text{a.e in } \Omega.$$

Also, for each $t \in [0,T]$, let $a_t(\cdot,\cdot)$ be the bilinear form defined by

(46)
$$a_t(G_1,G_2) := \int_\Omega \frac{1}{\sigma(\cdot,t)} \left(\frac{1}{r}\frac{\partial (rG_1)}{\partial r}\, \frac{1}{r}\frac{\partial (rG_2)}{\partial r} + \frac{\partial G_1}{\partial z}\frac{\partial G_2}{\partial z} \right) r\, drdz, \quad G_1, G_2 \in \widehat{\mathrm{H}}^1_r(\Omega).$$

From assumption H.2 it is easy to obtain the following result (see [4, Lemma 2.1]):

LEMMA 3. *The bilinear forms $a_t : \widehat{\mathrm{H}}^1_r(\Omega) \times \widehat{\mathrm{H}}^1_r(\Omega) \to \mathbb{R}$, $t \in [0,T]$, are continuous uniformly in t and they satisfy the Gårding's inequality*

$$a_t(G,G) + \lambda \|G\|^2_{\mathrm{L}^2_r(\Omega)} \geqslant \gamma \|G\|^2_{\widehat{\mathrm{H}}^1_r(\Omega)} \quad \forall G \in \widehat{\mathrm{H}}^1_r(\Omega), \quad \forall t \in [0,T], \tag{47}$$

with $\lambda = \gamma = 1/\sigma^*$. Moreover, there exists $\gamma_u > 0$ such that

$$a_t(G,G) \geqslant \gamma_u \|G\|^2_{\widetilde{\mathrm{H}}^1_r(\Omega)} \quad \forall G \in \mathscr{U}, \quad \forall t \in [0,T]. \tag{48}$$

Finally, we introduce the linear operator $A(t) : \widehat{\mathrm{H}}^1_r(\Omega) \to \widehat{\mathrm{H}}^1_r(\Omega)'$ induced by $a_t(\cdot,\cdot)$, namely,

$$\langle A(t)H, G\rangle_{\widehat{\mathrm{H}}^1_r(\Omega),\widehat{\mathrm{H}}^1_r(\Omega)'} := a_t(H,G) \quad \forall H, G \in \widehat{\mathrm{H}}^1_r(\Omega).$$

Clearly $A(t)$ is linear and continuous, i.e., it belongs to $\mathscr{L}(\widehat{\mathrm{H}}^1_r(\Omega), \widehat{\mathrm{H}}^1_r(\Omega)')$, for all $t \in [0,T]$.

REMARK 9. From the definition of $a_t(\cdot,\cdot)$, it follows that $a_t : \widetilde{\mathrm{H}}^1_r(\Omega) \times \widetilde{\mathrm{H}}^1_r(\Omega) \to \mathbb{R}$, $t \in [0,T]$, are continuous uniformly in t, and therefore, the linear operator $A(t) : \widetilde{\mathrm{H}}^1_r(\Omega) \to \widetilde{\mathrm{H}}^1_r(\Omega)'$ belongs to $\mathscr{L}(\widetilde{\mathrm{H}}^1_r(\Omega), \widetilde{\mathrm{H}}^1_r(\Omega)')$ for all $t \in [0,T]$.

The next section is devoted to study the existence of solutions to Problems 4 and 5. The proof is carried out through three different steps: time discretization, a priori estimates and passage to the limit by using compactness. This approximation procedure is often used in the analysis of equations that include a memory operator since at any time-step we solve a stationary problem in which this operator is reduced to a standard nonlinear mapping (see, for instance, [44]).

6.3. Existence of solutions

In this section we will prove that, under certain assumptions, there exist (H_N, B_N) solution of Problem 4.

Time discretization

Let us fix $m \in \mathbb{N}$ and set $\Delta t := T/m$. Now, for $n = 1, \ldots, m$, we define $t^n := n\Delta t$, $b^n := b(t^n)$, $\sigma^n(r,z) := \sigma(r,z,t^n)$, $f^n := f(t^n)$ and $A(t^n) := A^n$. Notation $\bar{\partial} z^n$ refers to the difference quotient

$$\bar{\partial} z^n := \frac{z^n - z^{n-1}}{\Delta t}.$$

A time discretization of Problem 4 based on backward Euler's scheme reads as follows:

Given $H_N^0 = H_{0N}$ and $W_N^0 = W_{0N}$ in Ω, find $H_N^n \in \mathscr{W}$ and $W_N^n \in \mathrm{L}_r^2(\Omega)$, $n = 1,\dots,m$, satisfying

$$\mu_0 \bar{\partial} H_N^n + \mu_0 \bar{\partial} W_N^n + A^n H_N^n = R_N^n \qquad \text{in } \mathscr{W}', \tag{49}$$

$$W_N^n = [\mathscr{F}(H_{N\Delta t^n}, \xi)](t^n), \tag{50}$$

where $H_{N\Delta t^n} : [0,t^n] \to \mathscr{W}$ is the piecewise linear in time interpolant of $\{H_N^i\}_{i=0}^n$ given by

$$H_{N\Delta t^n}(t^0) := H_{0N}; \tag{51}$$

$$H_{N\Delta t^n}(t) := H_N^{i-1} + (t - t^{i-1})\,\bar{\partial} H_N^i, \quad t \in (t^{i-1}, t^i], \quad i = 1,\dots,n, \tag{52}$$

and

$$\langle R_N^n, G\rangle_{\mathscr{W},\mathscr{W}'} := \langle f^n, G\rangle_{\mathscr{W},\mathscr{W}'} + \left(\bar{\partial} b^n - \langle f^n, r^{-1}\rangle_{\mathscr{W},\mathscr{W}'}\right)(rG)\,|_\Gamma.$$

We notice that, since for $n \in \{1,\dots,m\}$ we already know $H_N^1,\dots,H_N^{n-1}$, we have that $W_N^n(\cdot) = [\mathscr{F}(H_{N\Delta t^n}, \xi)](\cdot, t^n)$ depends only on $H_{N\Delta t^n}(\cdot,t)|_{[0,t^{n-1}]}$, which is known, and on H_N^n, which must be determined.

In order to analyze the discrete problem, we define $F^n : \Omega \times \mathbb{R} \longrightarrow \mathbb{R}$ as follows: given $s \in \mathbb{R}$

$$F^n(r,z,s) := [\mathscr{F}(U_s, \xi)](r,z,t^n) \quad \text{a.e. in } \Omega,$$

with U_s the piecewise linear in time function such that $U_s(r,z,t^l) = H_N^l(r,z)$, $l = 0,\dots,n-1$ and $U_s(r,z,t^n) = s$. This allows us to introduce the operator $\mathbb{F}^n : \mathrm{L}_r^2(\Omega) \to \mathrm{L}_r^2(\Omega)$ defined by $\mathbb{F}^n(G)(\cdot) := F^n(\cdot, G(\cdot))$ for all $G \in \mathrm{L}_r^2(\Omega)$. The following lemma provides some properties of $\mathbb{F}^n$ that will be used in the sequel.

LEMMA 4. *For all $n = 1,\dots,m$, $\mathbb{F}^n : \mathrm{L}_r^2(\Omega) \to \mathrm{L}_r^2(\Omega)$ is a continuous and monotone operator, namely*

$$\int_\Omega \left(\mathbb{F}^n(G_1) - \mathbb{F}^n(G_2)\right)(G_1 - G_2) r\, dr dz \geqslant 0 \qquad \forall G_1, G_2 \in \mathrm{L}_r^2(\Omega).$$

Moreover,

$$\int_\Omega \mathbb{F}^n(G) G r\, dr dz \geqslant -C_1 \|G\|_{\mathrm{L}_r^2(\Omega)} - C_2 \qquad \forall G \in \mathrm{L}_r^2(\Omega), \tag{53}$$

where $C_1, C_2 > 0$ depend on $\{H_N^l\}_{l=0}^{n-1}$ but are independent of G.

Proof. The continuity and non-decreasing properties of $\mathbb{F}^n$ follow from H.1 (cf. (7), (8) and (45)), whereas (53) is derived from (45). □

Thus, from the theory of monotone operators, it follows that (49)–(50) has a unique solution (see, for instance, [33, Theorem 2.18]).

A priori estimates

The aim of this section is to prove an a priori estimate for the solution of (49)–(50).

Here and thereafter C and c, with or without subscripts, will be used for positive constants not necessarily the same at each occurrence, but always independent of the time-step Δt.

LEMMA 5. *There exists $C>0$ such that, for all $l=1,\dots,m$,*

$$\Delta t\sum_{n=1}^{l}\left\|\bar{\partial}W_N^n\right\|_{\mathscr{W}'}^2+\left\|H_N^l\right\|_{\widehat{\mathrm{H}}_r^1(\Omega)}^2+\Delta t\sum_{n=1}^{l}\left\|\bar{\partial}H_N^n\right\|_{\mathrm{L}_r^2(\Omega)}^2\leqslant C.$$

Proof. Let apply (49) to $(H_N^n-H_N^{n-1})$. For $n=1,\dots,m$ we obtain

$$\begin{aligned}\mu_0\Delta t\left\|\frac{H_N^n-H_N^{n-1}}{\Delta t}\right\|_{\mathrm{L}_r^2(\Omega)}^2&+\int_\Omega\frac{\mu_0}{\Delta t}(W_N^n-W_N^{n-1})(H_N^n-H_N^{n-1})+\langle A^nH_N^n,H_N^n-H_N^{n-1}\rangle_{\mathscr{W},\mathscr{W}'}\\&=\langle f^n,H_N^n-H_N^{n-1}\rangle_{\mathscr{W},\mathscr{W}'}+\left(\bar{\partial}b^n-\langle f^n,r^{-1}\rangle_{\mathscr{W},\mathscr{W}'}\right)\left(rH_N^n-rH_N^{n-1}\right)|_\Gamma.\end{aligned}\tag{54}$$

First, we estimate the terms on the left hand side. From the piecewise monotonicity of $\mathscr{F}$ (cf. (8)) we have that

$$\int_\Omega\frac{1}{\Delta t}(W_N^n-W_N^{n-1})(H_N^n-H_N^{n-1})\,drdz\geqslant 0.\tag{55}$$

On the other hand, in order to estimate the last term on the left-hand side of (54) we use the identity $2(p-q)p=p^2+(p-q)^2-q^2$ to obtain that

$$\begin{aligned}&2\langle A^nH_N^n,H_N^n-H_N^{n-1}\rangle_{\mathscr{W},\mathscr{W}'}\geqslant\langle A^nH_N^n,H_N^n\rangle_{\mathscr{W},\mathscr{W}'}-\langle A^nH_N^{n-1},H_N^{n-1}\rangle_{\mathscr{W},\mathscr{W}'}\\&=\langle A^nH_N^n,H_N^n\rangle_{\mathscr{W},\mathscr{W}'}-\langle A^{n-1}H_N^{n-1},H_N^{n-1}\rangle_{\mathscr{W},\mathscr{W}'}+\langle(A^{n-1}-A^n)H_N^{n-1},H_N^{n-1}\rangle_{\mathscr{W},\mathscr{W}'}\end{aligned}\tag{56}$$

where

$$\left|\langle(A^{n-1}-A^n)H_N^{n-1},H_N^{n-1}\rangle_{\mathscr{W},\mathscr{W}'}\right|\leqslant C_\sigma\left\|\partial_t\sigma\right\|_{\mathrm{L}^\infty(0,T;\mathrm{L}^\infty(\Omega))}\Delta t\left\|H_N^{n-1}\right\|_{\widehat{\mathrm{H}}_r^1(\Omega)}^2.\tag{57}$$

Summing up (54) for $n=1,\dots,l$ with $l\in\{1,\dots,m\}$, from (55)–(57) we obtain

$$\begin{aligned}&\sum_{n=1}^{l}\mu_0\Delta t\left\|\bar{\partial}H_N^n\right\|_{\mathrm{L}_r^2(\Omega)}^2+\frac{1}{2}\langle A^lH_N^l,H_N^l\rangle_{\mathscr{W},\mathscr{W}'}\\&\qquad\leqslant\frac{1}{2}\langle A^0H_{0N},H_{0N}\rangle_{\mathscr{W},\mathscr{W}'}+\sum_{n=1}^{l}C_\sigma\left\|\partial_t\sigma\right\|_{\mathrm{L}^\infty(0,T,\mathrm{L}^\infty(\Omega))}\Delta t\left\|H_N^{n-1}\right\|_{\widehat{\mathrm{H}}_r^1(\Omega)}^2\\&\qquad+\sum_{n=1}^{l}\langle f^n,H_N^n-H_N^{n-1}\rangle_{\mathscr{W},\mathscr{W}'}+\sum_{n=1}^{l}\left(\bar{\partial}b^n-\langle f^n,r^{-1}\rangle_{\mathscr{W},\mathscr{W}'}\right)\left(rH_N^n-rH_N^{n-1}\right)|_\Gamma.\end{aligned}\tag{58}$$

Next, we estimate the last two terms on the right-hand side of (58). By summation by parts, Young's inequality and the fact that $(rG)\,|_\Gamma \leqslant C\,\|G\|_{\widehat{\mathrm{H}}^1_r(\Omega)}\ \forall G \in \mathscr{W}$, we have that

$$
\begin{aligned}
&\left| \sum_{n=1}^{l} \left(\bar{\partial} b^n - \langle f_{,}^n r^{-1}\rangle_{\mathscr{W},\mathscr{W}'}\right)\left(rH_N^n - rH_N^{n-1}\right)|_\Gamma \right| \\
&\qquad = \left| \left(\bar{\partial} b^l - \langle f^l, r^{-1}\rangle_{\mathscr{W},\mathscr{W}'}\right)\left(rH_N^l\right)|_\Gamma - \left(\bar{\partial} b^1 - \langle f^1, r^{-1}\rangle\right)(rH_{0N})\,|_\Gamma \right. \\
&\qquad\quad \left. - \sum_{n=1}^{l-1} \left(\bar{\partial} b^{n+1} - \bar{\partial} b^n - \langle f^{n+1} - f^n, r^{-1}\rangle_{\mathscr{W},\mathscr{W}'}\right)(rH_N^n)\,|_\Gamma \right| \\
&\qquad \leqslant C_\varepsilon \left\{ \|b\|^2_{\mathrm{H}^2(0,T)} + \|f\|^2_{\mathrm{H}^1(0,T;\mathscr{W}')} + \Delta t \sum_{n=1}^{l-1} \left| \frac{\bar{\partial} b^{n+1} - \bar{\partial} b^n}{\Delta t} \right|^2 + \Delta t \sum_{n=1}^{l-1} \left\| \bar{\partial} f^{n+1} \right\|^2_{\mathscr{W}'} \right\} \\
&\qquad\quad + \varepsilon \left\| H_N^l \right\|^2_{\widehat{\mathrm{H}}^1_r(\Omega)} + \Delta t \sum_{n=1}^{l-1} \|H_N^n\|^2_{\widehat{\mathrm{H}}^1_r(\Omega)} + \|H_{0N}\|^2_{\widehat{\mathrm{H}}^1_r(\Omega)}\,.
\end{aligned}
\tag{59}
$$

In a similar way,

$$
\left| \sum_{n=1}^{l} \langle f^n, H_N^n - H_N^{n-1}\rangle_{\mathscr{W},\mathscr{W}'} \right| \leqslant C_\varepsilon \|f\|^2_{\mathrm{H}^1(0,T;\mathscr{W}')} + \varepsilon \left\| H_N^l \right\|^2_{\widehat{\mathrm{H}}^1_r(\Omega)} + \Delta t \sum_{n=1}^{l-1} \|H_N^n\|^2_{\widehat{\mathrm{H}}^1_r(\Omega)} + \|H_{0N}\|^2_{\widehat{\mathrm{H}}^1_r(\Omega)}\,, \tag{60}
$$

for all $\varepsilon > 0$. On the other hand, in order to deal with the second term on the left-hand side of (58), we first notice that $H_N^l = H_{0N} + \Delta t \sum_{n=1}^{l} \bar{\partial} H_N^n$ and then

$$
\Delta t \sum_{n=1}^{l} \left\| \bar{\partial} H_N^n \right\|^2_{\mathrm{L}^2_r(\Omega)} \geqslant \frac{1}{T} \left\{ \frac{\left\| H_N^l \right\|^2_{\mathrm{L}^2_r(\Omega)}}{2} - \|H_{0N}\|^2_{\mathrm{L}^2_r(\Omega)} \right\}.
$$

Hence, from Lemma 3 (cf. (47)) we obtain that there exists $\widehat{\gamma} := \min\left\{\frac{\mu_0}{4T}, \frac{1}{2}\right\}\gamma$, such that

$$
\begin{aligned}
&\mu_0 \Delta t \sum_{n=1}^{l} \left\| \bar{\partial} H_N^n \right\|^2_{\mathrm{L}^2_r(\Omega)} + \frac{1}{2}\langle A^l H_N^l, H_N^l\rangle_{\mathscr{W},\mathscr{W}'} \\
&\qquad\qquad \geqslant \frac{\Delta t \mu_0}{2} \sum_{n=1}^{l} \left\| \bar{\partial} H_N^i \right\|^2_{\mathrm{L}^2_r(\Omega)} + \widehat{\gamma} \left\| H_N^l \right\|^2_{\widehat{\mathrm{H}}^1_r(\Omega)} - \mu_0 \frac{\|H_{0N}\|^2_{\mathrm{L}^2_r(\Omega)}}{2T}.
\end{aligned}
\tag{61}
$$

Then, by replacing (59)–(61) into (58) and choosing $\varepsilon = \dfrac{\widehat{\gamma}}{4}$ we obtain

$$\begin{aligned}
&\frac{\mu_0\Delta t}{2}\sum_{n=1}^{l}\left\|\bar{\partial}H_N^n\right\|^2_{\mathrm{L}^2_r(\Omega)}+\frac{\widehat{\gamma}}{2}\left\|H_{\Delta t}^l\right\|^2_{\widehat{\mathrm{H}}^1_r(\Omega)}\\
&\leqslant C\left\{\|b\|^2_{\mathrm{H}^2(0,T)}+\|f\|^2_{\mathrm{H}^1(0,T;\mathscr{W}')}+\Delta t\sum_{n=1}^{l}\left|\frac{\bar{\partial}b^n-\bar{\partial}b^{n-1}}{\Delta t}\right|^2+\Delta t\sum_{n=1}^{l}\left\|\bar{\partial}f^n\right\|^2_{\mathscr{W}'}\right\}\\
&\qquad+C\Delta t\sum_{n=1}^{l}\left\|H_N^{n-1}\right\|^2_{\widehat{\mathrm{H}}^1_r(\Omega)}+\left(\frac{\mu_0}{2T}+\frac{1}{2\sigma_*}+2\right)\|H_{0N}\|^2_{\widehat{\mathrm{H}}^1_r(\Omega)}.
\end{aligned}$$

Hence, by using the discrete Gronwall's lemma we obtain

$$\Delta t\sum_{n=1}^{l}\left\|\bar{\partial}H_N^n\right\|^2_{\mathrm{L}^2_r(\Omega)}+\left\|H_{\Delta t}^l\right\|^2_{\widehat{\mathrm{H}}^1_r(\Omega)}\leqslant C,\qquad l=1,\dots,m,$$

with $C>0$ depending on $\|b\|_{\mathrm{H}^2(0,T)}$, $\|H_{0N}\|_{\widehat{\mathrm{H}}^1_r(\Omega)}$, $\|f\|_{\mathrm{H}^1(0,T;\mathscr{W}')}$ and $\|\sigma\|_{\mathrm{W}^{1,\infty}(0,T;\mathrm{L}^\infty(\Omega))}$. Finally, we estimate $\sum_{n=1}^{l}\left\|\bar{\partial}W_N^n\right\|^2_{\mathscr{W}'}$ by using (49) and the last inequality. □

Convergence

Now, we will define a family of approximate solutions to Problem 4 and prove its weak convergence to a solution. With this aim, we introduce some notation: let $W_{N\Delta t}:[0,T]\to\mathrm{L}^2_r(\Omega)$ be the piecewise linear in time interpolant of $\{W_N^n\}_{n=0}^m$ (cf. (51)–(52)). We also introduce the step function $\overline{H}_{N\Delta t}:[0,T]\to\mathscr{W}$ by:

$$\overline{H}_{N\Delta t}(t^0):=H_{0N};\quad \overline{H}_{N\Delta t}(t):=H_N^n,\quad t\in(t^{n-1},t^n],\quad i=n,\dots,m,\tag{62}$$

and define the step functions $\overline{A}_{\Delta t}$ and $\overline{R}_{N\Delta t}$ in a similar way.

Using the above notation we rewrite equation (49) as follows:

$$\mu_0\frac{\partial H_{N\Delta t}}{\partial t}+\mu_0\frac{\partial W_{N\Delta t}}{\partial t}+\overline{A}_{\Delta t}\overline{H}_{N\Delta t}=\overline{R}_{N\Delta t}\qquad\text{in }\mathscr{W}',\quad\text{a.e. in }(0,T).\tag{63}$$

From Lemma 5 we deduce that there exists $C>0$ such that

$$\begin{aligned}
&\left\|\frac{\partial W_{N\Delta t}}{\partial t}\right\|_{\mathrm{L}^2(0,T;\mathscr{W}')}+\left\|\overline{A}_{\Delta t}\overline{H}_{N\Delta t}\right\|_{\mathrm{L}^\infty(0,T;\mathscr{W}')}\\
&\qquad+\|H_{N\Delta t}\|_{\mathrm{H}^1(0,T;\mathrm{L}^2_r(\Omega))\cap\mathrm{L}^\infty(0,T;\widehat{\mathrm{H}}^1_r(\Omega))}+\left\|\overline{H}_{N\Delta t}\right\|_{\mathrm{L}^\infty(0,T;\widehat{\mathrm{H}}^1_r(\Omega))}\leqslant C.
\end{aligned}\tag{64}$$

Moreover, since $\mathrm{H}^1(0,T;\mathrm{L}^2_r(\Omega))=\mathrm{L}^2_r(\Omega;\mathrm{H}^1(0,T))\hookrightarrow\mathrm{L}^2_r(\Omega;C([0,T]))$ with continuous injection, by using the affinely bounded assumption and (64) it follows that there exist $L_{\mathscr{F}}>0$ and $\tau\in\mathrm{L}^2_r(\Omega)$ such that

$$\begin{aligned}
\|W_{N\Delta t}\|_{\mathrm{L}^2_r(\Omega\times[0,T])}&\leqslant\sqrt{T}\,\|W_{N\Delta t}\|_{\mathrm{L}^2_r(\Omega;C([0,T]))}\\
&\leqslant\sqrt{T}L_{\mathscr{F}}\,\|H_{N\Delta t}\|_{L^2_r(\Omega;C([0,T]))}+\sqrt{T}\,\|\tau\|_{\mathrm{L}^2_r(\Omega)}\leqslant C.
\end{aligned}$$

This allows us to conclude that there exists H_N, W_N and X such that,

$$H_{N\Delta t} \longrightarrow H_N \quad \text{in } \mathrm{H}^1(0,T;\mathrm{L}^2_r(\Omega)) \cap \mathrm{L}^\infty(0,T;\widehat{\mathrm{H}}^1_r(\Omega)) \text{ weakly star}, \tag{65}$$

$$\overline{H}_{N\Delta t} \longrightarrow H_N \quad \text{in } \mathrm{L}^\infty(0,T;\widehat{\mathrm{H}}^1_r(\Omega)) \text{ weakly star}, \tag{66}$$

$$W_{N\Delta t} \longrightarrow W_N \quad \text{in } \mathrm{L}^2_r(\Omega\times[0,T]) \text{ weakly}, \tag{67}$$

$$\frac{\partial}{\partial t}H_{N\Delta t} \longrightarrow \frac{\partial}{\partial t}H_N \quad \text{in } \mathrm{L}^2(0,T;\mathscr{W}') \text{ weakly}, \tag{68}$$

$$\frac{\partial}{\partial t}W_{N\Delta t} \longrightarrow \frac{\partial}{\partial t}W_N \quad \text{in } \mathrm{L}^2(0,T;\mathscr{W}') \text{ weakly}, \tag{69}$$

$$\overline{A}_{\Delta t}\overline{H}_{N\Delta t} \longrightarrow X \quad \text{in } \mathrm{L}^\infty(0,T;\mathscr{W}') \text{ weakly star}. \tag{70}$$

Let $R_N \in \mathrm{H}^1(0,T;\mathscr{W}')$ defined by

$$\langle R_N, G\rangle_{\mathscr{W},\mathscr{W}'} := \langle f, G\rangle_{\mathscr{W},\mathscr{W}'} + \left(b'(t) - \langle f, r^{-1}\rangle_{\mathscr{W},\mathscr{W}'}\right)(rG)\,|_\Gamma \quad \forall G \in \mathscr{W}, \text{ a.e. in } [0,T].$$

By passing to the limit in (63) we obtain

$$\mu_0\frac{\partial H_N}{\partial t} + \mu_0\frac{\partial W_N}{\partial t} + X = R_N \qquad \text{in } \mathscr{W}', \quad \text{a.e. in } (0,T), \tag{71}$$

because $\overline{R}_{N\Delta t} \to R_N$ in $\mathrm{L}^2(0,T;\mathscr{W}')$, for $f \in \mathrm{H}^1(0,T;\mathscr{W}')$ and $b \in \mathrm{H}^2(0,T)$. The next step is to prove that $X = AH_N$ and $W_N = \mathscr{F}(H_N,\xi)$. The first equality, follows from (66), (70) and H.2. To prove the latter, first we recall that by virtue of the assumption on the domain (44), $\mathrm{L}^2_r(\Omega)$ and $\widehat{\mathrm{H}}^1_r(\Omega)$ are both identical to $\mathrm{L}^2(\Omega)$ and $\mathrm{H}^1(\Omega)$, respectively. Therefore, the last equality follows from the inclusions

$$\mathrm{H}^1(0,T;\mathrm{L}^2_r(\Omega)) \cap \mathrm{L}^2(0,T;\widehat{\mathrm{H}}^1_r(\Omega)) \subset \mathrm{H}^s(\Omega;\mathrm{H}^{1-s}(0,T)) \subset \mathrm{L}^2_r(\Omega;C([0,T])) \tag{72}$$

for $s \in (0,1/2)$, being the first continuous and the latter compact (see [44, Chapter IX, (1.45)]), and the strong continuity of $\mathscr{F}$.

As a consequence of this, we obtain the following result.

THEOREM 1. *Let us assume hypotheses H.1, H.2 and H.3. Then, Problem 4 has a solution.*

Proof. From (71) it follows that

$$\begin{aligned}\left\langle \frac{\partial B_N}{\partial t}, G\right\rangle_{\mathscr{W},\mathscr{W}'} &+ a_t(H_N,G)\\ &= \langle f, G\rangle_{\mathscr{W},\mathscr{W}'} + \left(b'(t) - \langle f, r^{-1}\rangle_{\mathscr{W},\mathscr{W}'}\right)(rG)\,|_\Gamma \quad \forall G \in \mathscr{W}, \text{ a.e. in } [0,T],\\ B_N &= \mu_0\left(H_N + \mathscr{F}(H_N,\xi)\right) \quad \text{in } \Omega\times(0,T).\end{aligned}$$

Moreover, from the compact inclusion (72) and the strongly continuous assumption (cf. (7)) we have that $H_{N\Delta t}(0) \to H_N(0)$ and $W_{N\Delta t}(0) \to \mathscr{F}(H_N,\xi)(0)$ in $\mathrm{L}^2_r(\Omega)$. Therefore (H_N, B_N) is a solution to Problem 4. □

A similar result hold for Problem 5.

THEOREM 2. *Let us assume hypotheses H.1, H.2 and H.3. Then Problem 5 has a solution.*

Proof. We only give a sketch of the proof. First, we consider a lifting of the boundary data. We notice that, from the regularity of g, there exists $H_g \in \mathrm{H}^2(0,T;\widetilde{\mathrm{H}}^1_r(\Omega))$ such that $H_g|_\Gamma = g$ and

$$\|H_g\|_{\mathrm{H}^k(0,T;\widetilde{\mathrm{H}}^1_r(\Omega))} \leqslant C\,\|g\|_{\mathrm{H}^k(0,T;\widetilde{\mathrm{H}}^{1/2}_r(\Gamma))}, \qquad k=1,2, \tag{73}$$

being C a constant independent of g (cf. [4, Section 2.3]). Then, we write $H_D = H_u + H_g$ with $H_u \in \mathscr{U}$, so that the existence of weak solutions can be deduced by applying arguments similar to those used to prove the existence of solution to Problem 4 (see also [44, Chapter IX]). Although the latter does not consider weighted Sobolev spaces, minor modifications of their arguments lead to the existence of solution to Problem 5. In particular, we obtain the corresponding compactness result (cf. (72)) by identifying the axisymmetric space $\mathrm{H}^1(0,T;\mathrm{L}^2_r(\Omega)) \cap \mathrm{L}^\infty(0,T;\widetilde{\mathrm{H}}^1_r(\Omega))$ with its respective 3D version $\mathrm{H}^1(0,T;\mathrm{L}^2(\widetilde{\Omega})^3) \cap \mathrm{L}^\infty(0,T;\mathrm{H}^1(\widetilde{\Omega})^3) \subset \mathbf{L}^2(\widetilde{\Omega};C([0,T]))$, the latter with compact inclusion.

□

REMARK 10. There is not a uniqueness result for a generic hysteresis operator satisfying (5)–(8), even though it is possible to prove such a result by choosing a particular operator, for instance, the Prandtl-Ishlinskiĭ operator of play type (see, for instance, [19] and more recently [13, Theorem 5.1]).

To end this section, we consider the following existence result:

THEOREM 3. *Let us assume that H.2 and H.3 hold true. Then, by choosing as hysteresis operator in the constitutive equations* (41) *and* (36) *the Preisach operator* $\mathscr{F}_p$ (*cf.* (9) *and* (10)), *it follows that there exist* (H_N, B_N) *and* (H_D, B_D) *solutions to Problems 4 and 5, respectively.*

Proof. From Lemma 2 we notice that $\mathscr{F}_p$ satisfies H.1. Then, the result follows from Theorems 1 and 2. Moreover, $\mathscr{F}_p$ is clearly affinely bounded (cf. (45)), since, as a consequence of (11), it is actually uniformly bounded in $\mathrm{L}^\infty(\Omega;C([0,T]))$. Moreover, instead of being affinely bounded (cf. (45)), because of (11) $\mathscr{F}_p$ is uniformly bounded in $\mathrm{L}^\infty(\Omega;C([0,T]))$. □

7. Numerical approximation

In this section we present a numerical procedure to solve a full discretization of Problem 5. The analogous procedure for Problem 4 is similar (see [37, 3] for more details about how to handle the non-standard boundary condition). For the sake of simplicity,

in what follows we will drop subscript D. Let us recall that different algorithms have been proposed to approximate non-linear partial differential equation with hysteresis; see, for instance [40, 41, 37, 38].

From now on we will assume that Ω is a convex polygon. We associate a family of partitions $\{\mathscr{T}_h\}_{h>0}$ of Ω into triangles, where h denotes the mesh size. Let $\mathscr{V}_h$ be the space of continuous piecewise linear finite elements vanishing on the symmetry axis ($r=0$), so that $\mathscr{V}_h \subset \widetilde{\mathrm{H}}^1_r(\Omega)$. We also consider the finite-dimensional space $\mathscr{U}_h := \mathscr{V}_h \cap \mathscr{U}$ and denote by $\mathscr{V}_h(\Gamma)$ the space of traces on Γ of functions in $\mathscr{V}_h$.

By using the above finite element space for the space discretization and the backward Euler scheme for time discretization, we are led to the following Galerkin approximation of Problem 5:

PROBLEM 6. Given $B_h^0 = \mu_0\left(H_h^0 + W_0\right)$ with $H_h^0 \in \mathscr{V}_h$ and $W_0 \in \mathrm{L}^2_r(\Omega)$, find $H_h^n \in \mathscr{V}_h$ and $B_h^n \in \mathrm{L}^2_r(\Omega)$, $n = 1,\dots,m$, such that

$$\begin{aligned}
\frac{1}{\Delta t}\int_\Omega B_h^n G_h r\, drdz + \int_\Omega \frac{1}{\sigma^n r}\left(\frac{\partial(rH_h^n)}{\partial r}\frac{\partial(rG_h)}{\partial r} + \frac{\partial(rH_h^n)}{\partial z}\frac{\partial(rG_h)}{\partial z}\right) drdz & \\
= \langle f^n, G_h\rangle_{\mathscr{U},\mathscr{U}'} + \frac{1}{\Delta t}\int_\Omega B_h^{n-1} G_h r\, drdz & \qquad \forall G_h \in \mathscr{U}_h, \\
B_h^n(r,z) = \mathscr{B}^n(H_h^n)(r,z) & \qquad \text{a.e. in } \Omega, \\
H_h^n = g_h^n & \qquad \text{on } \Gamma,
\end{aligned}$$

where $H_h^0 \in \mathscr{V}_h$ and $g_h^n \in \mathscr{V}_h(\Gamma)$ are convenient approximations of $H_0 \in \widetilde{\mathrm{H}}^1_r(\Omega)$ (cf. H.3) and $g(t^n)$, for $n = 1,\dots,m$, respectively, and $\mathscr{B}^n : \mathrm{L}^2_r(\Omega) \to \mathrm{L}^2_r(\Omega)$, $n = 1,\dots,m$, is such that, given $G \in \mathrm{L}^2_r(\Omega)$, and an initial state ξ

$$\mathscr{B}^n(G)(r,z) := \mu_0\left(u(r,z) + [\mathscr{F}(G_{h\Delta t^n},\xi)](r,z,t^n)\right) \quad \text{a.e. in } \Omega, \tag{74}$$

with $G_{h\Delta t^n}$ being the piecewise linear in time function such that $G_{h\Delta t^n}(r,z,t^l) = H_h^l(r,z)$, $l = 0,\dots,n-1$, and $G_{h\Delta t^n}(r,z,t^n) = G(r,z)$ a.e. in Ω. Notice that operator $\mathscr{B}^n$ is just a natural discrete version of the continuous operator defined by (34).

At each time step of the above algorithm, we must solve a non-linear problem. With this purpose, we have used a duality iterative algorithm which is based on some properties of the Yosida regularization of maximal monotone operators. This algorithm, introduced by Bermúdez and Moreno [5], has been extensively used for a wide range of applications with good numerical results. It seems to be very promising to handle the hysteresis non-linearity because it takes advantage of the spatial independence of the hysteresis operator.

In order to complete the proposed numerical scheme, a particular hysteresis operator must be considered (cf. (74)). In view of applications we have considered the classical Preisach model described in Section 4.

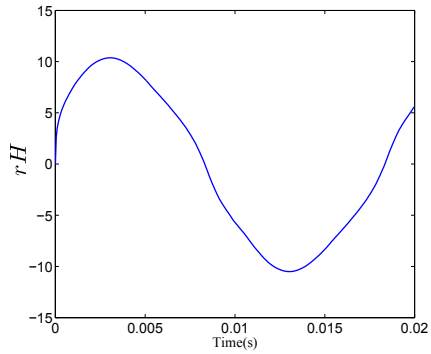

Figure 27: rH on the boundary.

8. Numerical example

In this section we report the results of a numerical test obtained with a Fortran code implementing the numerical method described in Section 7 to approximate the solution to Problem 5. Similar numerical tests for Problem 4 are currently in progress.

Let us consider the eddy current Problem 5 with $\Omega := [R_1, R_2] \times [0, d]$ and the non-homogeneous Dirichlet condition given by $g = (rH)/(2\pi r)$ where the constant value $rH(t)$ on the boundary is depicted in Figure 27 as a function of time which has been taken from a numerical simulation with the code described in [3]. The geometrical and physical data have been summarized in Table 5.1 below.

Table 5.1: Geometrical and physical data for the test

Internal radius, R_1:	0.0825 m
External radius, R_2:	0.0925 m
Thickness, d:	0.00065 m
Electrical conductivity, σ:	4×10^6 (Ohm/m)$^{-1}$
Frequency, f:	50 Hz

In practical applications the measurable data is the B-H curve, usually represented by the Everett function. We assume that the B-H relation (cf. (41)) is given by the Preisach operator characterized by the Everett function depicted in Figure 28 (left) which comes from experimental measurements. Figure 28 (right) shows the major loop of the B-H curve obtained with this Everett function.

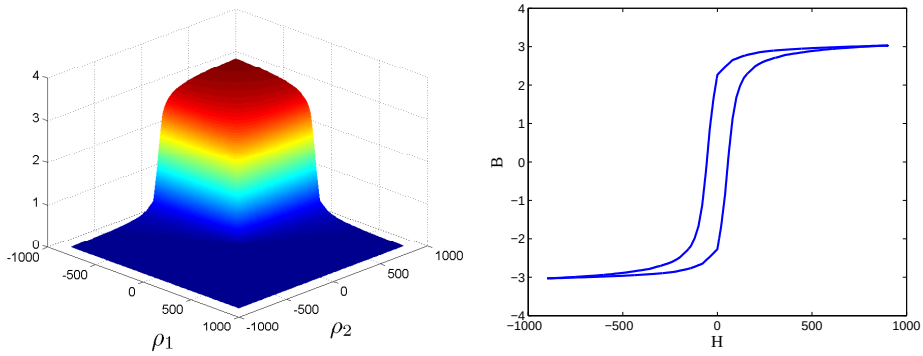

Figure 28: Everett function (left) and the corresponding B-H curve (right).

Figure 29 (left) shows the evolution of the B-H curve in a fixed point of the mesh and Figure 29 (right) the waveforms in the middle and at the surface of the domain. Whereas Figure 30 shows the magnetic field and magnetic induction, at different times on a fixed domain. In Figure 29 (right), we can see the presence of skin effect.

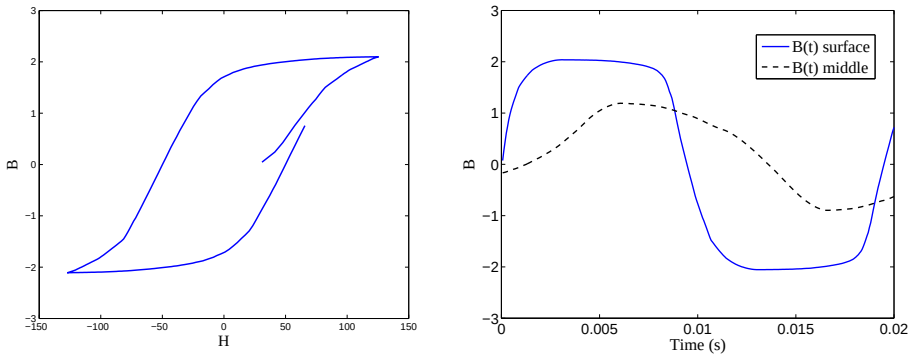

Figure 29: B-H curve at the surface of the domain (left) and B vs. time in the middle and at the surface of the domain (right).

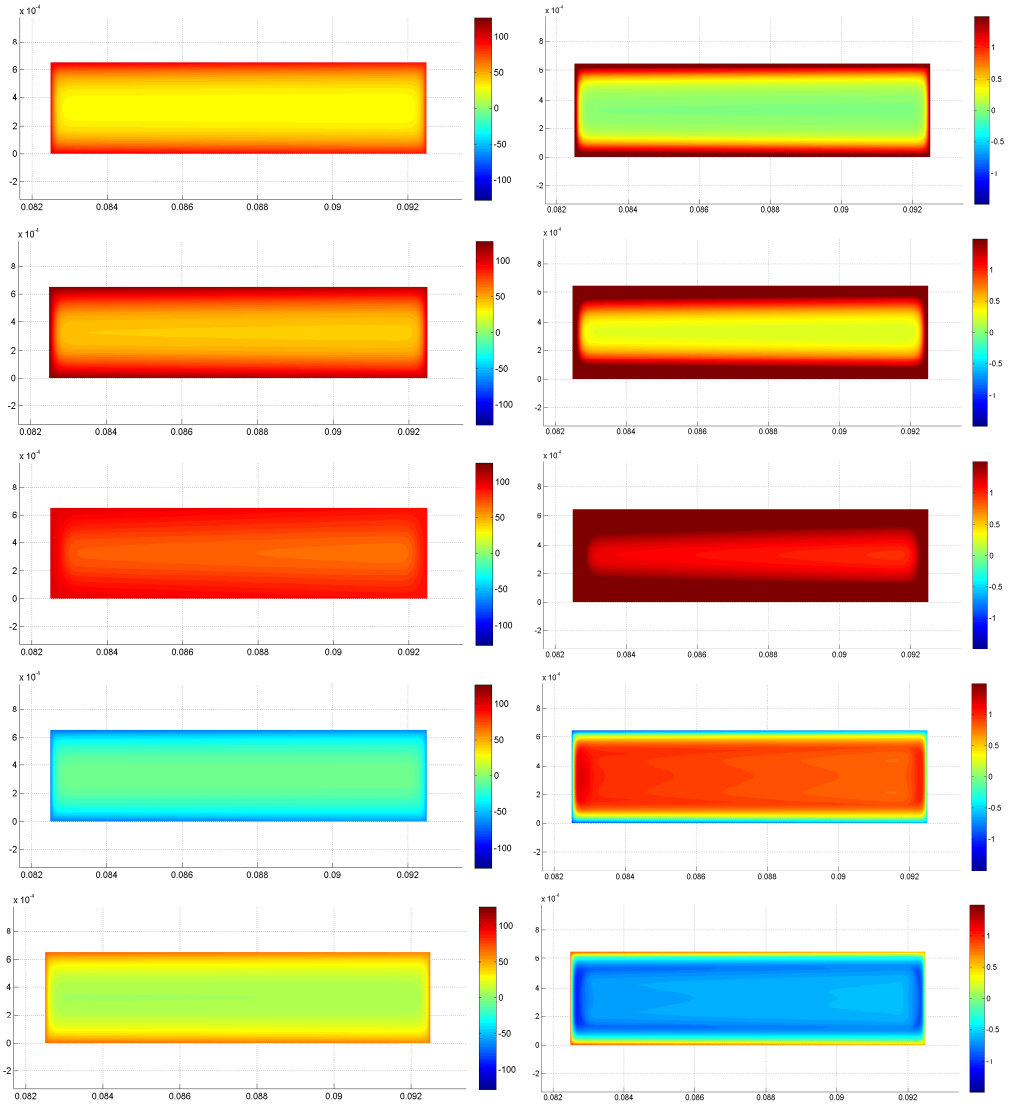

Figure 30: Magnetic field H (left) and magnetic induction B (right) at times $t = 0.00125$, 0.0025, 0.0050, 0.0100 and 0.0200 s.

Acknowledgment

The work of the authors from Universidade de Santiago de Compostela was supported by FEDER, Spanish Ministry of Science and Innovation under research project ENE2013-47867-C2-1-R. R. Rodríguez was partially supported by BASAL project, CMM, Universidad de Chile and Anillo ANANUM, ACT1118, CONICYT (Chile). P.

Venegas was partially supported by Centro de Investigación en Ingeniería Matemática (CI^2MA), Universidad de Concepción, through the BASAL project CMM, Universidad de Chile, CONICYT and MECESUP (Chile).

References

[1] A. BERMÚDEZ, J. BULLÓN, AND F. PENA, *A finite element method for the thermoelectrical modelling of electrodes*, Commun. Numer. Meth. Eng. **14** (1998), 581–593.

[2] A. BERMÚDEZ, J. BULLÓN, F. PENA, AND P. SALGADO, *A numerical method for transient simulation of metallurgical compound electrodes*, Finite Elem. Anal. Des. **39** (2003), 283–299.

[3] A. BERMÚDEZ, D. GÓMEZ, R. RODRÍGUEZ, P. SALGADO, AND P. VENEGAS, *Numerical solution of a transient non-linear axisymmetric eddy current model with non-local boundary conditions*, Math. Models Methods Appl. Sci. **23** (2013), 2495–2521.

[4] A. BERMÚDEZ, D. GÓMEZ, R. RODRÍGUEZ, AND P. VENEGAS, *Numerical analysis of a transient non-linear axisymmetric eddy current model*, (2014), (Submitted).

[5] A. BERMÚDEZ AND C. MORENO, *Duality methods for solving variational inequalities*, Comput. Math. Appl. **7** (1981), 43–58.

[6] G. BERTOTTI, *Hysteresis in Magnetism*, Academic Press, 1998.

[7] G. BERTOTTI AND I. D. MAYERGOYZ (eds.), *The Science of Hysteresis. Vol. I*, Elsevier/Academic Press, Amsterdam, 2006.

[8] M. BROKATE AND J. SPREKELS, *Hysteresis and Phase Transitions*, Springer, Berlin, 1996.

[9] E. DELLA TORRE, *Magnetic Hysteresis*, IEEE Press, New York, 1999.

[10] L. R. DUPRÉ, R. VAN KEER, AND J. A. A. MELKEBEEK, *Complementary 2-D finite element procedures for the magnetic field analysis using a vector hysteresis model*, International Journal for Numerical Methods in Engineering **42** (1998), no. 6.

[11] L.R. EGAN AND E.P. FURLANI, *A computer simulation of an induction heating system*, IEEE Trans. Magn. **27** (1991), 4343 – 4354.

[12] M. ELEUTERI, *An existence result for a P.D.E. with hysteresis, convection and a nonlinear boundary condition*, Discrete Contin. Dyn. Syst. (2007), 344–353.

[13] M. ELEUTERI, *Wellposedness results for a class of parabolic partial differential equations with hysteresis*, NoDEA Nonlinear Differential Equations Appl. **15** (2008), 557–580.

[14] M. ELEUTERI, J. KOPFOVÁ, AND P. KREJČÍ, *Magnetohydrodynamic flow with hysteresis*, SIAM Journal on Mathematical Analysis **41** (2009), no. 2, 435–464.

[15] M. ELEUTERI AND P. KREJČÍ, *Asymptotic behavior of a Neumann parabolic problem with hysteresis*, ZAMM Z. Angew. Math. Mech. **87** (2007), 261–277.

[16] M. ELEUTERI AND P. KREJČÍ, *An asymptotic convergence result for a system of partial differential equations with hysteresis*, Commun. Pure Appl. Anal. **6** (2007), 1131–1143.

[17] V. GIRAULT AND P.-A RAVIART, *Finite Element Approximations of the Navier-Stokes Equations, Theory and Algorithms*, Springer, Berlin, 1986.

[18] J. GOPALAKRISHNAN AND J. E. PASCIAK, *The convergence of V-cycle multigrid algorithms for axisymmetric Laplace and Maxwell equations*, Math. Comp. **75** (2006), 1697–1719.

[19] M. HILPERT, *On uniqueness for evolution problems with hysteresis*, Mathematical models for phase change problems, Internat. Ser. Numer. Math., vol. 88, Birkhäuser, Basel, 1989, pp. 377–388.

[20] R. INNVÆR AND L. OLSEN, *Practical use of mathematical models for Søderberg electrodes*, Elkem Carbon Technical Paper presented at the A.I.M.E. Conference (1980).

[21] P. KORDULOVÁ AND M. BENEŠ, *Solutions to the seepage face model for dual porosity flows with hysteresis*, Nonlinear Analysis: TMA **75** (2012), no. 18, 6473 – 6484.

[22] M.A. KRASNOSEL'SKIĬ AND A.V. POKROVSKIĬ, *System with Hysteresis*, Springer, Berlin, 1989, (Russian edition, Nauka, Moscow (1983)).

[23] P. KREJČÍ, *Hysteresis, Convexity and Dissipation in Hyperbolic Equations.*, Gakuto Int. Series Math. Sci. & Appl., vol. 8, Gakkotosho, Tokyo, 1996.

[24] M. KUCZMANN, *Identification of isotropic and anisotropic vector Preisach model*, Preisach Memorial Book, Akadémiai Kiadó, Budapest, 2005.

[25] M. KUCZMANN, *Vector preisach hysteresis modeling: Measurement, identification and application*, Physica B: Condensed Matter **406** (2011), no. 8, 1403 – 1409.

[26] M. MARKOVIC AND Y. PERRIARD, *Eddy current power losses in a toroidal laminated core with rectangular cross section*, 2009 International Conference on Electrical Machines and Systems (ICEMS) (New York), IEEE, 2009, pp. 1249–1252.

[27] I.D. MAYERGOYZ, *Mathematical Models of Hysteresis*, Springer, New York, 1991.

[28] I.D. MAYERGOYZ AND G. FRIEDMAN, *Isotropic vector Preisach model of hysteresis*, J. Appl. Phys. **61** (1987), 4022–4024.

[29] K.V. NAMJOSHI, J.D. LAVERS, AND P.P. BIRINGER, *Eddy-current power loss in toroidal cores with rectangular cross section*, IEEE Trans. Magn. **34** (1998), 636 –641.

[30] K. PREIS, *A contribution to eddy current calculations in plane and axisymmetric multiconductor systems*, IEEE Trans. Magn. **19** (1983), 2397–2400.

[31] F. PREISACH, *Über die magnetische nachwirkung*, Zeitschrift für Physik, **94** (1935), 277–302.

[32] E. ROTHE, *Zweidimensionale parabolische Randwertaufgaben als Grenzfall eindimensionaler Randwertaufgaben*, Math. Ann. **102** (1930), 650–670.

[33] T. ROUBÍČEK, *Non Linear Partial Differential Equations with Applications*, Birkhäuser, 2005.

[34] R. E. SHOWALTER, LITTLE T. D., AND U. HORNUNG, *Parabolic PDE with Hysteresis*, 1996.

[35] E. DELLA TORRE, E. PINZAGLIA, AND E. CARDELLI, *Vector modeling-part I: Generalized hysteresis model*, Physica B: Condensed Matter **372** (2006), no. 1-2, 111 – 114.

[36] E. DELLA TORRE, E. PINZAGLIA, AND E. CARDELLI, *Vector modeling-part II: Ellipsoidal vector hysteresis model. numerical application to a 2D case*, Physica B: Condensed Matter **372** (2006), no. 1-2, 115 – 119.

[37] R. VAN KEER, L. DUPRÉ, AND J. A. A. MELKEBEEK, *On a numerical method for 2D magnetic field computations in a lamination with enforced total flux*, J. Comput. Appl. Math. **72** (1996), 179–191.

[38] R. VAN KEER, L. DUPRÉ, AND J. A. A. MELKEBEEK, *Computational methods for the evaluation of the electromagnetic losses in electrical machinery*, Arch. Comput. Methods Engrg. **5** (1998), 385–443.

[39] P. VENEGAS, *Contribución al Análisis Matemático y Numérico de algunos problemas de Electromagnetismo*, Ph.D. Thesis, Universidad de Concepción, Chile, 2013.

[40] C. VERDI AND A. VISINTIN, *Numerical approximation of hysteresis problems*, IMA J. Numer. Anal. **5** (1985), 447–463.

[41] C. VERDI AND A. VISINTIN, *Numerical approximation of the Preisach model for hysteresis*, RAIRO Modél. Math. Anal. Numér. **23** (1989), 335–356.

[42] A. VISINTIN, *A model for hysteresis of distributed systems*, Ann. Mat. Pura Appl. **131** (1982), 203–231.

[43] A. VISINTIN, *On the Preisach model for hysteresis*, Nonlinear Anal. T.M.A. **8** (1984), 977–996.

[44] A. VISINTIN, *Differential Models of Hysteresis*, Springer, Berlin, 1994.

[45] A. VISINTIN, *Vector Preisach model and Maxwell's equations*, Physica B **306** (2001), no. 1-4, 21 – 25, Proceedings of the Third International Symposium on Hysteresis and Micromagnetics Modeling.

[46] A. VISINTIN, *Maxwell's equations with vector hysteresis*, Archive for Rational Mechanics and Analysis **175** (2005), no. 1, 1–37.

[47] A. VISINTIN, *Mathematical models of hysteresis*, The Science of Hysteresis (G. Bertotti, I. Mayergoyz, eds.), Elsevier, 2006.

AMS Subject Classification: 65N30 (78A55 78M10)

Alfredo BERMÚDEZ, Dolores GÓMEZ ,
Departamento de Matemática Aplicada, Universidade de Santiago de Compostela
Santiago de Compostela, SPAIN
e-mail: alfredo.bermudez@usc.es, mdolores.gomez@usc.es

Rodolfo RODRÍGUEZ,
CI^{2}MA, Departamento de Ingeniería Matemática, Universidad de Concepción
Concepción, CHILE
e-mail: rodolfo@ing-mat.udec.cl

Pablo VENEGAS,
Department of Mathematics, University of Maryland
College Park, USA
e-mail: pvenegas@umd.edu

Lavoro pervenuto in redazione il 29.01.2015.

Special Issues and Proceedings published in the Rendiconti

Some Topics in Nonlinear PDE's	(1989)
Mathematical Theory of Dynamical Systems and ODE, I-II	(1990)
Commutative Algebra and Algebraic Geometry, I-III	(1990–1991)
Numerical Methods in Applied Science and Industry	(1991)
Singularities in Curved Space-Times	(1992)
Differential Geometry	(1992)
Numerical Methods in Astrophysics and Cosmology	(1993)
Partial Differential Equations, I-II	(1993–1994)
Problems in Algebraic Learning, I-II	(1994)
Number Theory, I-II	(1995)
Geometrical Structures for Physical Theories, I-II	(1996)
Jacobian Conjecture and Dynamical Systems	(1997)
Control Theory and its Applications	(1998)
Geometry, Continua and Microstructures, I-II	(2000)
Partial Differential Operators	(2000)
Liaison and Related Topics	(2001)
Turin Fortnight Lectures on Nonlinear Analysis	(2002)
Microlocal Analysis and Related Topics	(2003)
Splines, Radial Basis Functions and Applications	(2003)
Polynomial Interpolation and Projective Embeddings - Lecture Notes of the School	(2004)
Polynomial Interpolation and Projective Embeddings - Proceedings of the Workshop of the School	(2005)
Control Theory and Stabilization, I-II	(2005–2006)
Syzygy 2005	(2006)
Subalpine Rhapsody in Dynamics	(2007)
ISASUT Intensive Seminar on Non Linear Waves, Generalized Continua and Complex Structures	(2007)
Lezioni Lagrangiane 2007–2008	(2008)
Second Conference on Pseudo-Differential Operators and Related Topics: Invited Lectures	(2008)
Second Conference on Pseudo-Differential Operators and Related Topics	(2009)
In Memoriam Aristide Sanini	(2009)
Workshop on Hodge Theory and Algebraic Geometry	(2010)
School on Hodge Theory	(2011)
Generalized Functions, Linear and Nonlinear Problems. Proceedings of the International Conference GF 2011	(2011)
Forty years of Analysis in Turin. A conference in honour of Angelo Negro	(2012)

Rendiconti del Seminario Matematico
dell'Università e del Politecnico di Torino

Volume 72, N. 1–2 (2014)

CONTENTS

ISSN 0373-1243

UNIVERSITÀ DEGLI STUDI DI TORINO
DIPARTIMENTO DI MATEMATICA